

Design and Evaluation of a Novel Ankle Joint for an Ankle Foot Orthosis for Individuals with Drop-Foot

Eileen Maya Baker
Marquette University

Recommended Citation

Baker, Eileen Maya, "Design and Evaluation of a Novel Ankle Joint for an Ankle Foot Orthosis for Individuals with Drop-Foot" (2019). *Master's Theses (2009 -)*. 550.
https://epublications.marquette.edu/theses_open/550

**DESIGN AND EVALUATION OF A NOVEL ANKLE JOINT FOR AN ANKLE
FOOT ORTHOSIS FOR INDIVIDUALS WITH DROP-FOOT**

by

Eileen Baker, B.S.

A Thesis submitted to the Faculty of the Graduate School,
Marquette University,
in Partial Fulfillment of the Requirements for
the Degree of Master of Science in Biomedical Engineering

Milwaukee, Wisconsin

August 2019

ABSTRACT
**DESIGN AND EVALUATION OF A NOVEL ANKLE JOINT FOR AN ANKLE
FOOT ORTHOSIS FOR INDIVIDUALS WITH DROP-FOOT**

Eileen Baker, B.S.

Marquette University, 2019

Individuals who have had a stroke often ambulate with an ankle foot orthosis (AFO) to treat drop-foot, a common impairment preventing active ankle dorsiflexion. AFOs limit ankle plantarflexion or drop-foot, but also restrict ankle motion that introduces additional gait pathologies during ambulation. The goal of this study was to design a mechanical ankle joint for an articulated thermoplastic AFO to permit enhanced motion during stance. This novel ankle joint operated in two stages: 1) locked during swing to prevent drop-foot and 2) unlocked during stance to allow motion.

This novel ankle joint was first tested with able-bodied subjects to ensure device function and safety, subsequent testing was conducted with post-stroke subjects to determine whether the novel design contributed to functional improvements during walking. Three able-bodied (23-26 years) and three post-stroke individuals (52-67 years) were recruited to complete custom AFO casting, fitting, and testing sessions with conventional and novel orthotic ankle joints. Testing included overground and variable slope treadmill walking trials. These gait analyses incorporated motion capture and kinetic data to calculate spatiotemporal, kinematic, and joint moment data. A survey was administered after testing to determine subject perception of the novel ankle joint in terms of comfort, walking performance, and perceived exertion. Paired t-tests were conducted to identify significant differences between orthotic ankle joint conditions.

Significant differences between ankle joint conditions were observed for stance duration, step length, and ankle plantarflexion during swing. Stance duration and step length increased for the paretic limb, and corresponding improved inter-limb symmetry for level and non-level terrain. Ankle plantarflexion during swing with the novel ankle joint was controlled, providing adequate foot clearance and increased ankle range of motion during early stance. These improvements in ankle mobility, however, did not contribute to consistent improvements in hip kinematics, nor significant differences in knee and hip kinetics.

Design refinement is recommended to support joint tuning and accommodate greater variation in spring stiffnesses. This novel orthotic ankle joint demonstrates promise and clinical potential to treat post-stroke individuals with drop-foot.

ACKNOWLEDGEMENTS

Eileen Baker, B.S.

This research could not have been completed without the help of a number of people, especially Dr. Barbara-Silver-Thorn and Dr. Philip Voglewede. They are some of the greatest educators and mentors a student could ever hope for, and without their guidance this project would not have been nearly as much fun. I would also like to thank Dr. Gerald Harris for sharing his expertise and motion capture equipment with me, making the last semester of TA duties a joy rather than a chore, and directing me to Dr. Jacob Rammer for additional support.

Tom Current, CPO is also thanked for his clinical expertise and willingness to mentor me in the specifics of orthotic fabrication, even when his own schedule was so crazy. I would like to thank John McGuire, MD and Rachel Minkin of the Stroke Rehabilitation Center for their assistance with subject recruitment. I also thank Dr. Aprill Dawson and Dr. Rebekah Walker for their statistical consultation.

Testing would not have been completed smoothly without the assistance of Yana Rawinski and Jessica Thayer, who helped with everything from data collection to subject entertainment. A big thank you to my subjects, who brought their stories and patience to make the process of testing my design less intimidating.

Finally, I'd like to thank my parents, the greatest support duo for a record breaking 25 years, for making it all possible.

This project was supported by funding from the National Center for Advancing Translational Sciences, National Institutes of Health, Award Number UL1TR001436. The Marquette University Biomedical Engineering Department is gratefully acknowledged for their providing of financial support to E. Baker.

TABLE OF CONTENTS

ACKNOWLEDGEMENTS.....	i
LIST OF TABLES.....	viii
LIST OF FIGURES.....	xi
LIST OF ACRONYMS.....	xvi
1 INTRODUCTION	1
2 LITERATURE REVIEW	4
2.1 STROKE.....	4
2.2 GAIT.....	6
2.2.1 <i>Able-Bodied Gait</i>	6
2.2.1.1 Temporal and Spatial Parameters of Gait	8
2.2.1.2 Gait Kinematics.....	10
2.2.1.3 Gait Kinetics.....	12
2.2.1.3.1 <i>Joint Moments</i>	12
2.2.2 <i>Post-stroke Gait</i>	14
2.3 ANKLE FOOT ORTHOSES.....	16
2.4 AFO TREATMENT OF DROP-FOOT.....	23
2.4.1 <i>Articulated vs. Solid AFOs</i>	23
2.4.1.1 Kinematics.....	26

2.4.1.2	Walking Speed	27
2.4.1.3	Symmetry	28
2.4.1.4	Variable Terrain	31
2.4.1.5	Kinetics.....	31
2.4.2	<i>Novel Orthotic Ankle Joint Designs</i>	33
2.5	SUMMARY	39
3	DESIGN SELECTION	40
3.1	DESIGN REQUIREMENTS	40
3.1.1	<i>Target Population</i>	40
3.1.2	<i>Design Specifications</i>	41
3.2	CONCEPT GENERATION.....	42
3.3	FINAL DESIGN	44
3.3.1	<i>Novel Ankle Joint Function</i>	44
3.3.2	<i>AFO-Orthotic Joint Interface</i>	45
3.3.3	<i>Bill of Materials</i>	48
3.4	FAILURE ANALYSES	48
3.4.1	<i>Failure Modes Analysis</i>	50
3.4.2	<i>Weakest Link Analysis</i>	51
3.5	SUMMARY	52
4	Methods.....	53

4.1	SUBJECT SELECTION.....	53
4.2	AFO FABRICATION AND FITTING	54
4.3	GAIT ANALYSIS	57
	4.3.1.1 Anthropometry Measurements.....	57
	4.3.1.2 Testing Protocol	61
	4.3.1.3 Metrics of Interest	63
4.4	KINEMATIC DATA PROCESSING.....	64
	4.4.1 2D to 3D Data Conversion	65
	4.4.2 Subject Specific Kinematic Models.....	66
	4.4.3 Lower Extremity Joint Angles.....	70
	4.4.4 Event Detection.....	71
	4.4.5 Data Parsing – Treadmill Walking Trials	73
	4.4.6 Data Parsing – Overground Walking Trials	75
	4.4.7 Symmetry.....	76
	4.4.8 Kinetic Data Analysis	76
4.5	STATISTICAL ANALYSIS	80
4.6	SUMMARY	81
5	Results.....	83
	5.1 SUBJECT CHARACTERISTICS	83
	5.2 CONFIRMATION OF DESIGN POTENTIAL AND SAFETY	84

5.3	HYPOTHESIS TESTING AND CLINICAL POTENTIAL	88
5.3.1	<i>Spatiotemporal Parameters</i>	89
5.3.2	<i>Kinematic Parameters</i>	94
5.4	KINETIC PARAMETERS	106
5.5	SUBJECT PERCEPTION	111
5.6	POWER ANALYSIS.....	112
5.7	SUMMARY	112
6	Discussion.....	113
6.1	DESIGN POTENTIAL – ABLE-BODIED SUBJECT TESTING	113
6.1.1	<i>Objective 1</i>	114
6.1.2	<i>Objective 2</i>	114
6.1.3	<i>Objective 3</i>	115
6.1.4	<i>Objective 4</i>	116
6.1.5	<i>Design Potential Summary</i>	116
6.2	POST-STROKE SUBJECT CHARACTERISTICS.....	117
6.3	HYPOTHESIS TESTING FOR POST-STROKE INDIVIDUALS	118
6.3.1	<i>Spatiotemporal Parameters</i>	119
6.3.1.1	Walking Speed	119
6.3.1.2	Stance Duration	121
6.3.1.3	Step Length	123

6.3.1.4	Spatiotemporal Parameters Summary	124
6.3.2	<i>Kinematic Parameters</i>	125
6.3.2.1	Peak Ankle Plantarflexion During Swing	126
6.3.2.2	Ankle ROM During Stance	128
6.3.2.2.1	<i>Early Stance (First Rocker)</i>	128
6.3.2.2.2	<i>Mid-Stance (Second Rocker)</i>	129
6.3.2.2.3	<i>Late Stance (Third Rocker)</i>	130
6.3.2.3	Knee Flexion during Stance	132
6.3.2.4	Hip Flexion during Stance.....	134
6.3.2.5	Kinematic Parameters Summary	136
6.3.3	<i>Kinetic Parameters</i>	136
6.3.3.1	Knee Extension Moment.....	137
6.3.3.2	Hip Extension Moment	138
6.3.3.3	Kinetic Parameters Summary.....	140
6.3.4	<i>Subject Perception</i>	140
6.3.4.1	Subject Perception Summary	141
6.4	CLINICAL RELEVANCE	142
6.4.1	<i>Prescription</i>	142
6.4.2	<i>Design Refinements</i>	143
6.4.3	<i>Fabrication and Fitting</i>	143

6.5	STUDY LIMITATIONS	144
6.5.1	<i>Subject Sample Size</i>	144
6.5.2	<i>Experimental Protocol Design</i>	145
6.5.3	<i>Kinematic Analysis</i>	147
6.6	PROTOCOL MODIFICATIONS AND FUTURE STUDIES	148
6.7	<i>Summary</i>	150
7	Conclusion	152
	Bibliography.....	156
	APPENDIX A: ALTERNATIVE DESIGNS.....	167
	APPENDIX B: DESIGN EVALUATION TOOLS.....	170
	APPENDIX C: SUBJECT FITNESS ASSESSMENT AND PERCEPTION.....	172
	APPENDIX D: RAW METRICS.....	177

LIST OF TABLES

Table 2.1 Spatial parameters for able-bodied men and women greater than 40 years of age [17].	10
Table 2.2 Summary of orthotic ankle joints, manufacturers, ROM, and design limitations	19
Table 2.3 Summary of investigations of articulated and solid AFO designs to treat drop-foot post-stroke	25
Table 2.4 Comparison of walking speed post-stroke individuals ambulating over level ground with various AFO designs.	28
Table 2.5 Step length [mean (standard deviation)] and corresponding SR and IA for post-stroke individuals (N=11) for three AFO conditions (no AFO, solid AFO, an articulated AFO) during level overground walking at self-selected speeds.	30
Table 2.6 AFO effects on symmetry for solid versus articulated AFOs when walking at self-selected speed: double and single support duration and step length for hemiparetic, post-stroke subjects and post-trauma drop-foot subjects.	31
Table 2.7 Changes in spatiotemporal, kinematic, and kinetic parameters for the three experimental conditions (no AFO, hydraulic AFO pre- and post-training for eight post-stroke individuals [56]).	36
Table 3.1 Analytic hierarchy process to determine weighting of design feasibility criteria for a novel ankle joint	42
Table 3.2 Decision matrix to rate each design concept based on requirement criteria.....	43
Table 3.3 Abbreviated FMEA for the novel ankle joint design, highlighting the four greatest risks to user safety based on rate of occurrence and severity.	50
Table 3.4 Weakest link analysis in the form of a pro/con list for each ankle joint component.....	51
Table 4.1 Description of anthropometric measurements taken during testing.	57
Table 4.2 Marker names and placement descriptions	60
Table 4.3 Metrics of Interest (%GC = normalized to gait cycle duration, SR = symmetry ratio, %height = normalized to subject height).	64

Table 4.4 Subject specific models and body segments.....	67
Table 4.5 Sagittal plane joint angles definitions for the ankle, knee, and hip (adapted from [81], [82]).....	71
Table 4.6 Summary of hypotheses between conventional and novel ankle joint conditions for able-bodied (able-bodied) and post-stroke (PS) subjects.....	81
Table 5.1 Able-bodied subject characteristics	83
Table 5.2 Post-stroke subject characteristics.....	84
Table 5.3 Subject self-selected walking speeds for conventional and novel ankle joint conditions during treadmill and overground walking trials, mean and standard deviation, S.D.).....	86
Table 5.4 Mean self-selected speeds during treadmill and overground walking trials for all AFO conditions (standard deviation, S.D.).....	89
Table 5.5 Survey responses regarding perceived relative walking performance, comfort, and ease (e.g., reduced exertion or effort) for the novel ankle joint relative to the conventional ankle joint.....	111
Table 6.1 Summary of the hypotheses tested.....	119
Table 6.2 Hypothesis testing results and trends.....	151
Table B.1 Bill of materials including manufacturer, specifications, cost, and function in the novel ankle joint design.....	170
Table B.2 Full FMEA for the novel ankle joint design to determine likely failure modes and severity.....	171
Table D.1 Spatiotemporal and kinematic parameters for the AFO side (right) of able-bodied subjects for each ankle condition	177
Table D.2 Spatiotemporal and kinematic parameters for the AFO side (right) of able-bodied subjects for each ankle condition during the middle 145 seconds of incline treadmill walking.....	178
Table D.3 Spatiotemporal and kinematic parameters for the AFO side (right) of able-bodied subjects for each ankle condition during the middle 145 seconds of decline treadmill walking	179

Table D.4 Kinetic parameters for able-bodied subjects during overground walking for each ankle joint condition; raw metrics are for the AFO side (right leg)	183
Table D.5 Spatiotemporal and kinematic parameters for the AFO side (right) of post-stroke subjects for each ankle condition during the middle 50% of incline treadmill walking.....	187
Table D.6 Spatiotemporal and kinematic parameters for the AFO side (right) of post-stroke subjects for each ankle condition during the middle 50% of decline treadmill walking.....	188

LIST OF FIGURES

Figure 2.1 Stance and swing periods of the GC (adapted from [12]).	7
Figure 2.2 Stance and swing phase durations of the GC for both limbs, defining periods of single versus double support (adapted from [12]).	9
Figure 2.3 Foot and ankle rockers during gait (adapted from [16]).	9
Figure 2.4 Joint (hip, knee and ankle) angle time series for able-bodied adults during level overground walking (adapted from [4]).	11
Figure 2.5 Joint (hip, knee, and ankle) moments for an able-bodied individual (adapted from [4]).	13
Figure 2.6 Drop-foot during swing phase of gait (adapted from [4]).	15
Figure 2.7 AFOs constructed from metal (a) and plastic (b) – solid, nonarticulated; (c) – articulated). (adapted from [33]–[35]).	17
Figure 2.8 Pin (a) and elastic (b) PF stops used to prevent PF motion in thermoplastic, articulated AFOs (adapted from [39]).	18
Figure 2.9 Becker double action joint internal mechanism (adapted from [40]).	20
Figure 2.10 MR fluid damping (a) and pneumatic muscle (b) actively powered AFOs (adapted from [45], [47]).	21
Figure 2.11 Ankle kinematics during level overground walking for a post-stroke subject with drop-foot wearing the MR damped AFO (adapted from [45]).	22
Figure 2.12 Ankle kinematics for individuals during overground walking at self-selected speed in various AFO designs(dotted line - shoes and no AFO, solid black line - solid AFO, solid gray line– DA-DS articulated AFO)	27
Figure 2.13 Knee extension moment in 30 post stroke subjects ambulating over level ground; dotted gray represents no AFO, solid black represents the solid AFO, and solid gray is the articulated dorsiflexion assist joint.	32
Figure 2.14 DACS AFO design (adapted from [69]).	34

Figure 2.15 Mean ankle (a) and knee angle (b) for five individuals with drop-foot. The dotted line is a metal AFO, dashed is a solid posterior support AFO, and the solid line is the DACS AFO.....	34
Figure 2.16 Articulated AFO design incorporating a hydraulic ankle damper.....	35
Figure 2.17 Spring adjustable resistance AFO joint from Becker Orthopedics	37
Figure 2.18 Comparison of ankle (top) and the knee (bottom) kinematics for a single post-stroke individual for variations in PF resistance (left), DF resistance (middle), and AFO alignment (right); low resistance setting (blue) and high resistance settings (purple). able-bodied comparative kinematic profiles (dotted line) are also shown.	38
Figure 2.19 Alternative orthotic ankle design with frictional clutch mechanism.....	39
Figure 3.1 Proposed function of the novel ankle joint during four different stages of gait: swing (a), heel strike (b), stance (c), and toe off (d) (adapted from [73]).	44
Figure 3.2 Final ankle joint body with SolidWorks isometric view (a), manufactured joint front view (b), and final joint integrated with the AFO (c).	45
Figure 3.3 Upright bar attachment front view with components exploded (a) and assembled (b).	46
Figure 3.4 Stirrup attachment to joint body using Chicago bolt and washers; side, exploded view (a) and assembled view (b).....	46
Figure 3.5 Fabricated AFO for the left leg, with a front view (a) and back view (b) displaying the conventional joint on the lateral side of the ankle and a Gaffney joint on the medial side.	47
Figure 3.6 Gaffney joint where originally there was only a fixed axis of rotation and no translation (a), and after modification the joint was free to translate upwards (b) and downwards (c) approximately 0.25cm each way.....	48
Figure 4.1 Casting of the affected limb for AFO fabrication: a) donned sock with rubber strip to aid cast removal, cast progression from (b) the foot to (c) the shank, and removal of the hardened cast using a saw (d).	55
Figure 4.2 Placement of the 29 markers for motion capture and kinematic data.	58
Figure 4.3 Ankle marker position on AFO for the Gaffney joint placed over the medial ankle (a) and lateral ankle joints [standard double action joint (b) and novel joint (c)]... ..	59
Figure 4.4 Marker placement on an able-bodied subject for gait analysis.	59

Figure 4.5 Testing protocol for overground and treadmill trials where SS indicates the trial was performed at the subject's self-selected speed; SM refers to the speed matched trial of the novel joint.....	61
Figure 4.6 Conversion of 2D marker data into 3D motion data using AMASS and Visual3D software.	65
Figure 4.7 Laboratory-based global coordinate system: positive Y-axis is the direction of travel, positive Z-axis is vertical, and positive X-axis is perpendicular to the other two axes according to the right-hand rule.....	66
Figure 4.8 Subject specific model creation and requisite segment input data.	67
Figure 4.9 Local coordinate system (X' , Y' , Z') with origin at the knee center for the right shank; the global, laboratory-based coordinate system (X , Y , Z) is shown for reference.....	68
Figure 4.10 Definition of the local coordinate system (i, j, k) for the hip joint relative to the knee joint for the thigh segment.....	69
Figure 4.11 Event detection algorithm for able-bodied and post stroke individuals based on kinematic profiles in the frontal plane. The purple vertical bars represent events: HS = maximum heel-pelvis angle, TO = minimum toe-pelvis angle.....	72
Figure 4.12 Stride cycle for right and left limbs based on HS and TO events; the corresponding stance and swing phases are also shown.	74
Figure 4.13 Definition of step length (adapted from [84]).	75
Figure 4.14 Conical frustrum used to approximate lower limb segment geometries in Visual3D for inverse dynamics calculation; R is the proximal and distal radii of the segment, L is the length of the segment and the coordinates shown are in the GCS.	77
Figure 4.15 Free body diagrams of the foot, shank, and thigh segments used to perform inverse dynamics calculations.....	79
Figure 5.1 Ankle plantarflexion during swing for able-bodied subjects during level treadmill walking for each orthotic ankle joint condition.....	87
Figure 5.2 Ankle ROM during stance for able-bodied subjects during level treadmill walking trials for each orthotic ankle joint conditions.....	88
Figure 5.3 Stance duration on the AFO side (normalized to %GC) during treadmill walking across all terrains for each orthotic ankle joint condition.	91

Figure 5.4 Inter-limb symmetry (SR) for stance duration during inclined, level, and declined treadmill walking for each orthotic ankle joint condition	92
Figure 5.5 Step length on the AFO side (normalized to % height) during treadmill walking across all terrains for each orthotic ankle joint condition.	93
Figure 5.6 Inter-limb symmetry (SR) for step length during inclined, level, and declined treadmill walking for each orthotic ankle joint condition.....	94
Figure 5.7 Ankle (left), knee (middle), and hip (right) angle time series for the paretic/AFO side of post-stroke subjects during level overground walking – a) Subject P1, b) Subject P2, c) Subject P3	97
Figure 5.8 Peak plantarflexion on the AFO side during treadmill walking across all terrains for each orthotic ankle joint condition.	99
Figure 5.9 Ankle ROM during early stance on the paretic/AFO side during level treadmill walking for each orthotic ankle joint condition.	100
Figure 5.10 Ankle dorsiflexion during mid-stance on the paretic/AFO side during level treadmill walking for each orthotic ankle joint condition.....	101
Figure 5.11 Plantarflexion of the ankle during late stance on the paretic/AFO side during level treadmill walking for each orthotic ankle joint condition.	102
Figure 5.12 Peak knee flexion during the loading phase of stance on the paretic/AFO side during level treadmill walking for each orthotic ankle joint condition.	103
Figure 5.13 Inter-limb symmetry (SR) for peak knee flexion during level treadmill walking for each orthotic ankle joint condition.	104
Figure 5.14 Peak hip flexion during stance on the paretic/AFO side during level treadmill walking for each orthotic ankle joint condition.	105
Figure 5.15 Inter-limb symmetry (SR) for peak hip flexion during level treadmill walking for each orthotic ankle joint condition	105
Figure 5.16 Ankle, knee, and hip moments for post-stroke subjects – a) Subject P2, and b) Subject P3, during level overground walking	108
Figure 5.17 Peak knee extension moment during stance for subjects P2 and P3 during overground walking for all ankle joint conditions.....	109
Figure 5.18 Inter-limb symmetry in peak knee extension moment during overground walking for each orthotic ankle joint condition for subjects P2 and P3.	110

Figure 5.19 Peak hip extension moment during stance for subjects P2 and P3 during overground walking for all ankle joint conditions.....	110
Figure 5.20 Inter-limb symmetry in peak hip extension during overground walking for each orthotic ankle joint condition for subjects P2 and P3.....	111
Figure A.1 Cam design with spring-loaded pin and unique cam shape.....	167
Figure A.2 Locking discs design.	168
Figure A.3 Initial prototype design sketch of linear spring system.	169
Figure C.1 Fugl-Meyer Assessment for the lower extremities [10].	172
Figure C.2a-b Berg Balance Test assessment of fall risk	173
Figure C.4 Subject perception survey results.	175
Figure D.1 Ankle (left), knee (middle), and hip (right) angle time series for the paretic/AFO side of able-bodied subjects during level walking.....	180
Figure D.2 Ankle (left), knee (middle), and hip (right) angle time series for the paretic/AFO side of able-bodied subjects during inclined walking.....	181
Figure D.3 Ankle (left), knee (middle), and hip (right) angle time series for the paretic/AFO side of able-bodied subjects during declined walking.	182
Figure D.4 Ankle, knee, and hip moments for the paretic/AFO side of control subjects walking over level ground..	184
Figure D.5 Ankle (left), knee (middle), and hip (right) angle time series for the paretic/AFO side of post-stroke subjects for inclined treadmill walking.	185
Figure D.6 Ankle (left), knee (middle), and hip (right) angle time series for the paretic/AFO side of post-stroke subjects for declined treadmill walking.....	186

LIST OF ACRONYMS

3D	Three-dimensional
2D	Two-dimensional
AB	Able-bodied
ADR	Adjustable Dynamic Response
AFO	Ankle Foot Orthosis
AHP	Analytic Hierarchy Process
CoR	Center of Rotation
CNC	Computer Numerical Control
DA-DS	Dorsi Assist – Dorsi Stop
DACS	Dorsiflexion Assist AFO Controlled by a Spring
DF	Dorsiflexion
EMG	Electromyography
FES	Functional Electrical Stimulation
FMEA	Failure Modes and Effects Analysis
GC	Gait Cycle
GCS	Global Coordinate System
GRF	Ground Reaction Force
HPL	Human Performance Lab
HS	Heel Strike
IA	Interlimb Asymmetry
IC	Initial Contact
LCS	Local Coordinate System
LHS	Left Heel Strike
LTO	Left Toe Off
MR	Magnetorheological
PF	Plantarflexion
PS	Plantarflexion Stop
RHS	Right Heel Strike

ROM	Range of Motion
RTO	Right Toe Off
SM	Speed Matched
SS	Self-Selected
TO	Toe Off

1 INTRODUCTION

Stroke is a major cause of disability worldwide, ranking fifth among causes of death and affecting 800,000 people every year [1]. The population of individuals who survive the initial stroke event often exhibit physical and cognitive impairments (paralysis, muscle weakness, speech, aphasia, and memory challenges). The primary goals of caregivers and patients during post stroke rehabilitation are the recovery of natural walking ability and increased independence [2]. To facilitate these goals, physicians and physical therapists commonly prescribe orthoses, also known as braces, to help correct gait deficits [3].

Patients who experience hemiplegia (lower extremity weakness or paralysis on one side of the body) after a stroke commonly exhibit drop-foot. Drop-foot is characterized by an inability to lift the foot (ankle dorsiflexion) during walking, causing the toes to drag or scuff on the ground thereby increasing fall risk [4]. The ankle foot orthosis (AFO) is a brace specifically designed to maintain ankle position to limit drop-foot; AFOs are commonly prescribed to individuals post stroke with impaired mobility [5].

An efficacious AFO selectively controls deleterious movements (dorsiflexion, plantar flexion, inversion, and eversion) without compromising healthy joint mechanics to provide stability [6]. However, many AFOs introduce additional gait pathologies during ambulation over level ground and complex terrain [7]. There is a need to explore

alternative AFO designs to minimize the effects of drop-foot gait and adverse biomechanics introduced by overly constrained orthotic designs.

The three purposes to this study were to: 1) design and construct a novel ankle joint for an AFO to treat drop-foot, 2) conduct gait analyses for able bodied subjects wearing this orthotic design to determine critical design features and refine testing protocols and 3) to perform additional human subject trials involving post stroke subjects, contrasting their gait in both a conventional AFO and an AFO incorporating this novel ankle joint, to confirm that the novel joint limits drop-foot while reducing gait pathologies and increasing kinematic symmetry. The specific research questions investigated were:

- 1) Does the novel ankle joint, integrated in a thermoplastic AFO, limit drop-foot in post stroke subjects?
- 2) Are kinematic and kinetic symmetry improved for the novel ankle joint design compared to a conventional model?
- 3) Does the enhanced ankle motion permitted by the novel ankle joint reduce gait compensation strategies (e.g., disparity in stride and step length, gait cycle timing, and knee flexion between the paretic and unaffected limbs) and improve ambulation over complex terrain?
- 4) Does the increased mobility permitted by the novel ankle joint support ambulation with greater ease (as perceived by questionnaire) than with a conventional orthosis?

These questions were addressed using 3D gait analysis to analyze bilateral lower extremity kinematics and kinetics in the sagittal plane while walking. Spatial and

temporal parameters (velocity, step length, stance time) were also evaluated to characterize the gait of able-bodied subjects and post-stroke individuals with drop-foot, contrasting the various measures for the novel and conventional orthotic ankle joints. The specific research hypotheses tested were:

- 1) The novel ankle joint improves walking speed, stance duration, and step length over a conventional ankle joint for post-stroke individuals with drop-foot.
- 2) The novel ankle joint reduces ankle plantarflexion (e.g., drop-foot) as well as a conventional ankle joint.
- 3) Ankle range of motion during stance improves during ambulation using the novel ankle joint compared to the AFO with conventional ankle joint.
- 4) The novel ankle joint reduces compensatory gait pathologies (e.g., increased hip and knee flexion during the loading phase of stance) introduced by conventional ankle joints incorporated in thermoplastic AFOs.
- 5) The novel ankle joint improves lower extremity spatiotemporal, kinematic, and kinetic interlimb symmetry relative to a conventional ankle joint.
- 6) Perceived exertion is reduced (e.g., increased ease of ambulation), comfort and walking performance are increased with the novel ankle joint design during inclined, neutral, and declined walking.

This investigation will provide clinicians and researchers with quantitative gait analysis data relevant to improved prescription of AFOs for post stroke individuals. These data will also advance the design of orthotic ankle joints for individuals with drop-foot; these designs may also affect the future design of AFOs for alternative populations with mobility impairments.

2 LITERATURE REVIEW

As noted in Chapter 1, the purpose of this study was to design, construct, and test a novel ankle joint for an AFO to limit drop-foot in post-stroke subjects, thereby resulting in reduced gait pathologies and increased kinematic symmetry. This literature review therefore summarizes the causes and incidence of stroke and drop-foot, gait biomechanics of able-bodied (able-bodied) and individuals with drop-foot, and specific AFO designs prescribed to treat drop-foot.

2.1 STROKE

Despite numerous medical and technological advances in the prevention of cerebrovascular accidents, a stroke occurs every 40 seconds in the U.S. and is still considered one of the leading causes of death in the world [8]. There are approximately 800,000 new or recurring cases of stroke in the U.S. per year [1]; of those that survive the event, 50% experience hemiparesis and 30% are unable to walk without assistance [8]. The cost of stroke, both in terms of medical expenses and decreased quality of life, makes it a serious cause of disability in the U.S.

A stroke results in neurological deficits caused by either an obstruction of blood vessels (ischemic stroke) or collection of blood in the brain (hemorrhagic stroke) that induces injury to the central nervous system [9]. Strokes can be treated soon after onset using a tissue plasminogen activator to dissolve blood clots in ischemic strokes; surgical intervention may be performed to stop bleeding in hemorrhagic strokes. The severity of

effects post-stroke depend on the affected location of the brain and time elapsed before medical treatment, but generally survivors exhibit both physical and cognitive impairments [9]. Physical effects include spasticity, weakened muscles, and gait asymmetry which can be targeted in rehabilitation incorporating physical therapy and assistive devices such as AFOs.

The severity of physical impairment following stroke is often assessed using the Fugl-Meyer Assessment and Berg Balance Scale. The Fugl-Meyer Assessment tests five deficit areas commonly observed for both the lower and upper extremities in individuals post-stroke: balance, motor function, joint range of motion (ROM), pain, and sensation [10]. Evaluated items are scored from 0-2 (0 = incomplete task, 1 = partially completed task, 2 = fully completed task). The Berg Balance Scale includes mobility based tests to assess balance impairment in elderly and other individuals, including the post-stroke population [11]. These tasks include standing, sitting, and transfers which are timed and scored from 0-4 based on level of completion (0 = incomplete task, 1= partially completed task with assistance, 2 = partially completed task with supervision, 3=partially completed task with time penalty, 4= fully completed task).

Physicians and physical therapists use these assessments to determine the best rehabilitation program for their post-stroke patients and document the effectiveness of treatment interventions (e.g., pre- versus post-treatment assessment). The primary goal of physical rehabilitation for both patients and caregivers is the recovery of normal walking ability [2]. To further goal progress, the selected treatment program can include strengthening exercises, improving motor coordination, and use of an assistive device.

Assistive devices commonly used to aid stroke patients include canes, crutches, walkers, and lower limb orthoses.

2.2 GAIT

As the goal of rehabilitation programs for individuals post-stroke is to regain normal walking ability, an understanding of able-bodied gait is required. Walking can be contrasted for able-bodied population and the post-stroke population to assist AFO design, prescription, and functional outcomes with orthotic use. As the purpose of this study was to design, construct, and test a novel ankle joint for incorporation in an AFO to aid persons with drop foot, only the biomechanics of the ankle and the knee joint are presented.

2.2.1 *Able-Bodied Gait*

Human locomotion is typically characterized as a series of repetitive motions that form a cycle. One full cycle of walking can be described as time spent in stance (contact with the ground) and swing (free motion through the air). There are eight phases of the gait cycle (GC): initial contact (IC), loading response, mid stance, terminal stance, pre-swing, initial swing, mid swing, and terminal swing (Figure 2.1). The phases of primary relevance to individuals with drop-foot are IC, loading response, and initial-mid swing, as well ankle mobility during mid-stance.

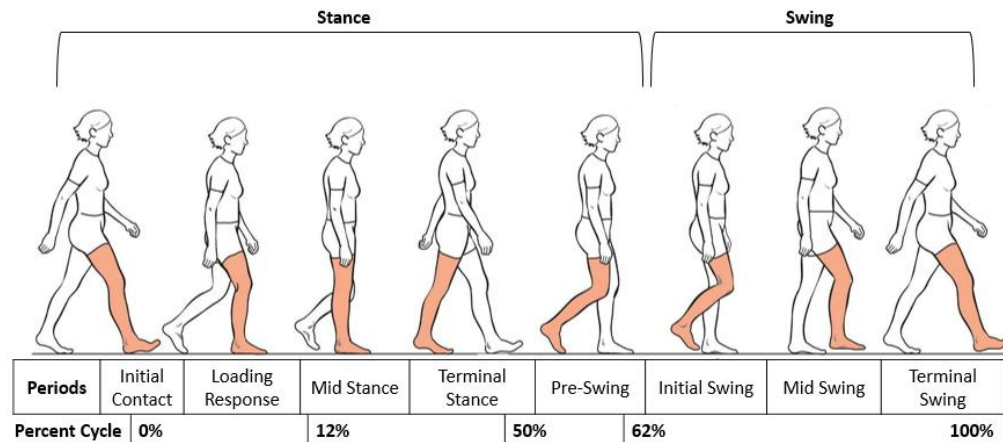


Figure 2.1 Stance and swing periods of the GC (adapted from [12]).

The first 2% of the GC is IC when the foot first strikes the floor. Typically, the heel is first structure to contact the floor, but this can change depending on the subject's velocity and ankle mobility. The function of this phase is to decelerate the limb and prepare for load acceptance; the ankle dorsiflexors (tibialis anterior) control the lowering of the foot to prevent it from slapping the ground [13]. The next phase is the loading response, which continues until contralateral foot off (2-12% GC). Momentum for forward progression is obtained as the tibia rotates about the heel and the ankle begins to dorsiflex (e.g., first rocker). As described by Perry, mid stance occurs from 12-31% GC, until the center of mass is positioned directly over the planted foot. The knee reaches maximum flexion during this stage, and the ankle is maximally dorsiflexed (Section 2.2.1.2). Terminal stance (31-50% GC) begins when the stance heel lifts off the ground and continues until contralateral foot contact.

After stance, the body enters pre-swing (50-62% GC) during which weight is transferred to the contralateral limb. The ankle is now in peak plantarflexion (PF);

plantarflexor muscle activity provides active push off to launch the limb into swing. Initial swing continues from 62-75% GC; foot clearance is achieved as the dorsiflexors activate to oppose gravity and the corresponding passive ankle plantarflexion. This dorsiflexion (DF) activity persists until the beginning of terminal swing (87% GC). Terminal swing closes out the gait cycle (87-100% GC); the ankle is now in a neutral position to prepare for IC of the heel with the ground for the subsequent GC.

2.2.1.1 Temporal and Spatial Parameters of Gait

Temporal (timing) and spatial (position) parameters are commonly used to evaluate and compare events in the GC [4], [13], [14]. Temporal parameters quantify the duration of the various phases in gait (Figure 2.2). The majority of time is spent in stance (60% versus 40% swing) during able-bodied walking; the relative duration of stance/swing varies with velocity [14]. The GC includes periods of single support (one limb in contact with the ground) and double support (both limbs in contact with the ground). The double support phase includes the loading response and pre-swing phases as load is transferred from one limb to the other; single support encompasses the remaining duration of stance [4].

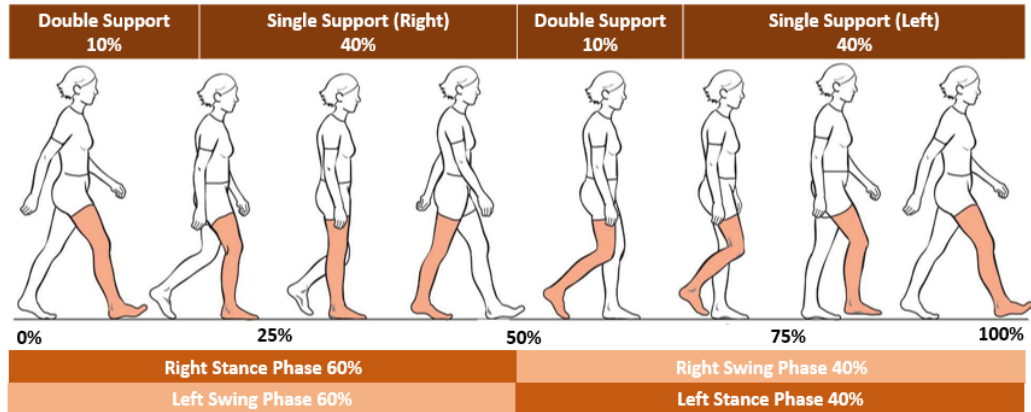


Figure 2.2 Stance and swing phase durations of the GC for both limbs, defining periods of single versus double support (adapted from [12]).

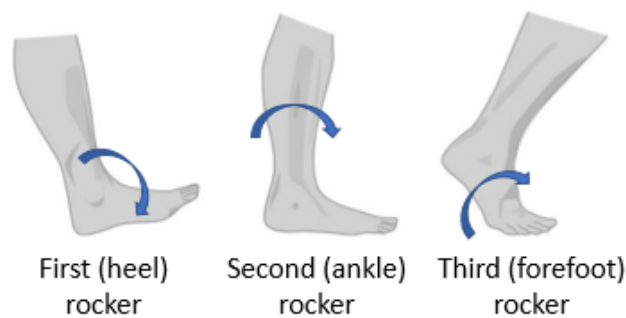


Figure 2.3 Foot and ankle rockers during gait (adapted from [15]).

Stance can also be studied in terms of three different rockers (Figure 2.3) [16]. The first rocker (IC through foot flat) during which the foot rotates about the heel. Subsequently, the tibia rotates about the ankle, defining the second rocker. Finally, the third rocker occurs during terminal stance, from pre-swing to toe off, as the mid- and hind-foot rotates about the metatarsal heads of the forefoot.

The primary spatial parameters used to characterize gait include velocity, cadence, stride length, and step length. Velocity is the speed of gait in the direction of

progression (distance/unit time) [14]. Cadence is defined as the number of steps that occur within a unit of time (e.g., steps/min). Stride length is the distance traveled between two successive ICs on the same foot (e.g., right heel strike to right heel strike). In contrast, step length measures the distance between heel contact of the ipsilateral to contralateral foot. Table 2.1 summarizes these spatial parameters for able-bodied men and women at their self-selected walking speed.

Table 2.1 Spatial parameters for able-bodied men and women greater than 40 years of age [17].

Age (years)		Velocity (m/s)	Cadence (steps/min)	Step Length (cm)
40-49	Male	1.328	120.6	64.7
	Female	1.247	129.6	57.1
50-59	Male	1.252	117.6	63.5
	Female	1.105	121.8	53.5
60-69	Male	1.277	117.0	65.0
	Female	1.157	123.6	55.3
70-79	Male	1.182	114.6	61.5
	Female	1.113	121.8	54.2

2.2.1.2 Gait Kinematics

Kinematics are defined as the geometry of motion, typically presented as joint angle time series for the hip, knee, and ankle; time is often normalized to percent GC. These angles in turn describe the orientation of the lower limb body segments. For able-bodied individuals, motion occurs primarily in the sagittal plane; therefore, only sagittal plane kinematics are presented. Figure 2.4 illustrates the ankle, knee, and hip angles in the sagittal plane during overground level walking for able-bodied individuals.

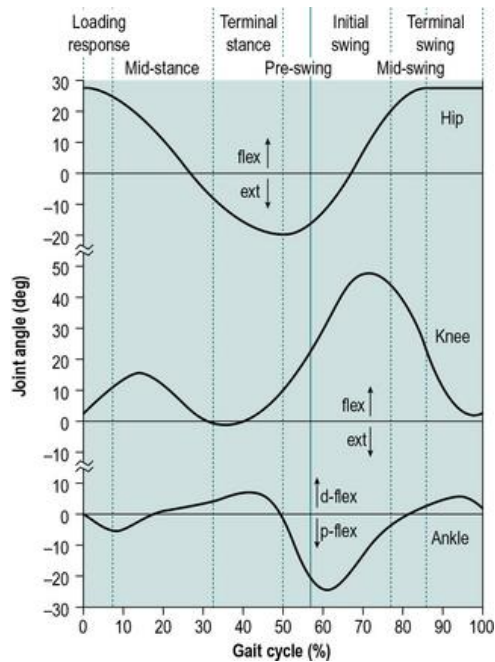


Figure 2.4 Joint (hip, knee and ankle) angle time series for able-bodied adults during level overground walking (adapted from [4]).

Ankle kinematics can be described in terms of four motion segments. From IC through loading response, the ankle transitions from a neutral to a plantarflexed position, as described by the first rocker [13]. During mid- through terminal-stance, the ankle dorsiflexes (second rocker) until pre-swing when it plantarflexes. Throughout swing, the ankle is dorsiflexed to provide foot clearance, returning to a neutral position in preparation for subsequent IC.

The knee undergoes a large ROM during gait, affected by the kinematics of the ankle, momentum, and the ground reaction forces (GRF) to maintain stability. At IC, the knee is slightly flexed and continues to flex until mid-stance, providing shock absorption

during the loading response. At mid-stance, the knee begins to extend; it then flexes again from terminal stance through mid-swing to assist with foot clearance. From mid- through terminal swing, the knee extends to advance the limb and prepare for the subsequent heel strike [14].

The hip goes through two arcs of motion during walking; the hip extends during stance and flexes during swing. Peak flexion of the hip is observed at IC; the hip then progressively extends to a neutral orientation through mid-stance. Peak hip extension occurs at TO; hip flexion then occurs through mid-swing.

2.2.1.3 Gait Kinetics

The study of kinetics refers to the forces (and moments) acting on the body during gait including GRFs to describe the sum of forces acting on all segments of the body through contact with the floor. These GRFs, measured with a force plate, can be used to calculate the respective internal joint forces and moments in concert with the lower limb kinematics via inverse dynamic analysis.

2.2.1.3.1 Joint Moments

The internal joint moments for an able-bodied individual, normalized with respect to body mass, during level overground walking are shown in Figure 2.5 for the ankle, knee, and hip.

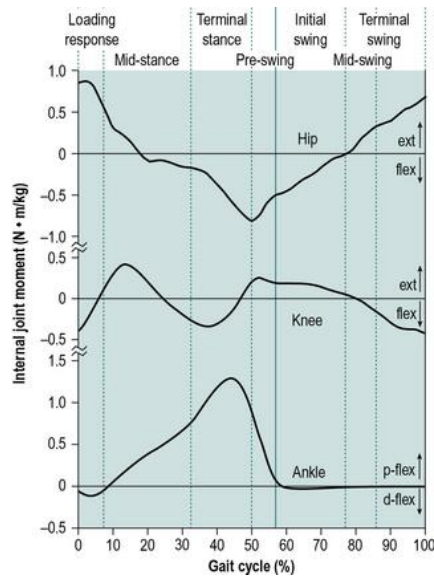


Figure 2.5 Joint (hip, knee, and ankle) moments for an able-bodied individual (adapted from [4]).

The ankle exhibits a small dorsiflexion moment at IC, transitioning to a plantar flexion moment during the loading phase. This internal plantarflexion moment continues until mid-stance; dorsiflexion activity is required to resist this plantarflexion moment and prevent foot slap. As the center of mass advances forward over the foot, the internal plantarflexion moment increases, peaking during terminal stance; concurrent plantarflexor activity provides active push-off. The plantarflexion moment decreases to nearly zero during pre-swing and remains minimal throughout the swing phase.

The knee moment time series during level overground walking is bi-phasic, characterized by two periods of extension and flexion. At IC, the internal flexion moment is observed at the knee and serves to decelerate the body and prevent knee hyperextension. The knee flexion moment then decreases and transitions to an internal extension moment during the loading and mid-stance phases of GC, ensuring stability in the joint. A peak internal knee extension moment occurs during early to mid-stance,

followed by an interval of internal knee flexion moment. A second internal knee extension moment duration is then observed from terminal stance through pre-swing, which controls the rate of knee flexion. During the transition to initial swing, the internal knee extension moment decreases; the knee moment is in flexion from mid- through terminal-swing. This transition to swing allows the muscles of the thigh to control the rate at which the knee extends before preparation for the next HS.

The impact of heel strike forces the hip to respond with a peak in hip extension moment, observed from IC through mid-stance, which continues to balance the increase in GRF during this time. The internal hip moment then transitions to a flexion moment as the hip progresses in front of the body's center of mass; flexion is maintained through weight transition to the contralateral limb and the swing phase. A low-level extension moment is present through swing to control the rate of thigh extension. The hip moment is a critical tool for characterizing compensatory gait strategies for aged or disabled populations, as the hip can compensate for reduced function of the ankle plantarflexor during push-off, causing gait pathologies [18].

2.2.2 *Post-stroke Gait*

After a stroke, individuals often experience weakness or paralysis in the muscles of the lower extremities that cause problems during ambulation. Hemiparesis, or paralysis/weakness on one side of the body following stroke, was found to persist in 50% of ischemic stroke survivors [8]. The most common impairment describing the hemiparetic disability is drop-foot, which results from weakness in the ankle dorsiflexors (Figure 2.6).



Figure 2.6 Drop-foot during swing phase of gait (adapted from [4]).

This unilateral neurological deficit prevents ankle flexion (or dorsiflexion), making it difficult for the subject to lift the toes and provide foot clearance during swing. Drop-foot contributes to a diminished walking velocity, shorter stride and step lengths, as well as temporal, spatial, and kinematic asymmetry between the lower limbs [19][20] [3].

Except for IC, the loading response, and swing phases, the gait of individuals post-stroke with drop-foot resembles that of able-bodied individuals. During IC, untreated drop-foot prevents IC with the heel due to the inability to actively dorsiflex the ankle and counter gravity, thereby causing IC via the forefoot. If some function of the tibialis anterior is retained, initial heel contact may occur; however, the individual is unable activate the dorsiflexors to gradually decelerate the foot during the first rocker, resulting in foot slap. For post stroke individuals with drop-foot, the loading response phase of the unaffected limb is typically lengthened due to decreased stability of the paretic limb [21]. The effects of drop-foot on gait are most apparent during swing phase, drop-foot contributes to foot clearance challenges that require compensatory mechanisms.

Common compensatory strategies have been observed for individuals with drop-foot (no orthotic intervention) characterized by gait deviations relative to able-bodied individuals. Both temporal and spatial asymmetry have been observed. At a basic level, weak ankle dorsiflexors reduce power generation, thereby requiring the paretic hip to perform more work [22]. This compensation can be especially tiring during uphill walking; the paretic limb is unable to provide sufficient distal power, requiring further hip musculature activation to compensate [23]. A specific strategy called steppage is characterized by increased hip and knee flexion, lifting the paretic limb higher to ensure that the foot clears the ground during swing [4], [24]. Many individuals with untreated drop-foot walk more slowly to increase stability during the transition to weight acceptance to and from the paretic limb [25]. Strategies have included prolonged single support stance on the unaffected limb to preserve strength, or altered foot placement relative to the body's midline [26] [27]. In general, the work of the unaffected limb increases to compensate for the weakened paretic limb [28].

2.3 ANKLE FOOT ORTHOSES

Ankle foot orthoses are prescribed to treat various physical impairments due to different causes (trauma, stroke, muscular dystrophy, multiple sclerosis, club foot, etc.) [6]. To be considered a rehabilitative device, lower limb orthoses need to provide at least one of the following four functions: correction of alignment, joint motion assistance/resistance, relief from loading force, or protection against physical impact [29]. AFOs are commonly designed to treat drop-foot due to weakness in the muscles of the lower extremity (tibialis anterior, quadriceps, etc.) post-stroke [5]. In addition to

correcting ankle angle during swing, AFOs can also be designed to contribute to work done at the ankle when facilitating powered push off during mid- to late-stance [30].

AFOs are primarily constructed from metal, plastic (typically polypropylene), or some combination of the two materials (Figure 2.7). Although both plastic and metal AFOs have been used to improve the gait of subjects post-stroke [31], plastic AFOs are most commonly prescribed in the U.S. [32] as polypropylene AFOs are lighter and accommodate more footwear options than custom metal orthoses [29].

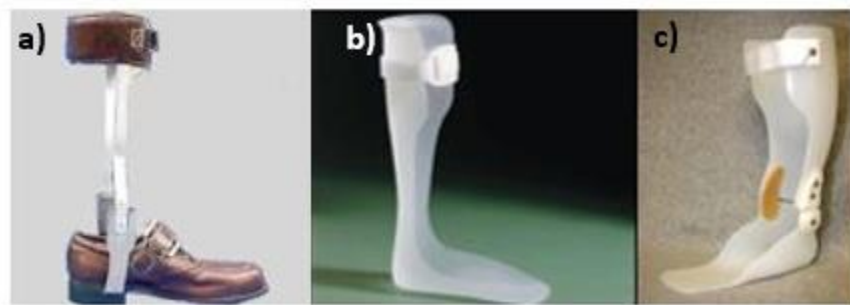


Figure 2.7 AFOs constructed from metal (a) and plastic (b) – solid, nonarticulated; (c) – articulated). (adapted from [33]–[35]).

Orthoses can also be classified in terms of solid versus articulated designs (Figure 2.7). The all-inclusive structure of solid AFOs makes precise fit difficult; errors during fabrication can adversely affect the intended stiffness and support [36]. The lack of an explicit joint near the location of the ankle of a solid AFO prevents both plantarflexion and dorsiflexion unless the model incorporates trimlines which increase ROM but decrease drop-foot prevention. plantarflexion restriction during IC results in the tibia being pulled forward as the foot moves to flat, increasing knee flexion that creates

potential knee instability [3], [32], [37]. Therefore, solid AFOs are contraindicated for patients with weakness of the quadriceps muscles. Additionally, constrained plantarflexion due to solid AFO construction limits powered push off during terminal stance and pre-swing, increasing the metabolic cost due to compensatory gait mechanisms [22]. A subset of solid AFOs are referred to as dynamic, and are constructed from materials with desirable elastic properties to decrease the impact on the body and increase ROM [38].

An articulated, plastic AFO consists of a plastic footplate and shaft, connected by metal or plastic ankle joints. Joint options support a variable range and resistance to motion. These joints can control the ankle to provide dorsiflexion assistance, constrain plantarflexion, allow free dorsiflexion, or some combination of all three [37]. Ankle joints are commonly used in conjunction with a posterior plantarflexion stop, which limits plantarflexion while supporting multiple options for manipulating dorsiflexion (Figure 2.8).

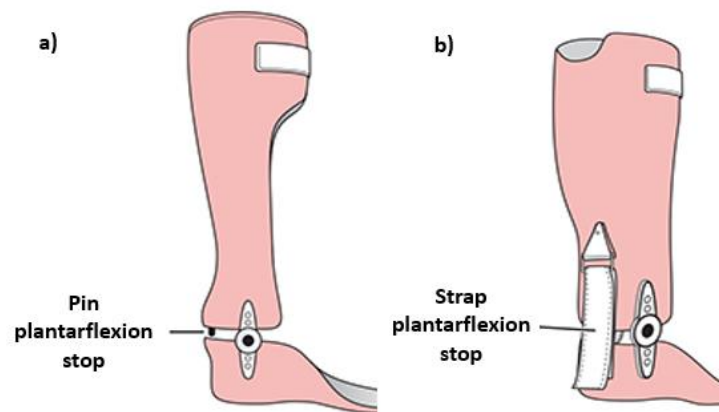






Figure 2.8 Pin (a) and elastic (b) PF stops used to prevent PF motion in thermoplastic, articulated AFOs (adapted from [39]).

Several of the common orthotic ankle joints and their limitations are summarized in Table 2.2.

Table 2.2 Summary of orthotic ankle joints, manufacturers, ROM, and design limitations

AFO Joint	Image	Material	ROM	Limitations
Double action [40]		Stainless steel aluminum	Limited DF and PF	Restricted ROM, inhibits normal movement of the ankle
Gaffney [41]		Stainless steel	Free motion, limited by posterior stop	Dependent on posterior stop
Tamarack [42]		Thermoplastic	DF assist	Easily deformable, stretch limits longevity
Oklahoma [43]		Thermoplastic	Free DF, limited by posterior stop	Dependent on posterior stop

The conventional orthotic ankle joint used in this study to contrast the performance of the novel ankle joint was the double action model manufactured by Becker Orthopedic (Figure 2.9). This joint consists of ball bearings that sit atop the footplate, anterior and posterior channels that run the length of the joint, springs/pins inside the channels, and set screws at the top of the joint to adjust the neutral position and

resistance to dorsi/plantar flexion. The ball bearings provide a smooth rolling motion between the springs (and/or pins) and the footplate during stance. Joint resistance to motion can be tuned by the orthotist by adjusting the set screws, using springs of variable stiffness, or replacing the springs with pins.

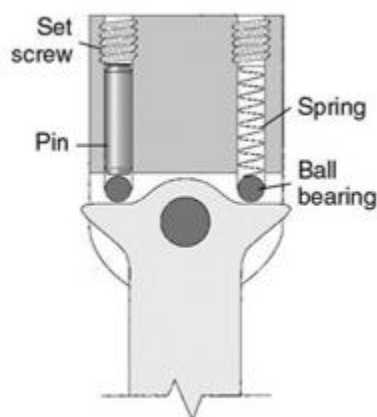


Figure 2.9 Becker double action joint internal mechanism (adapted from [40]).

The primary advantage to this design is its adjustability and ability to support each individual's ankle ROM. The metal material is less prone to elongation under load, a common limitation of thermoplastic joints that can make a brace ineffective or contribute to failure modes [44]. Additionally, the option to lock the ankle at a specific ROM, restrict plantarflexion, or permit dorsiflexion, makes this joint appropriate for many individuals and impairments. The disadvantages of this joint include its larger size and mass (typical of metallic orthotic joints) and ROM constraints.

To address the increased metabolic cost due to plantarflexor weakness and steppage gait of individuals with drop-foot, active, powered AFO designs have been

proposed. Promising options include both the use of magnetorheological (MR) fluid damping and pneumatic artificial muscles [45]–[48] (Figure 2.10).

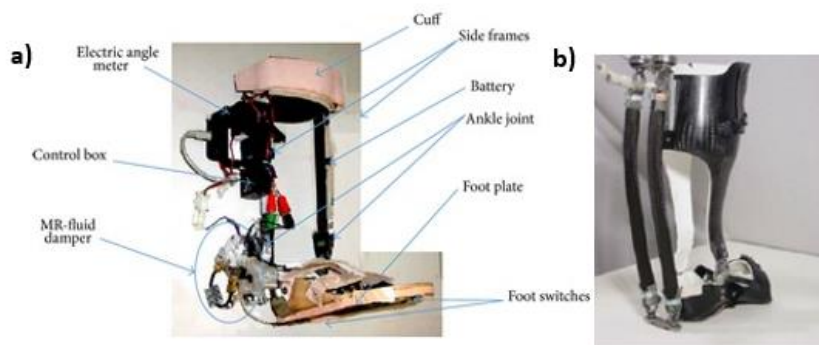


Figure 2.10 MR fluid damping (a) and pneumatic muscle (b) actively powered AFOs (adapted from [45], [47]).

The MR design employs a polypropylene hose that carries MR fluid between cylinder chambers; the proximity of the magnet can be adjusted to change the viscosity of the fluid. This adjustment controls the resistance torque of the cylinder at the ankle joint. The activation of the pneumatic muscle AFO can be controlled via forefoot contact with the ground or electromyographic (EMG) activity of the lower extremity muscles. The artificial muscle is constructed of inflatable material; pressurization produces plantarflexor torque to power movement. These designs provide both powered plantar flexion or push-off during terminal-stance to pre-swing, as well as active ankle dorsiflexion during swing.

These actively powered AFOs, however, have not yet progressed to commercialization as the designs incorporate bulky batteries or remain tethered to

provide power, thereby adversely affecting cosmesis and inhibiting unrestricted ambulation [5]. Regardless, these devices are promising as control algorithms can be tuned on an individual basis during specific gait phases, minimizing potential compensatory gait mechanisms (Figure 2.11). For a post-stroke individual with drop-foot, the adjustable, orthotist-tuned MR damping resulted in ankle kinematics that better approximated that of able-bodied gait (Figure 2.4 and Figure 2.11), outperforming a fixed resistance setting. Both MR damping conditions prevented drop-foot during swing phase. However, only the adjustable damping supported IC with the heel.

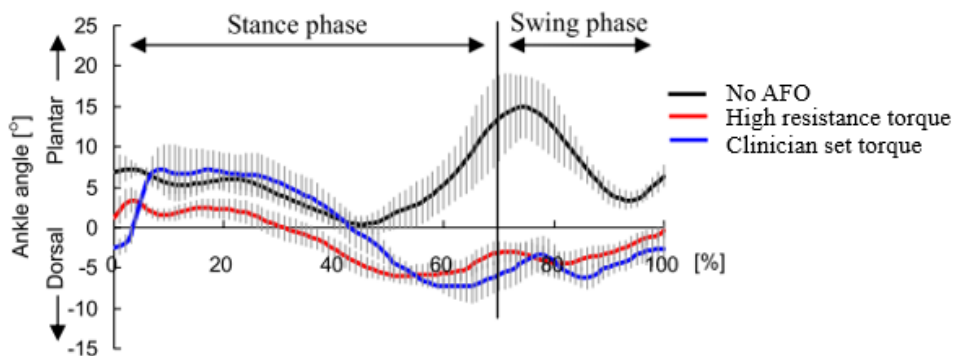


Figure 2.11 Ankle kinematics during level overground walking for a post-stroke subject with drop-foot wearing the MR damped AFO (adapted from [45]).

While these active orthotic systems may provide the ability to better replicate able-bodied gait kinematics with the application of torque, several design limitations must still be addressed. Individuals with drop-foot are reluctant to adopt orthotic designs that are bulky, complex, and with high power needs that are less cosmetic than conventional AFOs.

2.4 AFO TREATMENT OF DROP-FOOT

AFOs are commonly prescribed to enhance gait function in individuals with drop-foot, with many design options available to address specific patient needs. While all AFOs change how the user walks, design variations typically target specific phases of gait. This section describes the impact of these AFO designs (solid, articulated, novel ankle joints) on the gait of post-stroke individuals.

Gait improvement of post-stroke individuals with AFO treatment has been characterized by increased stride and step length, enhanced gait symmetry (temporal, spatial, and kinematic), and increased walking speed [26], [27]. These spatial-temporal parameters are benchmarks of gait performance, affecting both walking speed and aesthetics [49]. The more closely the gait matches that of able-bodied individuals, the greater the individual's satisfaction and independence [38]. The success of solid AFOs in restoring normal gait patterns to individuals with drop-foot has been tempered by a greater understanding of the design limitations restricting existing ankle mobility. While solid AFOs support the foot during swing and prevent drop-foot due to gravity, the restricted ankle motion often adversely affects the stance phase of the gait cycle. This limitation is addressed by use of articulated AFOs incorporating ankle joints.

2.4.1 *Articulated vs. Solid AFOs*

Improvements in ankle ROM, symmetry (temporal, spatial, kinetic, and kinematic), increased stride length, step length of the paretic limb, and increased cadence

have been observed for ambulation with articulated AFOs in comparison to solid AFOs [24], [50]–[53]. Several key studies investigating the effects of articulated orthoses on drop-foot are summarized in Table 2.3.

Table 2.3 Summary of investigations of articulated and solid AFO designs to treat drop-foot post-stroke

Study	Subject Population	Orthosis Type	Parameters of Interest	Key Findings
Kerkum et al., 2015 [54]	11 male, 4 female cerebral palsy (10±2 yrs.)	Solid & Articulated (stiff and flexible)	Kinematics, kinetics	<u>Articulated AFO</u> : Increased ankle angle at IC, decreased knee flexion moment at IC
van Swigchem et al., 2014 [55]	15 male, 4 female post-stroke (55.0 ± 10.1 yrs.)	Solid & Articulated	Kinematics, step length, obstacle avoidance	<u>Solid AFO</u> : Reduced ability to avoid obstacles, greater kinematic pathologies
Tyson et al., 1998 [20]	3 male, 1 female various causes (43.3 ± 16.8 yrs.)	Articulated	Spatiotemporal, symmetry	<u>Articulated AFO</u> : Increased velocity, stride/step length, and spatial symmetry
Singer et al., 2014 [56]	3 male, 2 female post-stroke (62 ± 9 yrs.)	Solid & Articulated	Kinematics, kinetics	<u>Articulated AFO</u> : Increased ankle stiffness, DF moment (1 st rocker), knee extension moment (2 nd rocker)
Romkes & Brunner, 2002 [53]	9 male, 3 female cerebral palsy (11.9 ± 4.9 yrs.)	Dynamic & Articulated	Kinematics, spatiotemporal, power absorption	<u>Articulated AFO</u> : Restore heel first IC, increased stride/step length, reduced knee flexion at IC
Mulroy et al., 2010 [37]	23 male, 7 female post-stroke (58.3 avg. yrs.)	Articulated (2 settings) & Solid	Kinematics, kinetic, spatiotemporal, plantar and dorsiflexor EMG	<u>Articulated AFO</u> : Improved ankle DF in swing & loading response, decreased knee flexion moment at IC
Kobayashi et al., 2015 [50]	8 male, 3 female post-stroke (56 ± 11 yrs.)	Articulated	Kinematics, kinetics	<u>High PF spring stiffness</u> : Decreased ankle & knee joint ROM
Kobayashi et al., 2017 [30]	8 male, 2 female post-stroke (56 ± 11 yrs.)	Articulated	Kinematics, kinetics	<u>S3 & S4 spring levels</u> : IC with heel, knee angle & moment controlled
Lewallen et al., 2010 [57]	10 male, 3 female post-stroke (58±11.98 yrs.)	Solid & Articulated	Velocity, step length, single support time, user satisfaction	<u>Solid AFO</u> : Shorter step length for both limbs, poor user satisfaction
Deng et al., 2016 [38]	1 male post-polio weakness (74 years)	Articulated & ADR (adjustable dynamic response)	Velocity, step length, usage, activity level, user satisfaction	<u>ADR</u> : Improved activity level, velocity, user satisfaction

2.4.1.1 Kinematics

The studies summarized above demonstrate that kinematics are significantly affected by the type of AFO used, with articulated ankle joint designs more closely replicating normal gait. Improved walking ability was demonstrated by enhancing ankle ROM during stance [52], [57], [58], reducing ankle plantarflexion during swing [37], promoting IC at the heel [30], [37], [54], and reducing peak knee flexion at IC to emulate able-bodied walking [19], [53]. During swing, the ankle is slightly dorsiflexed to provide foot clearance, with a neutral orientation at terminal stance to prepare the limb for IC. Ankle angle at IC is an important metric of AFO ankle joint efficacy with heel first contact (not forefoot) attesting to effective drop-foot treatment [58].

As shown in Figure 2.12, ankle ROM improved during the entire gait cycle with an articulated AFO when compared to both the no AFO and solid AFO conditions for a large number of subjects (N=30). The Dorsi Assist/Stop (DA-DS) articulated AFO increased plantarflexion (up to 17°) compared to the solid AFO design, facilitating foot flat after IC and push off during terminal stance. Foot drop was effectively controlled after TO, as no movement beyond -5° was observed, as compared to the shoes only condition (-13°). The ability of an articulated AFO to concurrently control foot alignment and plantarflexion resistance makes it a more efficacious treatment than solid AFOs for individuals post- stroke [36].

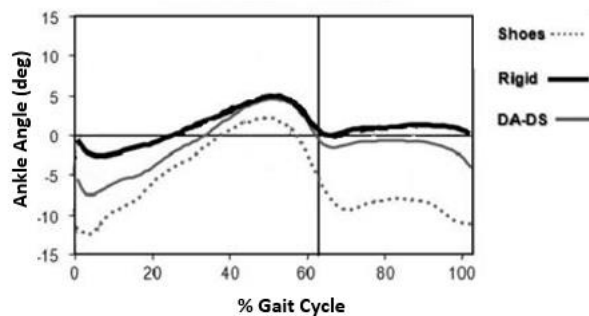


Figure 2.12 Ankle kinematics for individuals during overground walking at self-selected speed in various AFO designs (dotted line - shoes and no AFO, solid black line - solid AFO, solid gray line - DA-DS articulated AFO) (adapted from [37]).

Comparison of a solid dynamic AFO and an articulated AFO on the knee joints for 12 individuals with cerebral palsy walking over level ground demonstrated that an articulated brace controlled peak knee flexion to occur earlier in the stance phase (articulated: 73.3% vs solid: 75.3%; $p < 0.05$), more consistent with that observed for able-bodied individuals [53]. Similarly, a comparative study of the Air-Stirrup (articulated AFO) and a solid AFO on the gait of 15 individuals post-stroke demonstrated reduced peak knee flexion during midstance (articulated: 11.2°, solid: 16.9°) [59].

2.4.1.2 Walking Speed

Increased walking velocity, or the ability to move faster and farther, can improve access to goods and services in the community, improving quality of life [60]. The use of articulated AFO designs to treat drop-foot has consistently demonstrated increased walking speed compared to both no-AFO and solid AFO treatments ([37], [38], [58], [61], [62]; Table 2.4). The increased walking speed likely contributes to higher self-

reported level of satisfaction and increased activity level, all of which are primary goals for recovery after a stroke [38].

Table 2.4 Comparison of walking speed post-stroke individuals ambulating over level ground with various AFO designs.

Walking Speed (m/s)				
	<i>Device Type</i>			
<i>Population</i>	No AFO	Solid	Articulated Dorsi-Assist	Articulated PF Stop
Active DF post stroke (N=9) [37]	-	0.528	0.615	0.647
Limited DF post stroke (N=21) [37]	-	0.375	0.377	0.388
Post-polio (N=1) [38]	0.746	0.778	-	0.816
Spastic hemiplegia (N=15) [58]	1.12	1.21	-	1.23
Post-stroke (N=12) [61]	0.32	0.37	0.41	
Cerebral palsy (N=12) [62]	0.906	0.947	-	0.996

2.4.1.3 Symmetry

Reduced compensatory gait mechanisms with AFO treatment of drop-foot can also be characterized in terms of improved symmetry (or reduced asymmetry).

For unilateral impairments, interlimb asymmetry (IA) may be defined in terms of the IA index for spatial, temporal and kinematic parameters [63]. The IA index for comparison between the limbs of lower extremity amputees is calculated (1).

$$IA = \frac{x_{prosthetic}}{x_{intact}} \quad (\text{Eq 1})$$

where x may refer to step length, stance and swing duration, and specific kinematic parameters between the affected and unaffected limbs. A value of 1.0 indicates symmetry between the limbs and an $IA < 1.0$ indicates the measure for the intact limb exceeded that of the prosthetic limb. For this study, the IA index was modified to produce the symmetry ratio (SR) (2).

$$SR = \frac{x_{affected} - x_{unaffected}}{x_{unaffected}} \cdot 100\% \quad (\text{Eq 2})$$

which characterizes the percent difference in a given parameter between limbs normalized to the unaffected side [64]. A SR of zero represents symmetry; non-zero measures reflect asymmetry (e.g., negative SR values indicate the unaffected limb measure exceeds that for the unaffected side). Temporal parameters were normalized to percent GC and spatial parameters to percent subject height before use in (2). The advantage to this definition is that visualization of asymmetry is enhanced through an understanding that zero is perfect symmetry. The calculation of a percent difference is more intuitive than remembering 1.0 represents symmetry, and any asymmetrical value must be a ratio of that metric.

Step length is contrasted using both SR and IA for individuals post-stroke with hemiplegia for various AFO conditions in Table 2.5. These results indicate that step length symmetry is improved with the articulated AFO; the IA and SR measures are reduced when comparing the solid to the articulated values (IA 1.27 to 1.12 and SR 27.5% to 11.7%). Note that walking speed varied for each AFO condition, contributing to the comparable SR and IA measures for the no AFO and articulated AFO conditions.

Table 2.5 Step length [mean (standard deviation)] and corresponding SR and IA for post-stroke individuals (N=11) for three AFO conditions (no AFO, solid AFO, an articulated AFO) during level overground walking at self-selected speeds. (adapted from [59]).

	Affected Limb Step Length (cm)	Unaffected Limb Step Length (cm)	IA (ratio)	SR (%)
No AFO	29.8 (11.4)	26.4 (11.9)	1.13	12.9
Solid AFO	33.4 (9.8)	26.2 (11.5)	1.27	27.5
Articulated AFO	33.3 (11.2)	29.8 (17.3)	1.12	11.7

Many prior studies have compared temporal and spatial parameters between the no AFO and articulated AFO conditions [22], [65]–[67]. Fewer studies compared such measures between solid and articulated AFOs. Data including double support time, single support time, and step length were contrasted in terms of the SR and IA for two different populations ([68], N=8, post-stroke, solid AFO; [23], N=12, post-trauma, articulated AFOs) in Table 2.6. All the metrics for the solid AFO indicate prolonged loading of the non-paretic limb. The corresponding temporal and spatial symmetry and asymmetry are reflected in the SR and IA measures, respectively. While the population and walking speed differed, greater symmetry was observed with articulated AFO treatment.

Table 2.6 AFO effects on symmetry for solid versus articulated AFOs when walking at self-selected speed: double and single support duration and step length for hemiparetic, post-stroke subjects and post-trauma drop-foot subjects. Aff. is an abbreviation for the affected side, and Unaff. is the unaffected limb.

	Solid AFO [68] (N=8)				Articulated AFO [23] (N=12)			
	Aff.	Unaff.	IA (ratio)	SR (%)	Aff.	Unaff.	IA (ratio)	SR (%)
Double Support Duration (s)	0.45	0.47	0.96	-4.26	0.27	0.27	1.0	0%
Single Support Duration (s)	0.41	0.57	0.72	-28.1	0.56	0.57	0.98	-1.79
Step Length (m)	0.37	0.31	1.19	19.4	0.71	0.72	0.99	-1.39

2.4.1.4 Variable Terrain

While solid AFOs enhance ankle and subtalar joint stability over level terrain, ambulation over uneven terrain and/or over inclines and declines are often challenging with this design [57]; obstacle avoidance (during treadmill ambulation) is also often problematic with solid AFOs. In fact, the use of a solid AFO adversely affected subjects' ability to avoid obstacles relative to the no AFO condition; wearing a solid AFO required more time to re-establish steady gait after perturbation [55]. Uphill walking still poses a significant challenge to post-stroke individuals ambulating with an AFO, as constrained ROM decreases adaptability to terrain variations.

2.4.1.5 Kinetics

In addition to the effects of AFO design on spatial, temporal, and kinematic parameters, the internal joint moments at the knee and hip are also affected. While few studies directly compare the moments at the hip between solid and articulated AFO

designs, there is information about the differences between no AFO and AFO joint moments, and different settings for articulated AFOs.

Post-stroke individuals (N=30) walking over level ground with two different types of AFO (solid and articulated DA-Ds) had larger peak knee extension moments than when compared to shoes only, but the articulated AFO showed a reduction in that peak versus the solid AFO [37] (Figure 2.13). A similar response was seen when changing the spring stiffness in an articulated AFO joint, where a stiffer spring (analogous to a rigid AFO) increased the peak knee extension moments during stance [56]. This effect on the knee was most pronounced for individuals with severely restricted plantarflexion, forcing the tibia to rotate in the sagittal plane to increase knee flexion and produce a balancing knee extension moment.

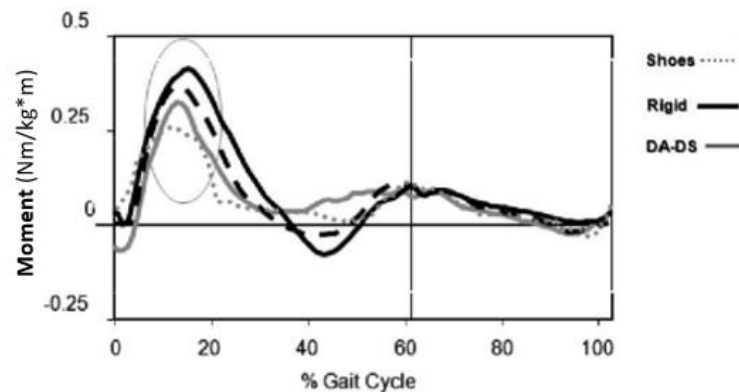


Figure 2.13 Knee extension moment in 30 post stroke subjects ambulating over level ground; dotted gray represents no AFO, solid black represents the solid AFO, and solid gray is the articulated dorsiflexion assist joint. (adapted from [37]).

The same trend is seen at the hip, where Bregman et al. found that 10 post stroke or multiple sclerosis subjects with drop-foot who walked with an AFO had higher peak hip extension moments than able-bodied individuals [22].

2.4.2 *Novel Orthotic Ankle Joint Designs*

Several alternative orthotic ankle joints have been designed to address treatment goals and improve ambulation of individuals with drop-foot. The primary objectives of these devices are to provide support and foot clearance during swing while preserving plantarflexion mobility during IC and free dorsiflexion throughout stance, without adversely affecting active plantarflexion during push off.

Yamamoto et al. designed a dorsiflexion assist AFO controlled by a spring (DACS) [69]. As illustrated in Figure 2.14, this AFO incorporates a spring, piston and slider assembly that link the plastic footplate and shank sections. The compressed spring of the spring/piston/slider assembly helps lift the foot during swing; the spring compresses during stance allowing free ankle motion. Preliminary testing of five individuals with chronic hemiplegia was conducted. The spring stiffness was tuned for each subject; four stiffness configurations were tested over five gait cycles of level overground walking. The self-selected walking speed was increased for three subjects (DACS AFO: 0.65 ± 0.20 ; no AFO: 0.63 ± 0.06 ; solid AFO: 0.60 ± 0.16). The DACS AFO also resulted in reduced knee hyperextension and increased dorsiflexion ROM (Figure 2.15). Despite these promising functional outcomes, the durability of the DACS AFO was questionable. The plastic components of the DACS AFO often deformed beyond acceptable limits. Design refinement is necessary.

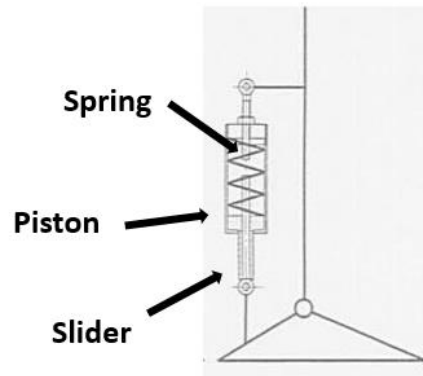


Figure 2.14 DACS AFO design (adapted from [69]).

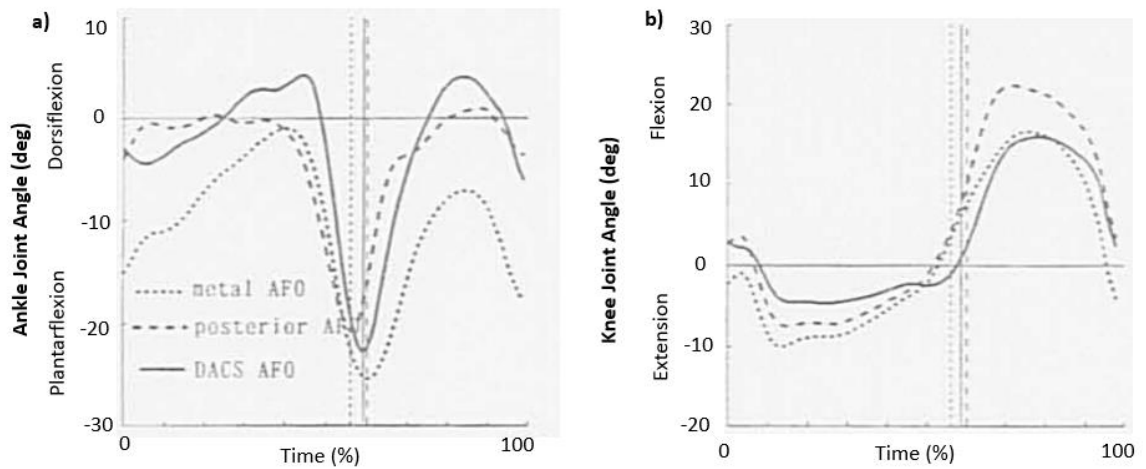


Figure 2.15 Mean ankle (a) and knee angle (b) for five individuals with drop-foot. The dotted line is a metal AFO, dashed is a solid posterior support AFO, and the solid line is the DACS AFO. (adapted from [69]).

The same group also developed an alternative articulated AFO incorporating a hydraulic damper to provide a moment to resist drop-foot during swing (Figure 2.16) [52].

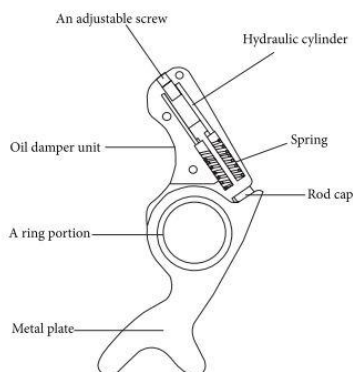


Figure 2.16 Articulated AFO design incorporating a hydraulic ankle damper (adapted from [52]).

The neutral ankle angle of the AFO was adjustable, accommodating individual variations at IC. To investigate the utility of this hydraulic orthotic ankle, kinematic and kinetic data were collected during overground walking for eight post-stroke subjects; comparative trials were conducted with the hydraulic orthotic ankle and the no AFO condition. Trials with the hydraulic AFO were conducted before and after a three-week (20 min/day) acclimation period. Walking speed, step length of the non-paretic limb, and ankle angle at IC all improved with the hydraulic AFO relative to the no AFO condition; further improvements were often noted after acclimation (Table 2.7).

Despite the improved performance in ankle kinematics to the hydraulic ankle AFO with acclimation, knee kinematics were not improved. In particular, the knee angle at IC, peak knee flexion during swing, and peak knee extensor moment during loading response were comparable to values observed for the no AFO. Gait performance relative to conventional AFO treatment was not conducted, nor were trials conducted for a control

group of able-bodied individuals limiting conclusions regarding clinical potential of this design. While some improvements in ankle function were noted, the inability to control the resistive moment of the ankle during plantarflexion was reported as a design limitation.

Table 2.7 Changes in spatiotemporal, kinematic, and kinetic parameters for the three experimental conditions (no AFO, hydraulic AFO pre- and post-training for eight post-stroke individuals [56]).

	w/o AFO Mean (SD)	AFO before Mean (SD)	AFO after Mean (SD)
Walking Speed (m/s)	0.40 (0.18)	0.45 (0.18)	0.56 (0.27) *
Step Length (non-paretic) (m)	0.17 (0.08)	0.20 (0.07)	0.23 (0.08) *
Ankle Angle at IC (°)	-2.08 (3.80)	4.06 (7.77)	4.11 (6.16) *
Knee angle at IC (°)	11.86(8.67)	12.13(6.38)	11.06(5.94)
Peak knee flexion during swing (°)	35.15(14.20)	34.74(12.73)	35.58(12.02)
Knee peak extensor moment (Nm/(kg.m))	0.21(0.11)	0.18(0.11)	0.23(0.13)

* statistically significant; p-value < 0.005; Friedman analysis

While the above novel designs have been tested in the laboratory only, the Triple Action Ankle Joint has progressed from research environment to a commercially available product (Becker Orthopedic). The objective of this design is to provide adjustable plantar and dorsiflexion resistance (Figure 2.17) [36].

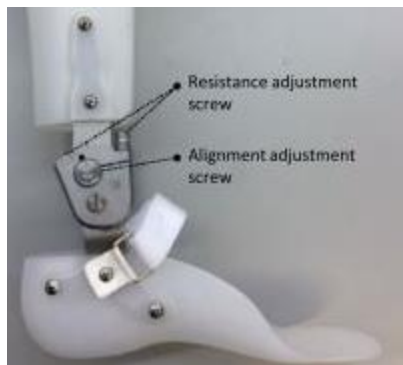


Figure 2.17 Spring adjustable resistance AFO joint from Becker Orthopedics (adapted from [36]).

This orthotic ankle joint incorporates three springs to control ankle resistance; the joint also facilitates neutral alignment modifications. Preliminary testing was conducted for a single post-stroke subject with drop-foot. Twelve combinations of plantarflexion and dorsiflexion resistance levels were tested during level overground walking; additional trials at the subject's self-selected speed (0.36 m/s) were also conducted on an instrumented split belt treadmill. The resultant ankle and knee kinematics of the paretic limb are shown in Figure 2.18 for various resistances. The ankle and knee kinematics were most sensitive to variations in dorsiflexion resistance and ankle alignment, though the plantarflexion resistance joint was able to closely approximate the double-bump shape of the knee joint profile. However, no resistance nor alignment setting resulted in ankle and knee kinematics that matched able-bodied data. The clinician-selected ankle resistance for knee joint stability differed from subject preference; subject preference may have been influenced by training and/or previous AFO usage.

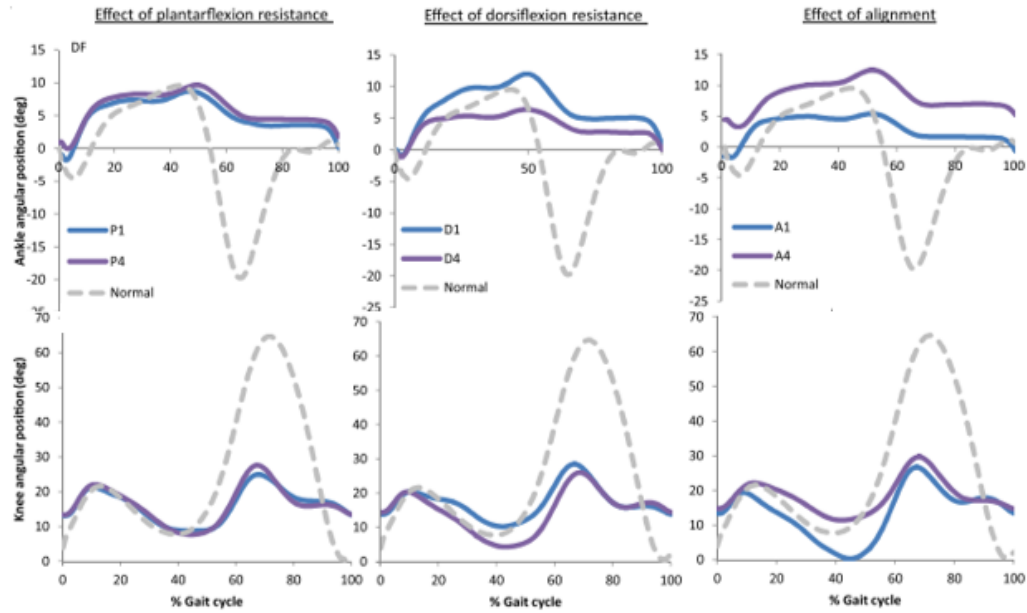


Figure 2.18 Comparison of ankle (top) and the knee (bottom) kinematics for a single post-stroke individual for variations in PF resistance (left), DF resistance (middle), and AFO alignment (right); low resistance setting (blue) and high resistance settings (purple). able-bodied comparative kinematic profiles (dotted line) are also shown. (adapted from [36]).

A final alternative orthotic ankle design, the Dream Brace by ORTHO Inc.

(Japan), incorporated a one-way frictional bearing clutch to control ankle movement [5].

The orthotic ankle includes three different settings for plantarflexion resistance;

dorsiflexion is free (Figure 2.19).

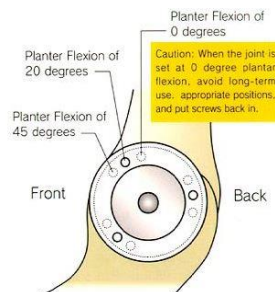


Figure 2.19 Alternative orthotic ankle design with frictional clutch mechanism (adapted from [5]).

To date, clinical assessment of this joint has not been reported; however, the joint is commercially available. Limitations reportedly include fixed plantarflexion resistance, which adversely affects plantarflexion push off during late stance.

2.5 SUMMARY

In summary, AFO use has improved ambulation of individuals post-stroke, demonstrating increased walking speed, improved temporal symmetry, increased stride length, and increased step length of the paretic limb. While both solid and articulated designs demonstrate clinical efficacy, articulated AFOs preserve ankle ROM and decrease knee and hip compensatory strategies and gait pathologies. While alternative articulated AFO designs have been proposed and demonstrate some potential, further orthotic ankle design refinement is needed to treat individuals with drop-foot.

3 DESIGN SELECTION

An overview of the process for ankle joint design selection and prototype fabrication is presented in this chapter.

3.1 DESIGN REQUIREMENTS

The need for a novel orthotic ankle joint was confirmed by a local orthotist, addressing the aforementioned limitations of current articulated AFO designs in during stance for individuals with drop-foot. Conventional AFOs constrain ankle plantarflexion or drop-foot during swing to improve foot clearance; however, this also restricts ankle ROM during stance adversely affecting forward progress (see Chapter 2, section 2.3.1). The desired device should permit ankle motion during stance while constraining ankle motion during swing to prevent drop-foot.

Knowledge of the target post-stroke population combined with the review and analysis of current commercially available joint designs determined important functional requirements to design a more effective joint for incorporation in thermoplastic AFOs to treat drop-foot.

3.1.1 Target Population

The high incidence of stroke leading to drop-foot in the U.S. contributes to the demand for articulated AFOs permitting increased ankle ROM during stance. The anticipated target user of this device is a community ambulator, walking daily without a

walking aid (e.g., cane or walker), assisted solely by an AFO to prevent drop-foot. Users should be able to modestly vary their cadence and speed, increasing the likelihood that an AFO that might restore more natural walking patterns. The weight range accommodated by the novel ankle joint was determined to be 45-114kg, which accommodates 5th percentile women to 90th percentile men in North America [70].

3.1.2 Design Specifications

Consultation with the local orthotist and review of clinical and technical literature, as well as orthotic product documentation for commercially available orthotic ankle joint designs identified several design requirements for clinical adoption,

- 1) Size and weight should be minimized, and at least match current conventional joints (Becker Double Action Ankle Joint, approximate size 5.72cm x 3.81cm x 1.02cm, and 98.7 grams [71]).
- 2) Custom manufacturing should be minimized; the joint should interface with conventional stirrup (e.g., Double Action Y-Stirrup 2810, Becker Orthopedic) and upright for integration with articulated thermoplastic AFOs.
- 3) Joint life must be at least 3 years (e.g., typical AFO lifetime) without total failure.
- 4) Body weight of the user, up to 114kg, must be fully supported by the ankle joint and integrated thermoplastic AFO during ambulation and activities of daily living
- 5) Joint range of motion should accommodate a minimum of 10° plantarflexion and 20° dorsiflexion.

- 6) Joint settings must permit adjustability (e.g., maximum plantarflexion, maximum dorsiflexion, and resistance to plantarflexion and dorsiflexion motion) to accommodate variable user needs and preference.

3.2 CONCEPT GENERATION

A series of potential designs to address the design specifications were developed and evaluated to determine the most promising design option. Design mechanisms included cam and pin, interlocking plates, and a linear spring system (see Appendix A, Figures A.1-A.3). Feasibility was evaluated in terms of device size, weight, manufacturability, ROM, adjustability, jamming risk, durability, and reliability. These factors were weighted in terms of their relative importance using the analytic hierarchy process, AHP, see Table 3.1.

Table 3.1 Analytic hierarchy process to determine weighting of design feasibility criteria for a novel ankle joint

Scale (Row vs Column)	Value	Size	Weight	Manufacturability	ROM	Adjustability	Jamming	Durability	Reliability
Extremely Less Important	1/9		4	3	4	4	1/2	3	1/3
Strongly Less Important	1/5	1/4		1/4	1/6	1	1/5	1/5	1/8
Moderately Less Important	1/3	1/3	4		3	4	1/3	3	1/3
Equal Importance	1	1/4	6	1/3		4	1/4	2	1/7
Moderately More Important	1/3	1/4	1	1/4	1/4		1/7	1/4	1/8
Strongly More Important	1/5	2	5	3	4	7		3	1
Extremely More Important	1/9	1/3	5	1/3	1/2	4	1/3		1/7
		3	8	3	7	8	1	7	

The AHP serves to help assign and weight priorities of the important design mechanisms to allow direct comparisons between difficult descriptors such as “durability” and “reliability”. The end metric, consistency index, describes how

consistent the rankings were assigned to rate one design feature more highly than another. The consistency index was 9.66%, which being less than 10% indicates a general consistency in assigning weighting to each of the design mechanisms [72]. Once the weight of each design requirement was assigned, a decision matrix (Table 3.2) was constructed and evaluated for each of the three design concepts: cam and pin, interlocking plates, and a linear spring system.

Table 3.2 Decision matrix to rate each design concept based on requirement criteria

Importance (1-10)	8	3	7	6	2	8	5	10	39
Relative Weight (%)	14.8%	2.8%	11%	7.9%	2.7%	22.9%	7.2%	30.6%	100%
Design Requirement	Size	Weight	Manufacturability	ROM	Adjustability	Jamming	Durability	Reliability	Score
Cam and Pin	50	70	10	80	40	70	60	60	18
Interlocking Plates	50	50	10	70	60	90	90	80	17
Linear Spring System	90	70	70	50	70	50	70	60	29

The decision matrix analysis identified the linear spring system design as the most feasible, ranking highly in size, manufacturability, and adjustability compared to the alternate designs. The linear spring system design was therefore selected for further development.

3.3 FINAL DESIGN

3.3.1 Novel Ankle Joint Function

The novel orthotic ankle joint function varies between four phases of gait: swing, heel strike, stance, and toe off by switching between locked and unlocked modes. When the joint is not bearing weight during swing (Figure 3.1a), the mechanism is locked by springs and drop-foot is prevented. When the user heel strikes the ground (Figure 3.1b), the force depresses the springs, allowing the CoR to translate $\sim 0.5\text{cm}$. This translation lifts the stirrup away from the tabs that prevented movement during swing, allowing rotation to occur and lower the foot to the ground in a controlled manner. The joint remains unlocked throughout stance (Figure 3.1c), permitting $\sim 25^\circ$ ROM through late stance. Once the user begins unloading the leg to prepare for toe off (Figure 3.1d), the load reduces enough for the spring plungers to extend, locking the stirrup back into place to prevent toe drop through the next swing phase.

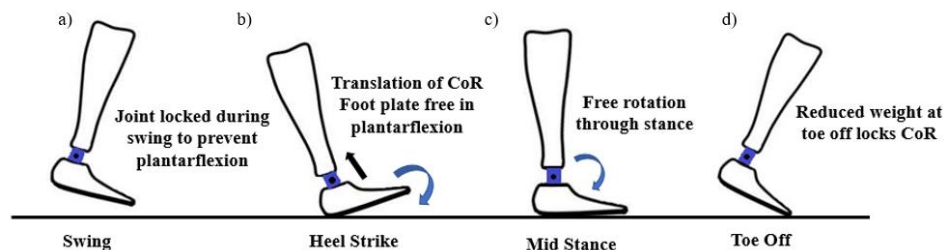


Figure 3.1 Proposed function of the novel ankle joint during four different stages of gait: swing (a), heel strike (b), stance (c), and toe off (d) (adapted from [73]).

3.3.2 AFO-Orthotic Joint Interface

The final joint body was iteratively modified until the design was approved by the collaborating orthotist for testing (Figure 3.2).

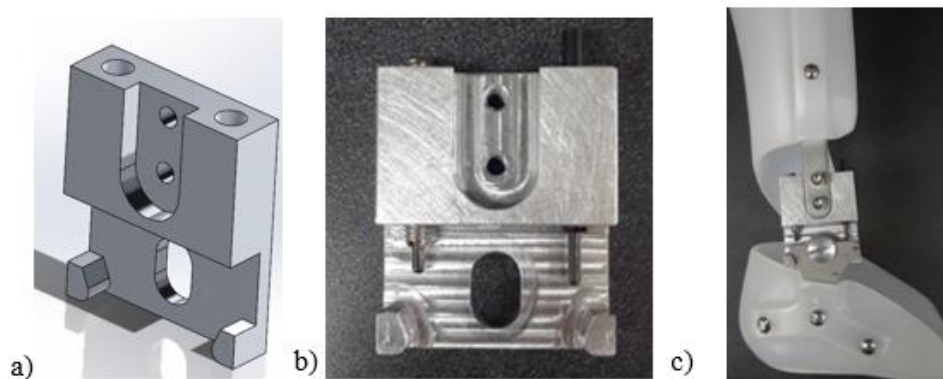


Figure 3.2 Final ankle joint body with SolidWorks isometric view (a), manufactured joint front view (b), and final joint integrated with the AFO (c).

The novel joint connected to the lateral upright bar and stirrup on the lateral ankle of the AFO with upright screws (M5x0.8) and a Chicago bolt (M8) (Figures 3.3-3.4). A Delrin washer was placed between the stirrup and the joint, as well as on the other side of the joint between the joint body and head of the female Chicago bolt. Delrin is very efficient in reducing friction between moving parts [74], enhancing smooth motion and reducing the wear of the joint during use. Two different spring plungers were incorporated in the joint, which allowed the dorsiflexion and plantarflexion stiffness to be

controlled independently. The stiffer spring was placed posteriorly, enabling larger plantarflexion resistance during swing, when drop-foot occurs.

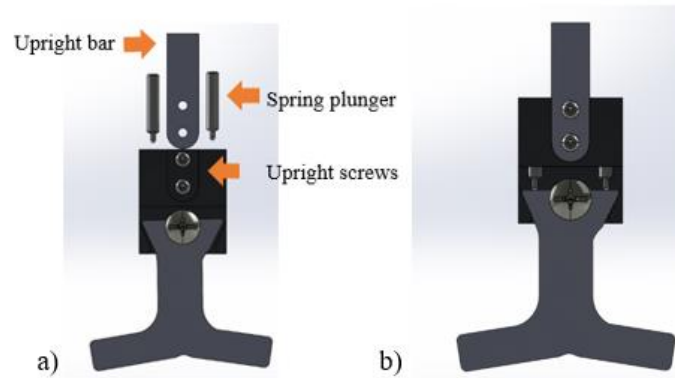


Figure 3.3 Upright bar attachment front view with components exploded (a) and assembled (b).

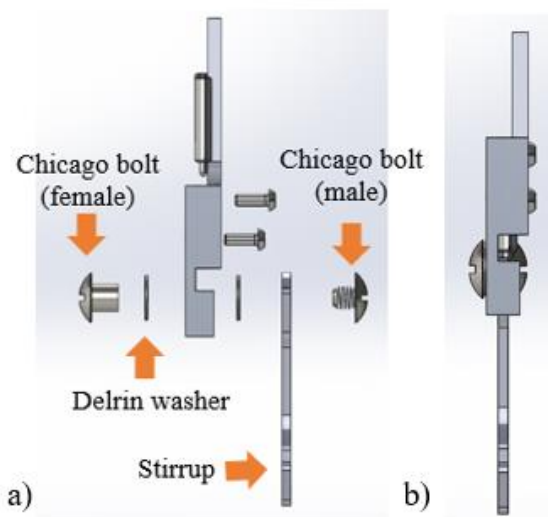


Figure 3.4 Stirrup attachment to joint body using Chicago bolt and washers; side, exploded view (a) and assembled view (b).

The AFO interface for the novel ankle joint was the same as that for the conventional orthotic ankle joint (Becker Orthopedic Double Action Ankle Joint) selected for related comparative functional analysis. The conventional and novel joint were always placed on the lateral ankle side of the AFO, and a free rotation Gaffney joint [75] on the medial side (Figure 3.5) (see Chapter 4, section 4.2 for more details). The articulated ankle joint was placed only on the lateral side of the AFO to prevent potential misalignment of the joint and ankle axis of rotation (personal communication, 6/2018).

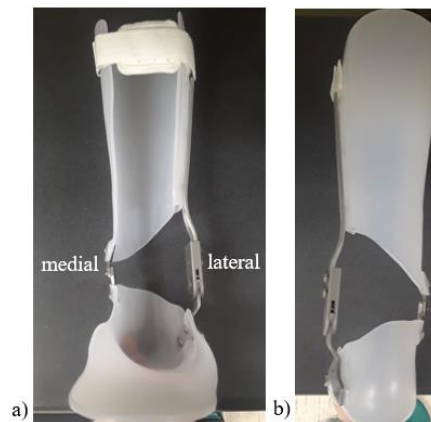


Figure 3.5 Fabricated AFO for the left leg, with a front view (a) and back view (b) displaying the conventional joint on the lateral side of the ankle and a Gaffney joint on the medial side.

In contrast to the conventional Double Action joint that permits only rotational movement, the novel ankle joint incorporates both rotation and a small amount of translation (~0.5cm) at heel strike to disengage the locking mechanism. When initial incorporated, the medial Gaffney joint constrained this translation. A slot was cut into the Gaffney joint, allowing a small amount of translation without bending of the brace

(Figure 3.6-7), to address the kinematic incompatibility between the medial and lateral orthotic joints.

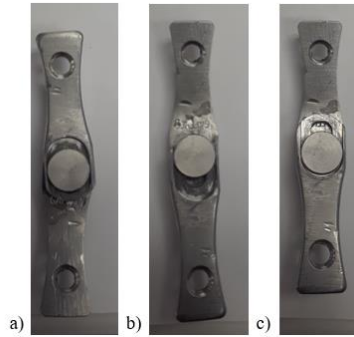


Figure 3.6 Gaffney joint where originally there was only a fixed axis of rotation and no translation (a), and after modification the joint was free to translate upwards (b) and downwards (c) approximately 0.25cm each way.

3.3.3 Bill of Materials

The bill of materials (BOM) specifying the parts used to manufacture and produce the novel orthotic joint prototype are summarized in the Appendix B (Table B.1).

3.4 FAILURE ANALYSES

Physical testing to assess cycle life and fatigue were not conducted. The size and material of the novel joint closely corresponded to that of the commercially available Double Action joint used clinically. Structural failure risk due to normal operational loads was considered minimal and highly unlikely during the limited laboratory testing.

In lieu of destructive physical testing, theoretical analyses were performed to determine the possible failure modes and the components at greatest risk. These analyses guided the subsequent design process.

3.4.1 Failure Modes Analysis

A Failure Modes and Effects Analysis (FMEA) was performed to determine the most likely and catastrophic failures of the novel ankle joint. The FMEA is performed frequently in designing new products, catching reliability problems, ensuring adherence to customer needs, and performing early quality control [76]. The assessment is generally performed as a team, and the components are evaluated to assess both the severity of failure and the probability of occurrence, which are combined as a weighted sum to produce a risk priority number (RPN). The four areas of the joint most likely to fail based on the calculated RPN are summarized in Table 3.3. The full design FMEA can be found in the Appendix B (Table B.2).

Table 3.3 Abbreviated FMEA for the novel ankle joint design, highlighting the four greatest risks to user safety based on rate of occurrence and severity. The component with the highest priority was determined to be the interface bolt.

Feature	Failure Mode	Cause	Severity	Occurrence	RPN
Spring channels	Thin walls: <i>springs pushed out</i>	Design flaw, improper machining	7	3	84
Springs	Too weak: <i>breakage</i>	Improper material selection, large subject	7	4	112
Stirrup interface	Too thin: <i>stirrup jams and scrapes</i>	Improper material selection, design flaw	6	3	90
Chicago bolt	Too weak: <i>shears</i>	Improper material selection, wrong size	7	3	126

The FMEA demonstrated a need to shift load from the primary interface bolt to prevent potential shearing. The original design was modified to move the center slot of the bolt downwards such that at its lowest position, the stirrup rested on the stop tabs promoting load sharing thereby reducing shearing failure risk.

3.4.2 Weakest Link Analysis

The weakest link analysis utilized the modes of failure for all components as identified in the FMEA. Further design refinement was then conducted such that any potential such failures would result in minimal injury to the user; regular AFO inspection might also be conducted and components replaced as needed to ensure joint integrity (Table 3.4).

Table 3.4 Weakest link analysis in the form of a pro/con list for each ankle joint component

Component	Failure Pros	Failure Cons
Stop Tabs	Failure is not catastrophic since the main bolt catches footplate	Not used regularly so failure wouldn't be first unless using inferior materials
		Impossible to replace without remanufacturing
Main Bolt	Easy to replace without re-machining	Catastrophic, causes user to trip or fall
		Expensive to replace
Spring Plungers	Easy to replace and predict wear	Broken springs could be difficult to remove from threaded holes
	Not catastrophic	
Footplate	Easy to predict due to deformation	Damages multiple components on joint body
		Difficult to replace without remaking thermoplastic brace
Upright	Unlikely to damage the joint	Difficult to replace without remaking thermoplastic brace
		Challenging to cause failure first without another component damage
Upright Screws	Easy and cheap to replace	Abrupt and jarring to user

The analysis revealed that damage or failure of the main bolt and/or upright screws are easy and inexpensive to replace; such failures pose potentially high injury risk to the user (e.g., fall). It was determined that the novel ankle joint should fail at either the springs or the stop tabs as such failures are easy to predict, may perhaps be viewed via inspection or simply replaced as regular maintenance with wear use; these failures also correspond to user noninjuries. Even if failure does occur, the ankle joint is still safe to use, as the main bolt will support the weight of user in the event of stop tab fracture and diminished spring function only affects the level of drop-foot prevention. While the user might scuff their toe more than usual, it is a good visual aid to prompt replacement of the springs.

3.5 SUMMARY

The novel ankle joint design was produced to enhance walking function during stance when using an AFO is prescribed and worn to treat drop-foot after a stroke. Three designs were evaluated; the final design incorporated a linear spring system with translation at heel strike to absorb energy and disengage the locking mechanism. Analyses were performed to determine the most likely modes of failure, refining the design to minimize such risk, prior to human subject testing.

4 Methods

The methodology related to data collection and processing to assess the efficacy of the novel orthotic ankle joint for post-stroke individuals is summarized. This methodology includes details regarding subject selection and recruitment, orthotic fabrication, human subject test protocols, data collection, data processing, and statistical analysis to test the respective research hypotheses.

4.1 SUBJECT SELECTION

The research protocol was approved by the Institutional Review Boards at Marquette University and the Medical College of Wisconsin. Two populations were recruited: 1) able-bodied control subjects and 2) individuals post-stroke with drop foot. Control subjects were recruited through word of mouth and recruitment fliers. The specific inclusion criteria for the control subjects were greater than 18 years of age and in good health; the exclusion criterion was any musculoskeletal injury to either lower limb during the past two years that would affect gait. The post-stroke subjects were recruited through the Stroke Subject Recruitment Database of a local physiatrist (J. McGuire, MD). The inclusion criteria for these subjects were at least 6 months post-CVA, unilateral drop-foot, the ability to walk at least 5 minutes without assistance or rest, and regular use of an AFO to ambulate.

Database review was performed by clinical staff. Subjects who met the eligibility criteria and expressed interest in study participation were contacted by clinical staff and

provided consent to be contacted by phone by study personnel. During this call, an in-depth description of the study, eligibility requirements, and procedures were shared. If the individual passed the screening and continued to have interest in participating in the study, AFO fabrication was scheduled.

4.2 AFO FABRICATION AND FITTING

Study participation included three sessions: 1) orthotic casting (1 hour), 2) orthotic fitting (30 min), and 3) gait analysis (90-120 min). The first two sessions were conducted at either the orthotist's office (Hanger Clinic, Milwaukee, WI) or Marquette University; for the control subjects, both sessions were completed at Marquette University. The final test session took place in the Human Performance Laboratory (HPL) at Marquette University.

Prior to casting, written informed consent was obtained after confirming subject eligibility. A brief medical history was solicited from the post-stroke subjects; questions included: date of stroke event, type of AFO used for daily community ambulation, daily walking activity, and the date of the last Botox injection (if applicable).

A certified orthotist cast the lower limb of each subject, wrapping synthetic fiberglass casting material around the lower leg distal to the knee to the toes (Figure 4.1). The right leg was casted for all control subjects; the affected leg was casted for the post-stroke subjects.

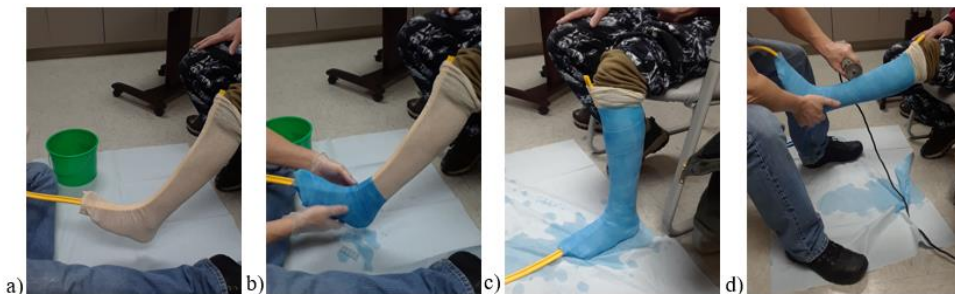


Figure 4.1 Casting of the affected limb for AFO fabrication: a) donned sock with rubber strip to aid cast removal, cast progression from (b) the foot to (c) the shank, and removal of the hardened cast using a saw (d).

After the fiberglass hardened, the cast was cut with a rotating saw and removed. This mold was then filled with plaster to create a positive model of the limb. The upright, stirrup (Becker Orthopedic, 2810 Slim Line Stirrup), and Gaffney joint (Gaffney Technology LLC, Bronco) used to accommodate the addition of an articulated ankle joint were placed over the plaster mold to create voids for orthotic joint placement after vacuum bagging. A 0.8cm thick sheet of medical grade polypropylene thermoplastic (PolyPro) was heated to 350°F (or until the plastic turned clear); it was then draped over the mold and AFO components; finally, the thermoplastic was vacuum formed to the mold. After cooling, the AFO was split at the level of the ankle joint; holes were drilled on the medial ankle to place a Gaffney free motion joint. Similarly, holes were drilled on the lateral ankle side to secure the upright and stirrup. A Double Action Ankle Joint (Becker Orthopedic) was installed between the upright and stirrup, secured to the upright with screws (M5x0.8); the stirrup was secured with a bolt (M8 Chicago). Springs were inserted in the Double Action Joint channels to control dorsiflexion and plantarflexion resistance (see Figure 2.9, Chapter 2, section 2.3). Pins were not employed, preventing

hard stops, similar to the spring plungers of the novel ankle joint. The AFO was then trimmed, sanding rough edges prior to adding straps and padding to facilitate secure, comfortable donning.

During the AFO fitting session, the orthotist modified the AFO shape as needed to maximize comfort. After satisfactory fit was achieved, the subject ambulated (within parallel bars, if needed) with the AFO incorporating the conventional, double-action ankle joint; the orthotist adjusted the set screws to preload the springs in the anterior/posterior channels to adjust plantarflexion resistance as needed to prevent foot drop and toe drag. Subjects were encouraged to walk with a heel strike first strategy. This fitting process was then repeated to configure the novel ankle joint; the spring plungers were exchanged or tightened to provide sufficient resistance to prevent toe drag.

During the AFO fitting session, the general fitness of the post-stroke subjects was assessed via the Fugl-Meyer Assessment (lower extremities only) and Berg Balance Scale (Chapter 2, section 2.1). The Fugl-Meyer Assessment tool characterizes balance, motor function, joint range of motion (ROM), pain, and sensation [10]. Specific tasks include: testing patellar and Achilles tendon reflexes, performing coordinated movements with each leg, assessment of sensation on the lower extremity with eyes closed, and manipulation of ankle, knee, and hip joints with a maximum score of 86 (see Appendix C, Figure C.1). Higher scores reflect less sensory and mobility impairment. The Berg Balance Scale characterizes general balance during a series of timed tests [11]. Tasks include moving from a sit to stand, standing unsupported, retrieving an object from the floor, etc.; the maximum score is 56 (see Appendix C, Figure C.2a-c). Similar to the

Fugl-Meyer Assessment, a higher Berg Balance Scale score is indicative of enhanced function (e.g., reduced impairment).

4.3 GAIT ANALYSIS

With one exception (subject P2), gait analysis inclusive of both overground and treadmill ambulation trials for the two orthotic ankle conditions was conducted during a single session. Data acquired included: bilateral anthropometric measurements, lower limb kinematics, kinetic data, and survey responses.

4.3.1.1 Anthropometry Measurements

Anthropometric measurements including: height, weight (with orthosis), orthosis mass, bilateral length and girth of the lower extremities and limb segments (Table 4.1).

Table 4.1 Description of anthropometric measurements taken during testing.

Measurement (cm)	Landmarks for measurements
ASIS Distance	left and right anterior superior iliac spine (ASIS)
ASIS to lateral malleoli	ipsilateral ASIS to lateral malleoli
Knee width	medial and lateral femoral epicondyles
Ankle width	medial and lateral malleoli
Foot length	first cuneiform and fifth metatarsal
Thigh length	greater trochanter to lateral femoral epicondyle
Thigh proximal circumference	Circumference at just distal to the ischial tuberosity
Thigh distal circumference	Circumference at the distal portion of the limb, superior to the patella

Twenty-nine reflective markers were secured bilaterally with double sided tape; marker locations were based on the Helen Hayes pelvis model [77] (Figure 4.2 and Table 4.2). For the right limb of the control subjects and affected limb of the post-stroke subjects, the lateral and medial ankle marker positions were placed on the AFO over the center of rotation of the medial (Gaffney) and lateral (conventional and novel) orthotic ankle joints (Figure 4.3). Marker placements were recorded in static photographs (anterior and posterior views) in the frontal plane; subject anonymity was maintained (Figure 4.4).

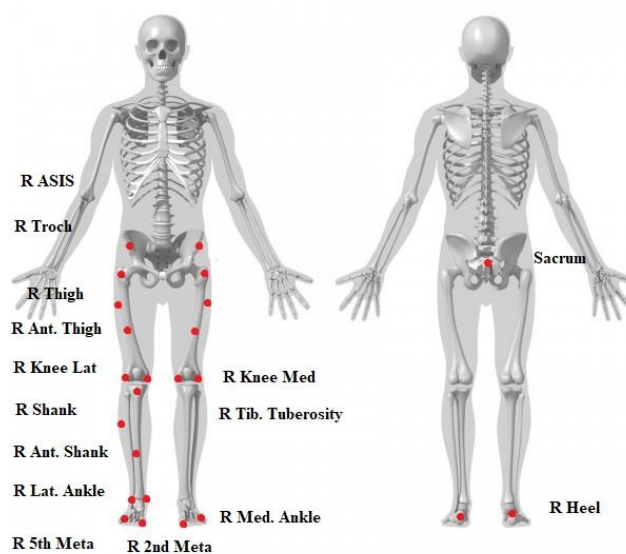


Figure 4.2 Placement of the 29 markers for motion capture and kinematic data.

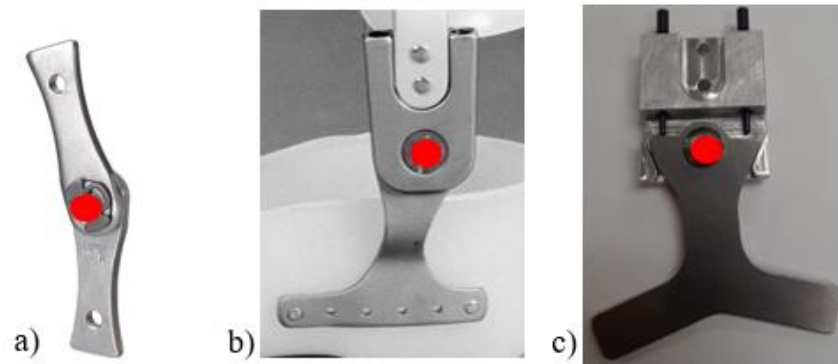


Figure 4.3 Ankle marker position on AFO for the Gaffney joint placed over the medial ankle (a) and lateral ankle joints [standard double action joint (b) and novel joint (c)].



Figure 4.4 Marker placement on an able-bodied subject for gait analysis.

Table 4.2 Marker names and placement descriptions

Region	Marker Name	Description
Unaffected Leg	Sacrum	Sacrum
	R and L Ilium	Iliac crest, posterior
	R and L ASIS	ASIS
	R and L Trochanter	Greater trochanter
	R and L Thigh**	Thigh, lined up with lateral knee and ASIS
	R and L Anterior Thigh**	Thigh, 3" below and anterior to thigh marker
	R and L Lateral Knee	Lateral femoral epicondyle
	R and L Medial Knee	Medial femoral epicondyle
	R and L Tibial Tuberosity	Tibial tuberosity
	R and L Shank**	Shank, in line with lateral knee and ankle at widest
	R and L Anterior Tibia**	Shank, anterior tibia
	R and L Lateral Ankle	Lateral malleolus
	R and L Medial Ankle	Medial malleolus
	R and L 5 th Metatarsal	5 th metatarsal, positioned on shoe
	R and L 2 nd Metatarsal	2 nd metatarsal, positioned on shoe
R and L Heel	Calcaneus, positioned on shoe	
Orthosis	Affected Lateral Ankle	Center of mechanical joint (standard and novel)
	Affected Medial Ankle	Center of Gaffney joint

** used for tracking purposes only

4.3.1.2 Testing Protocol

Gait analyses were conducted for both overground and treadmill walking trials for both orthotic ankle joint conditions. The specific test protocol is summarized in Figure 4.5. With the exception of the final treadmill trial with the novel orthotic ankle joint, all trials were conducted at the subject's self-selected (SS) speed during level walking for the respective joint and interface (overground or treadmill); the SS speed was not altered when inclined or declined. The final trial was conducted at the previously evaluated self-selected walking speed for the conventional AFO, thereby providing speed matched (SM) data.

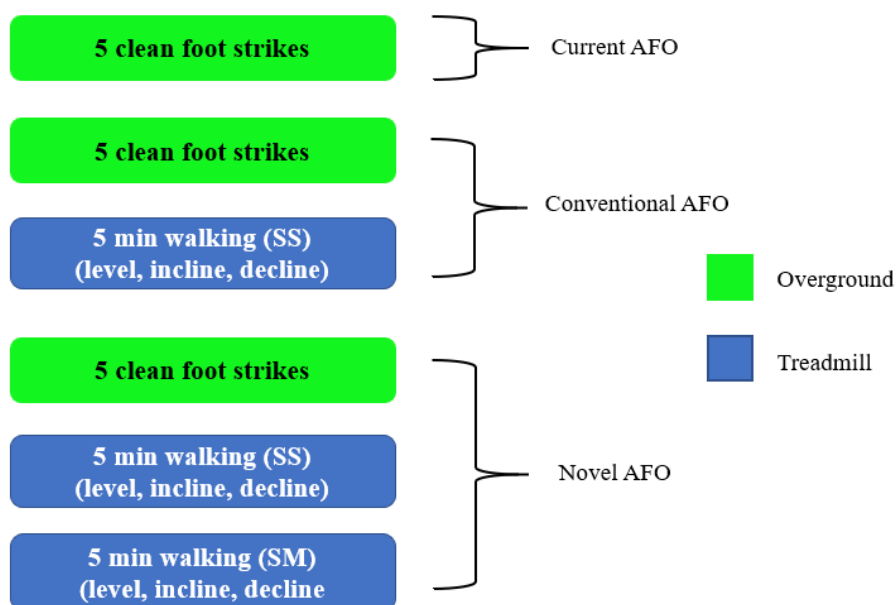


Figure 4.5 Testing protocol for overground and treadmill trials where SS indicates the trial was performed at the subject's self-selected speed; SM refers to the speed matched trial of the novel joint (performed at the self-selected speed for the conventional joint trial).

Kinematic data were collected at 120Hz using a 14 camera OptiTrack motion capture system (Corvalis, OR). Kinetic data were recorded at 1200Hz on the split belt treadmill (vertical force only; Woodway, Waukesha, WI) and force plates (AMTI, Watertown, MA) embedded in the level walkway.

Testing commenced with overground walking; static trials were recorded in the middle of the walkway with the subject positioned such that each foot was on separate force plates. The subjects walked at SS speed over the walkway while kinematic and kinetic data were collected. Trials were repeated until five clean foot strikes were achieved for each testing condition; 10-minute breaks were given between conditions for rest and acclimation to the alternative orthotic ankle joint. A clean foot strike is defined as single foot contact within the force plate area. The current AFO (no AFO for able-bodied subjects) was tested first, followed by the AFO with conventional double action joint until a total of 5 clean trials for each condition were obtained. The two force plates facilitated acquisition of force data for both limbs in a single trial.

Treadmill walking included level, inclined and declined treadmill orientations; the treadmill was mounted on a 6 DOF motion base system (MOOG, Inc., Alma, NY). The subject was secured to the treadmill with a safety harness and familiarized with the emergency stop button; an additional static trial was conducted for calibration. Five-minute walking trials consisting of 8 sec of level walking followed by eight repeated cycles consisting of: 6 sec inclined walking (7% grade), 8 sec level walking, 6 sec declined walking (7% grade), and finally, 14 sec level walking. To facilitate the

automated, programmed changes in grade, the current and anticipated terrain was projected on three large monitors in front of the subject.

For gait analyses of the post-stroke subjects, the treadmill walking protocol was revised to collect shorter trial segments. The single 5-min trial was divided into a 2 min trial, 1 min trial, and second 2 min trial; the inter-trial duration was less than 30 sec.

The AFO was then doffed; the double action ankle joint was removed and replaced with the novel ankle design. The subject then donned the AFO and walked around the laboratory for up to 20 min to acclimate to the novel orthotic ankle joint. Overground walking trials were then repeated to acquire five clean foot strikes for each limb. The subject then returned to the treadmill to complete two trials. These treadmill walking trials again included level, inclined and declined treadmill orientations. The initial trials were conducted at the SS speed for novel orthotic ankle joint condition; a second (SM) trial was conducted at the SS walking speed for the initial, conventional AFO configuration. The subject was blinded to their SS speeds.

Upon completion of all walking trials, each subject completed a survey noting their perceived relative comfort, level of exertion, and walking performance for the two orthotic ankle joint conditions (Appendix C).

4.3.1.3 Metrics of Interest

As noted by the research hypotheses (Chapter 1), the variables used to assess the functional performance of the novel ankle joint include temporal, spatial, kinematic, kinetic, and perception measures (Table 4.3).

Table 4.3 Metrics of Interest (%GC = normalized to gait cycle duration, SR = symmetry ratio, %height = normalized to subject height).

	Measurement	Units
Temporal	velocity	<i>m/s</i>
	stance duration	<i>%GC, SR (%)</i>
Spatial	step length	<i>%height, SR (%)</i>
Kinematic	ankle plantarflexion (during swing, AFO side)	<i>degrees</i>
	ankle ROM for three rockers (during stance)	<i>degrees</i>
	knee flexion (during loading response)	<i>degrees, SR (%)</i>
	hip flexion (during response)	
Kinetic	peak internal knee extension moment (during loading response)	<i>Nm/kg, SR (%)</i>
	peak internal hip extension moment (during loading response)	
Perception	relative comfort relative exertion relative performance	

4.4 KINEMATIC DATA PROCESSING

The kinematic data processing required: 1) conversion of marker data from 2D to 3D, 2) development of subject-specific kinematic models, 3) heel strike and toe off event detection, 4) parsing data into gait cycles and the respective stance and swing periods, and 5) averaging across gait cycles. The ankle joints being tested only attempted to modify gait in the sagittal plane; potential inversion or eversion of the ankle was controlled by the AFO structure which did not vary between orthotic ankle conditions. As

such, the study focused on ankle motion in the sagittal plane. Additionally, as knee and hip motion during gait is greatest in the sagittal plane for able-bodied individuals [50], [53], [59], analysis of hip and knee motion was also restricted to sagittal plane analysis.

4.4.1 2D to 3D Data Conversion

The 2D data from motion capture were converted to 3D using the process detailed in the flowchart illustrated in Figure 4.6. The motion data were recorded as a series of 2D coordinates that corresponded to the location of each marker and were converted to 3D coordinates via Direct Linear Transformation using the ADTech Motion Analysis Software System (AMASS) (Version2.0.0, C-Motion, Germantown MD). The 3D coordinates were reported in terms of the global coordinate system (GCS) shown in Figure 4.7.

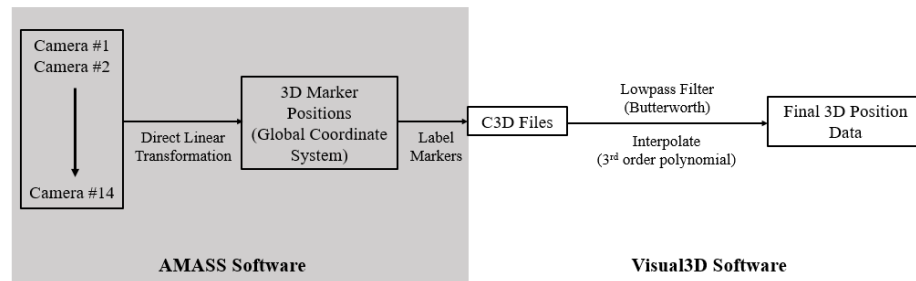


Figure 4.6 Conversion of 2D marker data into 3D motion data using AMASS and Visual3D software.

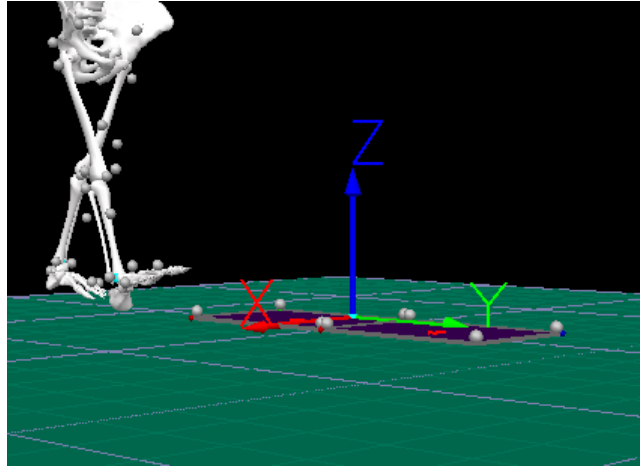


Figure 4.7 Laboratory-based global coordinate system: positive Y-axis is the direction of travel, positive Z-axis is vertical, and positive X-axis is perpendicular to the other two axes according to the right-hand rule.

The marker data for static and dynamic trials from each testing session were further labeled in AMASS to define the anatomical landmarks (Table 4.2); these data were then exported as a C3D file and imported to Visual3D (V6, C-Motion, Germantown, MD). For each marker, the 3D kinematic data were lowpass filtered (Butterworth, cutoff frequency 10Hz) to remove noise [78]. Gaps (less than 20 frames) in marker motion were interpolated using a 3rd order polynomial; polynomial interpolation was based on three frames prior and three frames after the respective frame gap.

4.4.2 Subject Specific Kinematic Models

Specific subject models were created using the C3D file in Visual3D according to the Helen Hayes Pelvis model [77]. Model segments and the corresponding local coordinate systems were defined in terms of the respective segment markers, body landmarks and the anthropometric measurements (Figure 4.8 and Table 4.4).

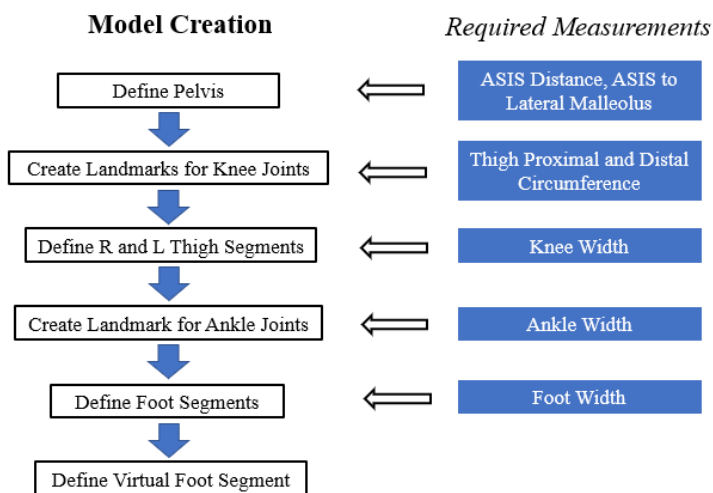


Figure 4.8 Subject specific model creation and requisite segment input data.

Table 4.4 Subject specific models and body segments

Segment	Origin	Landmarks	Markers	Tracking Markers
Pelvis	Midpoint between R and L ASIS	None	R ASIS, L ASIS, Sacrum	R ASIS, L ASIS, Sacrum, R Iliac, L Iliac
Thigh	Hip joint	Hip and knee joint center	Lat Knee, Med knee	Lat Knee, Med Knee, Troch
Shank	Knee joint	Knee and ankle joint center	Lat Knee, Med Knee, Lat Ankle, Med Ankle	Lat Knee, Med Knee, Lat Ankle, Med Ankle, Tib Tuberosity
Foot	Right ankle joint	Lateral and medial ankle, 2 nd meta	Lat Ankle, Med Ankle, 2 nd meta, 5 th meta	Lat Ankle, Med Ankle, Heel, 2 nd Meta, 5 th Meta
Virtual Foot	Midpoint between Lat and Med Ankle	Lat and med ankle, 2 nd meta projections	Lat Ankle, Med Ankle, 2 nd Meta	Lat Ankle, Med Ankle, Heel, 2 nd Meta, 5 th Meta

With the exception of the ankle width inclusive of the AFO, the process for defining the right and left side segments was the same. The local coordinate system, with origin at the proximal joint center, for each body segment also defined the anatomical planes and sign convention for joint motion. For example, the local coordinate system (with origin at the knee center) for the right shank is shown in Figure 4.9; flexion is defined as rotation about the local X'-axis (where positive values represent flexion and negative represent extension). The local coordinate systems are defined relative to the fixed global coordinate system using the static trial marker data.

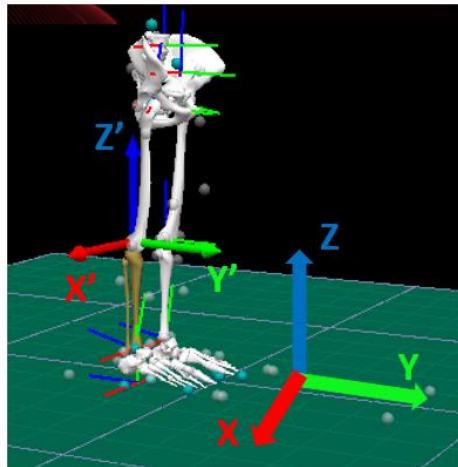


Figure 4.9 Local coordinate system (X' , Y' , Z') with origin at the knee center for the right shank; the global, laboratory-based coordinate system (X , Y , Z) is shown for reference.

The aforementioned local coordinate system for each body segment is defined using vectors connecting the proximal and distal segment endpoints (Figure 4.10 for the hip relative to the knee joint [79]). The superior/inferior axis (\hat{k}), from the distal (shank) segment endpoint (knee) towards, is defined first. The vector (v) between the medial to

lateral landmarks of the distal segment endpoint is then crossed with the \hat{k} vector; this resultant vector, \hat{j} , defines the local anterior/posterior axis, again with origin at the proximal segment endpoint (e.g., hip). Finally, the mediolateral axis (\hat{i}), perpendicular to the superior/inferior and anterior/posterior axes, is calculated as the cross product of \hat{j} and \hat{k} .

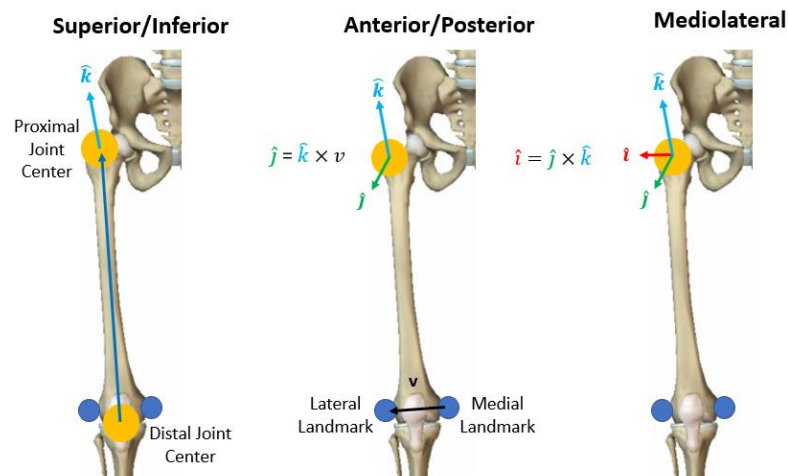


Figure 4.10 Definition of the local coordinate system ($\hat{i}, \hat{j}, \hat{k}$) for the hip joint relative to the knee joint for the thigh segment.

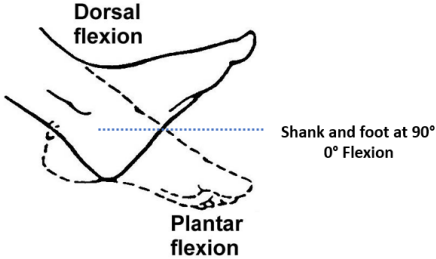
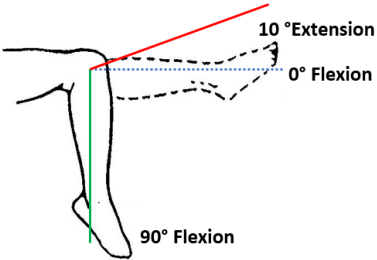
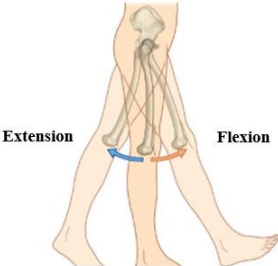
A virtual foot segment was created to enable calculation of ankle joint angles [80]. The virtual foot was defined using the lateral and medial ankle, second and fifth metatarsal, and the heel markers projected onto the floor. With the origin of the segment's local coordinate system at the ankle, the local Y'-axis was parallel to the floor along the length of the foot, the X'-axis was lateral, and the Z'-axis was perpendicular; the corresponding rotations were inversion/eversion, dorsi-/plantarflexion, and

abduction/adduction, respectively. As this virtual segment has no associated mass, it cannot be used to calculate ankle joint moment or power via inverse dynamics.

4.4.3 Lower Extremity Joint Angles

The joint angle time series were computed in Visual3D, based on the segment origin and local coordinate system. In these local coordinate systems, rotation in the sagittal (Y'-Z') plane occurs about the local X'-axis. These lower extremity joint rotation angles are detailed in Table 4.5.

Table 4.5 Sagittal plane joint angles definitions for the ankle, knee, and hip (adapted from [81], [82]).

Joint	Segment	Reference	X'-Axis Rotation	Definition
Ankle	Foot	Shank	Ankle flexion (dorsiflexion) and extension (plantarflexion)	
Knee	Shank	Thigh	Knee flexion and extension	
Hip	Thigh	Pelvis	Hip flexion and extension	

4.4.4 Event Detection

Treadmill heel strike (HS) and toe off (TO) events were initially detected for able-bodied subjects using a custom pipeline in Visual3D. The angle between the calcaneal marker (heel) and pelvis segments was computed for each side to determine HS events;

similarly, the angle between the 2nd metatarsal marker (toe) and pelvis was used to determine TO events [83]. These joint angles were reviewed in the frontal plane.

While this process worked well for the gait trials for the control subjects, errors occurred during analysis of post-stroke subject walking trials (Figure 4.11). The abnormal motion of the paretic limb resulted in both missed events and erroneously identified using the above event detection algorithm. As such, for both populations, HS and TO event detection was manually processed for all motion trials (treadmill and overground). The process included of the heel and toe markers time series, relative to the pelvis, to ensure identification of a single maximum (e.g., HS event) for the heel marker with respect to pelvis angle and a single minimum (e.g., TO event) for the toe with respect to the pelvis angle.

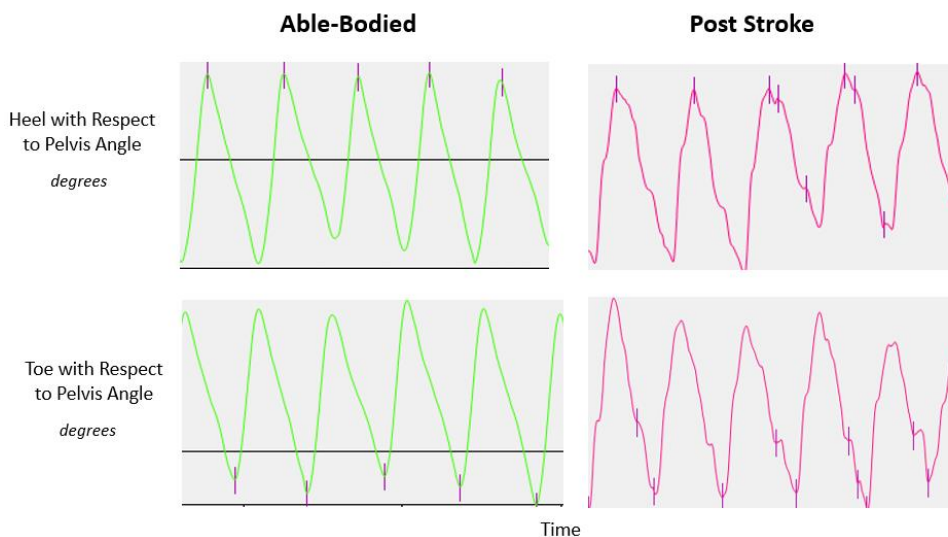


Figure 4.11 Event detection algorithm for able-bodied and post stroke individuals based on kinematic profiles in the frontal plane. The purple vertical bars represent events: HS = maximum heel-pelvis angle, TO = minimum toe-pelvis angle. Note the extraneous events identified for the kinematic profiles for the post-stroke population when this process was automated.

To ensure accuracy and repeatability, the timing of these manually identified events were contrasted with the initial automated event detection process. For the control subjects, peak timing differences between manual and automated identified events never exceeded 7 frames (0.058 seconds).

During overground walking trials, HS and TO events were defined based on vertical force magnitude. Specifically, HS was defined as the time when vertical force exceeded a threshold of 7N to account for noise; TO events were defined as the time when vertical force fell from positive to below the threshold magnitude. Only the gait cycles inclusive of force plate contact were used for subsequent analysis.

The time for each HS and TO event for all gait cycles was exported for future analysis in MATLAB, facilitating data parsing into gait cycles and stance/swing periods.

4.4.5 Data Parsing – Treadmill Walking Trials

The treadmill trials included multiple gait cycles and various treadmill orientations. These data therefore needed to be parsed based on HS and TO events, as well as treadmill orientation. Data parsing was performed using custom MATLAB code (Version 9.2.0.556344 (R2017a), The MathWorks, Inc., Natick, MA). For able-bodied control subjects, treadmill data analysis was limited to the middle 145 sec of the 5-min trial, minimizing potential effects of training and fatigue. For the post-stroke subjects, for whom the 5 min walking trials were acquired in two 2-min and 1-min sub-trials, treadmill data analysis was restricted to the middle 60 sec of the two 2-min trials and the middle 30

sec of the 1-min trial. Treadmill orientations were parsed into level, inclined, and declined data sets by matching the time change of each terrain (see section 4.3.1.2) to the index of the events (e.g., the first 8 seconds of level walking collected at 120Hz corresponded to the data index of 1-960). Each terrain data set was processed separately, with common procedures to calculate the respective output metrics.

The above time segments were refined to start with the first right HS event. Stride cycles for the right leg were defined from the first right HS to the subsequent right HS; left stride cycles were similarly defined (Figure 4.12). The correct progression of events (right HS to left TO to left HS to right TO) was ensured by calculating the cycle duration; cycle durations less than 90% or greater than 110% of the mean cycle duration were re-examined in Visual3D to correct potential missed or extraneous events. The amended data and stride cycles were then sub-divided into stance (ipsilateral HS to TO) and swing (ipsilateral TO to HS) phases.

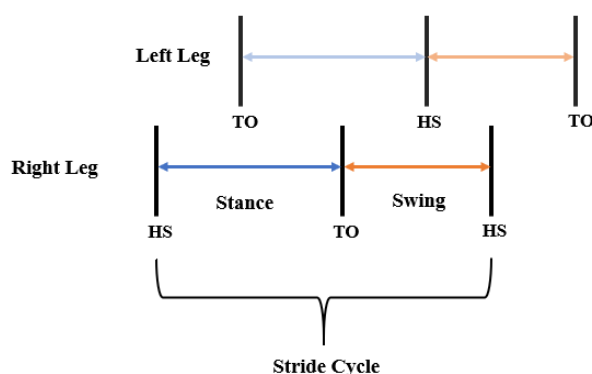


Figure 4.12 Stride cycle for right and left limbs based on HS and TO events; the corresponding stance and swing phases are also shown.

The HS events were also used to calculate the sole spatial parameter investigated in this study: step length, or the distance between the heel contact position at HS of the leading limb to trailing limb (Figure 4.13). For treadmill walking, step length was calculated as the product of the step duration (between successive contralateral HS events) and treadmill speed.

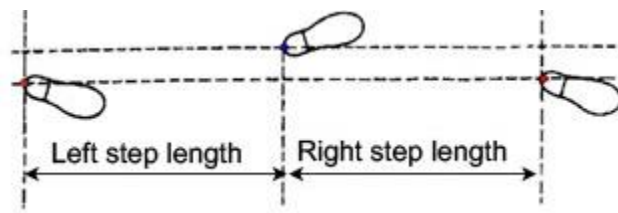


Figure 4.13 Definition of step length (adapted from [84]).

All treadmill metrics of interest were calculated for every gait cycle and averaged across gait cycles for each respective orthotic condition.

4.4.6 Data Parsing – Overground Walking Trials

Overground walking trials consisted solely of steps during which the force plates were contacted. For a given limb, analysis frames were limited to those in which the respective foot was in contact with the plate.

4.4.7 Symmetry

To assess inter-limb symmetry for various gait metrics, the symmetry ratio, SR, was calculated (see Chapter 2, section 2.4.1.3) [63], [64].

$$SR = \frac{x_{AFO} - x_{unaffected}}{x_{unaffected}} \cdot 100\% \quad (\text{Eq 2})$$

In (2), x refers to the specific metric (e.g., step length, stance duration, peak joint angle, joint ROM, peak joint moment), AFO refers to the paretic/AFO side, and $unaffected$ refers to the non-paretic side for post-stroke subject data. A SR value of zero represents inter-limb symmetry; negative SR's indicate that the respective measure for the unaffected limb exceeds that for the AFO side.

4.4.8 Kinetic Data Analysis

The peak extension moments at the knee and hip during stance were calculated as the maximum of the moment about the sagittal plane (global X+ direction). This study defined an extension moment as positive, (see Chapter 2, section 2.2.1.3.2). The corresponding measure of inter-limb symmetry was calculated for each of these metrics for each trial, and then averaged across trials for each orthotic condition.

The internal joint moments at knee and hip were calculated using inverse dynamics modeling, a built-in Visual 3D function that analyzes the synchronously acquired motion and GRF data from overground walking trials in the GCS [85]. The model treats the segments of the lower extremities (foot, shank, and thigh) as rigid linkages, with equal and opposite joint reaction forces and moments at the respective

connections at the joints [86]. In addition to segment kinematics and GRFs, inverse dynamic modeling also requires segment mass and inertial properties. In Visual3D, the lower extremity segments are approximated as a conical frustrum (Figure 4.14); the corresponding geometry is based on related anthropometric measurements [87] to define the proximal and distal radii of the frustrum. The estimated segment inertial properties including segment mass, center of mass location, and moments of inertia are calculated using this geometry, anthropometric measurements, and subject body mass.

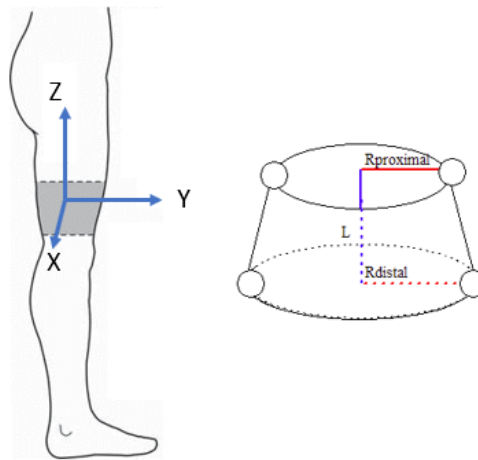


Figure 4.14 Conical frustrum used to approximate lower limb segment geometries in Visual3D for inverse dynamics calculation; R is the proximal and distal radii of the segment, L is the length of the segment and the coordinates shown are in the GCS.

The segment mass is approximated as a fraction of the total body mass [ref], as described by (3).

$$m_s = p_s M \quad (\text{Eq 3})$$

where p_s is the fraction of the segment mass (m_s) relative to total body mass (M). For the lower extremities, p_s is 0.0145, 0.0465, and 0.1 for the foot, shank and thigh, respectively.

The location of the segment center of mass along the segment length, x , is described by (4) and either (5a) or (5b) depending on the segment.

$$x = \frac{R_{proximal}}{R_{distal}} \quad (\text{Eq 4})$$

$$c = 1 - \frac{1+2x+3x^2}{4(1+x+x^2)} \text{ for } R_{proximal} < R_{distal} \quad (\text{Eq 5a})$$

$$c = \frac{1+2x+3x^2}{4(1+x+x^2)} \text{ for } R_{distal} < R_{proximal} \quad (\text{Eq 5b})$$

Relevant geometry includes R , the radius (either proximal or distal) of the segment and c , the distance of the segment center of mass relative to the proximal end of the segment.

Finally, the segment mass moments of inertia are defined in (6) and (7),

$$I_{xx} = I_{yy} = \frac{a_1 a_2 M^2}{\delta L} + b_1 b_2 M L^2 \quad (\text{Eq 6})$$

$$I_{zz} = \frac{2a_1 a_2 M^2}{\delta L} \quad (\text{Eq 7})$$

where I is the moment of inertia, xx defined as the moment of inertia about the X axis, yy about the Y axis, and zz about the Z axis (Figure 4.14). The derivation of a_1 , a_2 , b_1 , b_2 , and δ can found in Appendix C (C.1-5).

Segment analyses are based on free body diagrams of the respective lower limb segments; inverse dynamics modeling begins with the most distal segment, the foot (Figure 4.15), for which the GRFs are known. The foot orientation in the global

coordinate system, the GRFs measured with the force plates, estimated segment mass, center of mass location, and the segment mass moment of inertia are used to compute the reaction forces and moment at the ankle for each frame during stance via equilibrium analysis of forces and moments in the sagittal plane (8-11). The resultant internal moment at the ankle (local coordinate system for foot segment) is converted to the global coordinate system using the corresponding angles and rotation transformation acquired during motion capture calibration.

The reaction forces and moments at the ankle are then applied (equal and opposite) to a free body diagram of the shank segment, facilitating calculation of the knee reaction forces and moments. This procedure is then repeated for the thigh segment to calculate the reaction forces and moments at the hip joint.

These hip and knee moment time series were then reviewed to identify the peak knee and hip moments during stance; these peaks were then averaged across the five trials for each orthotic condition.

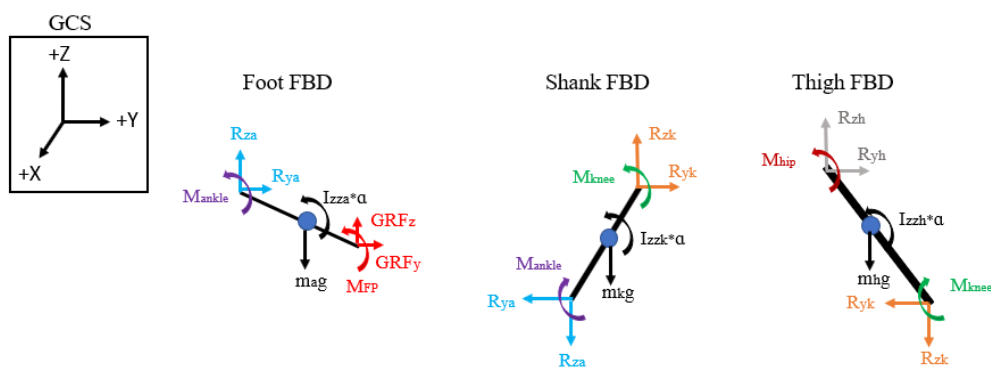


Figure 4.15 Free body diagrams of the foot, shank, and thigh segments used to perform inverse dynamics calculations.

$$\sum F_y = ma_y \quad (\text{Eq 7})$$

$$\sum F_z = ma_z \quad (\text{Eq 8})$$

$$\sum M_x = I_{xx}\alpha \quad (\text{Eq 9})$$

where m is the mass of the segment, a is the linear acceleration, I is the mass moment of inertia, and α is the angular acceleration.

4.5 STATISTICAL ANALYSIS

Statistical analyses were performed using SPSS (v 25.0, IBM Inc., Armonk, NY) to contrast the various parameters between orthotic ankle joint conditions. Analyses were conducted for overground walking and each treadmill orientation. The normality of the specific metric was assessed across all gait cycles (overground or treadmill) for each AFO condition using the Shapiro-Wilk test ($p=0.05$). As data for all metrics were normally distributed, a two-tailed paired t-test ($p=0.05$) was performed to identify potentially significant differences between AFO conditions for control and post-stroke walking according to the hypotheses in summarized Table 4.6.

Due to the small sample size of both populations and large variations in gait between post-stroke individuals of different functional levels, the data were not averaged across subjects. Instead, the hypotheses were assessed on the intra-subject basis with the multiple stride cycles for each condition.

Table 4.6 Summary of hypotheses between conventional and novel ankle joint conditions for able-bodied (able-bodied) and post-stroke (PS) subjects.

Hypothesis	Description	Population	Null Hypothesis
1	Walking speed, step length and stance duration on the paretic limb are increased with the novel ankle joint.	AB, PS	$\bar{X}_{conv} \geq \bar{X}_{novel}$
2	Peak ankle plantarflexion during swing with the novel ankle joint does not exceed the conventional.	AB, PS	$\bar{X}_{conv} \leq \bar{X}_{novel}$
3	Ankle ROM during stance is greater with the novel ankle joint	AB, PS	$\bar{X}_{conv} \geq \bar{X}_{novel}$
4	Compensatory gait (peak hip and knee flexion during stance) is reduced with the novel ankle joint	PS	$\bar{X}_{conv} \leq \bar{X}_{novel}$
5	Kinematic and kinetic symmetry is improved (reduced SR) with the novel ankle joint	PS	$\bar{X}_{conv} \leq \bar{X}_{novel}$
6	Perceived exertion is reduced with novel ankle joint. Perceived comfort and walking performance are improved with the novel ankle joint design	PS	$\bar{X}_{conv} \leq \bar{X}_{novel}$
			$\bar{X}_{conv} \geq \bar{X}_{novel}$

Using GPower (Version 3.1.9.4, Dusseldorf, Germany), a post-hoc power analysis was performed on the ankle ROM during stance and self-selected speed during overground trials for post-stroke subjects only. This analysis determined the power of the current study with 95% confidence and provided a recommendation for the sample size necessary to achieve 80% power for both metrics.

4.6 SUMMARY

Able-bodied and post-stroke subjects were recruited to participate in this study. Subjects were fitted with a custom AFO prior to completion of overground and treadmill

walking trials. Kinematic data were processed to determine spatiotemporal parameters and joint angle time series, particularly of the ankle and knee; these data were then contrasted between the conventional and novel ankle joint conditions. Kinetic data (peak knee and hip moments) during overground walking trials were also contrasted between AFO conditions. Data comparisons were statistically analyzed to test the research hypotheses and efficacy of novel ankle joint, assess study power, and evaluate recommended sample size for future testing.

5 Results

Able bodied and post-stroke subjects completed gait analyses with conventional and novel ankle joints incorporated within the study AFO. Spatio-temporal, kinematic, and kinetic data were collected and compared to assess the function of the novel ankle joint relative to the conventional joint. This chapter summarizes the results of these comparisons, including 1) preliminary evaluation of the design based on able-bodied control subject testing and 2) investigation of the design efficacy and research hypotheses based on post-stroke subject testing.

5.1 SUBJECT CHARACTERISTICS

Three able-bodied control subjects and three post-stroke individuals with drop foot were recruited, provided written informed consent and completed the full study test protocol. The characteristics for these control and post-stroke subjects are summarized in Table 5.1 and Table 5.2, respectively.

Table 5.1 Able-bodied subject characteristics

	Subject C1	Subject C2	Subject C3
Age (yrs.)	23	26	25
Gender	Female	Male	Male
Height (cm)	176.8	183.5	186.5
Weight (w/o orthosis, kg)	76.0	88.8	90.4

Table 5.2 Post-stroke subject characteristics.

	Subject P1	Subject P2	Subject P3
Age (yrs.)	67.1	56.8	52.7
Gender	Female	Male	Male
Height (m)	1.626	1.727	1.690
Weight (w/o orthosis, kg)	67.9	74.3	94.5
Time Post-stroke (yrs.)	2.9	5.6	11.0
Affected Side	Left	Left	Left
Current AFO type	non-articulated	articulated with plantarflex stop	articulated with plantarflex stop
Current AFO ankle joint	n/a	Tamarack	Tamarack
Fugl-Meyer Assessment Score (max 86)	27	56	46
Berg Balance Test Score (max 56)	27	55	52

5.2 CONFIRMATION OF DESIGN POTENTIAL AND SAFETY

Preliminary testing of able-bodied control subjects was performed to confirm that the novel joint could be swapped with the conventional joint, that its function was comparable to the conventional joint and that the novel joint did not introduce risk during future testing of post-stroke subjects. The specific objectives of these preliminary trials were: 1) demonstrating that the novel ankle joint could be safely and consistently installed in the same custom AFO, swapping it with the conventional joint, 2) ankle plantarflexion during swing was comparable to the conventional ankle joint to confirm

efficacy in the prevention of drop foot and potential toe drag, and 3) ankle range of motion during stance was enhanced in the novel joint compared to the conventional joint. The remainder of the metrics assessed during able-bodied testing are summarized in Appendix D [spatiotemporal and kinematic metrics (Tables D.1-3 and Figures D.1-3) and kinetics (Table D.4 and Figure D.4)].

All spatiotemporal and kinematic measures were evaluated using data from the treadmill trials, as this protocol ensured the greatest number of steps without marker drop out. No significant differences in parameters were observed for various treadmill orientations (level, incline, and decline); the average of all steps during the middle 145 sec of the level walking trials is presented for these preliminary able-bodied control subjects. Treadmill data for inclined and declined walking can be found in Appendix D (inclined: Table D.2 and Figure D.2; declined: Table D.3 and Figure D.3). The overground walking trials were used solely to determine self-selected speed and kinetic measures including knee and hip extension moments.

The self-selected (SS) walking speeds for each AFO condition and testing protocol are summarized in Table 5.3. The speed measured during the conventional ankle joint treadmill walking trial was also used for the novel ankle joint speed matched (SM) treadmill walking trial. For overground walking, self-selected walking speed was averaged across five trials. All subjects walked faster with the novel ankle joint condition during treadmill walking when compared to the conventional joint velocities. During overground trials, the self-selected walking speed was significantly faster with the novel ankle joint for subject C2. While not statistically significant, slower walking speeds were

observed during overground walking with the novel ankle joint trial for the other subjects.

Table 5.3 Subject self-selected walking speeds for conventional and novel ankle joint conditions during treadmill and overground walking trials, mean and standard deviation, S.D.).

Speed (m/s)	Treadmill		Overground		
	Conventional	Novel	No AFO	Conventional	Novel
Subject C1	0.849	1.03	1.25(0.06)	1.20(0.08)	1.18(0.04)
Subject C2	0.849	0.984	1.08(0.06)	1.04(0.07)	1.12(0.08)*
Subject C3	0.894	0.984	1.10(0.04)	1.15(0.04)	1.13(0.03)
Mean (S.D.)	0.864(0.03)	0.999(0.03)*	1.15(0.09)	1.13(0.09)	1.14(0.05)

* significant difference (0.05 level, intra-subject basis) between conventional and novel ankle joint

Ankle plantarflexion during swing for each step (AFO side only) was measured as a metric of drop foot prevention for level treadmill walking (Figure 5.1). Variations in peak plantarflexion of 1-3° during swing were observed for all orthotic conditions for each subject. Statistically significant differences were observed between AFO conditions (both SM and SS) for subjects C1 and C3 ($p < 0.001$); significant differences in ankle plantarflexion between orthotic conditions were only observed during SM testing for subject C2 ($p = 0.006$). Peak ankle plantarflexion during swing occurred during the first 5% of swing, immediately after toe off, for all subjects. During the remainder of swing phase, plantarflexion did not exceed 2° for all individuals.

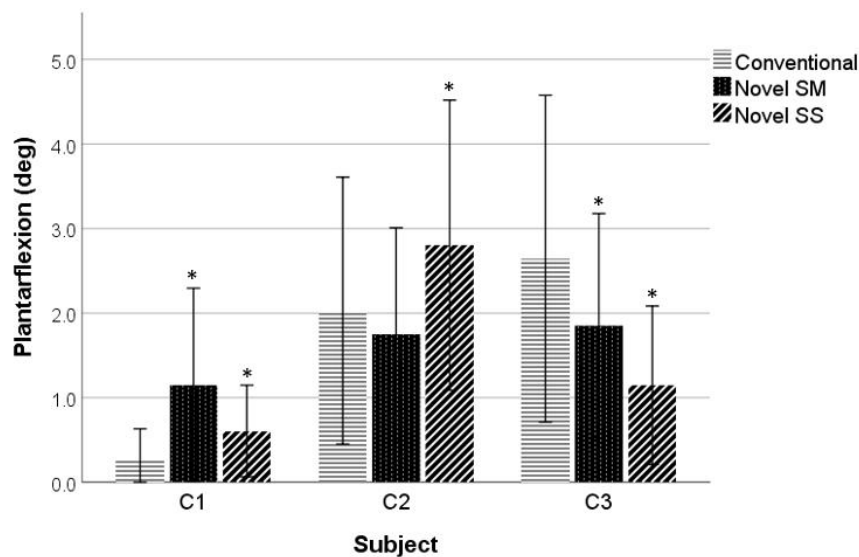


Figure 5.1 Ankle plantarflexion during swing for able-bodied subjects during level treadmill walking for each orthotic ankle joint condition. * indicates a statistically significant intra-subject difference between conventional and novel joint conditions (0.05 level). SS indicates the trial was performed at the subject's self-selected speed; SM refers to the speed matched trial of the novel joint (performed at the self-selected speed for the conventional joint trial).

The second metric used to assess function of the novel ankle joint was ankle ROM during stance (Figure 5.2). A statistically significant difference in ankle ROM (plantar and dorsiflexion) between AFO conditions was only observed for subject C1, with increased ROM with the novel ankle joint during SM testing (conventional: $21.0 \pm 2.48^\circ$, novel SM: $24.2 \pm 2.57^\circ$; $p=0.007$). The ankle ROM during stance ranged from 21-28° for all trials, AFO conditions, and subjects.

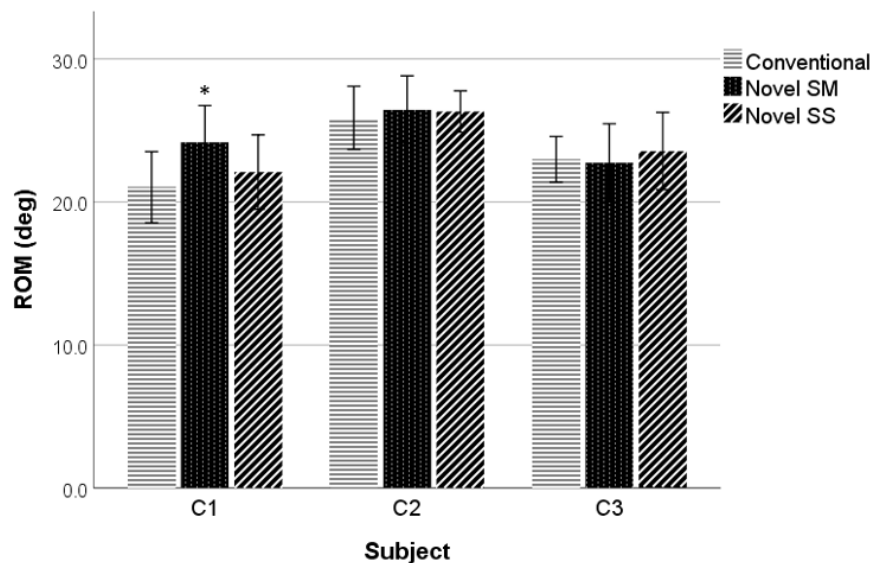


Figure 5.2 Ankle ROM during stance for able-bodied subjects during level treadmill walking trials for each orthotic ankle joint conditions. * indicates a statistically significant intra-subject difference between conventional and novel joint conditions (0.05 level). SS indicates the trial was performed at the subject's self-selected speed; SM refers to the speed matched trial of the novel joint (performed at the self-selected speed for the conventional joint trial).

These preliminary results demonstrated minimal risk with the novel orthotic ankle joint and readiness to safely proceed to post-stroke trials for hypothesis testing and evaluation of clinical treatment potential.

5.3 HYPOTHESIS TESTING AND CLINICAL POTENTIAL

Testing of post-stroke individuals was conducted to compare the ankle joint designs and conditions in terms of kinematic, kinetic, and spatiotemporal parameters to assess the relative efficacy of the novel orthotic ankle joint design. In contrast to the control subject testing, significant differences in some output metrics were noted with treadmill orientation and are reported as such. For metrics for which no differences were noted with terrain, only level treadmill walking data are contrasted here. Inclined and

declined results are summarized in Appendix D. Metrics were contrasted on an intra-subject basis, accounting for the greater inter-subject variability amongst the post-stroke population.

5.3.1 Spatiotemporal Parameters

The self-selected speeds for both treadmill and overground walking trials are shown in Table 5.4. Only subject P2 demonstrated an increased self-selected speed during treadmill trials with the novel ankle joint versus the conventional ankle joint (conventional 0.492 m/s, novel 0.536 m/s); all other subjects maintained the same speed for each condition. During overground walking, subjects P2 and P3 had statistically significant increases in self-selected speeds with the novel joint when compared to their current AFO and the conventional ankle joint (P2 increased by 0.012 m/s, P3 increased by 0.022 m/s). Subject P1 walked more slowly with the novel ankle joint than either of the other conditions.

Table 5.4 Mean self-selected speeds during treadmill and overground walking trials for all AFO conditions (standard deviation, S.D.).

Speed (m/s)	Treadmill		Overground		
	Conventional	Novel	Current AFO	Conventional	Novel
Subject P1	0.268	0.268	0.847(0.13)	0.703(0.04)	0.705(0.08)
Subject P2	0.492	0.536	0.723(0.03)	0.749(0.06)	0.761(0.06)* ¹
Subject P3	0.447	0.447	0.709(0.01)	0.711(0.02)	0.733(0.02)* ¹
Mean(S.D)	0.402(0.12)	0.417(0.14)	0.754(0.09)	0.721(0.05)	0.733(0.06)

+ significant difference (0.05 level) between current AFO and the novel joint

* significant difference (0.05 level) between conventional and novel ankle joint

Stance duration (time from ipsilateral HS to ipsilateral TO) on the AFO side was compared for each ankle joint condition during treadmill walking for all orientations (Figure 5.3). Time was normalized to percent GC to facilitate comparisons between conditions, regardless of walking speeds. All subjects spent longer time in stance on the AFO side when traversing the inclined terrain; stance duration on the AFO side was reduced during declined walking. Stance duration was greatest for subject P1 for all terrains and ankle joint conditions. While not statistically significant, stance duration tended to be prolonged with the novel joint at both SS and SM speeds. Subject P2 demonstrated increased stance duration with the novel joint walking on declined terrain (SM only, $p=0.011$). The same result was seen with subject P3, where stance duration was increased with the novel joint over declined terrain (SM only, $p=0.021$) and inclined terrain (SM only, $p=0.001$).

To quantify potential inter-limb asymmetry for stance duration (percent GC), the symmetry ratio (SR) was evaluated (Figure 5.4). A SR value of 0 indicates symmetry between limbs; a negative SR reflects prolonged stance duration on the unaffected limb. Subject P1 exhibited extensive step variability; no statistically significant differences in stance duration SR were observed. Subjects P2 and P3 consistently demonstrated prolonged stance duration on the unaffected limb (e.g., $SR < 0$). Subjects P2 and P3 demonstrated reduced stance duration asymmetry with the novel ankle joint at both speeds; these differences were statistically significant during declined (P2-SM, $p=0.036$; P3-SM, $p=0.031$) and inclined walking (P3 only, SM, $p=0.021$).

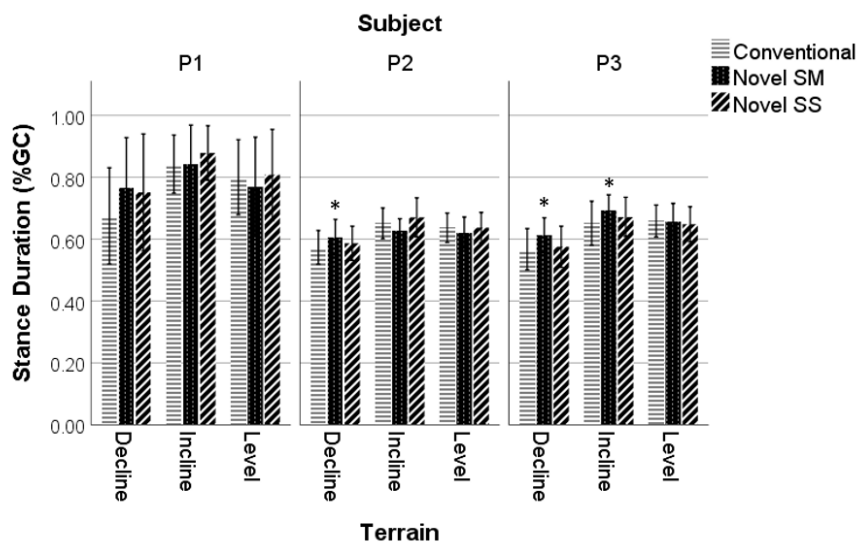


Figure 5.3 Stance duration on the AFO side (normalized to %GC) during treadmill walking across all terrains for each orthotic ankle joint condition. * statistically significant difference between conventional and novel joint conditions (0.05 level, intra-subject comparison). SS indicates the trial was performed at the subject's self-selected speed; SM refers to the speed matched trial of the novel joint (performed at the self-selected speed for the conventional joint trial).

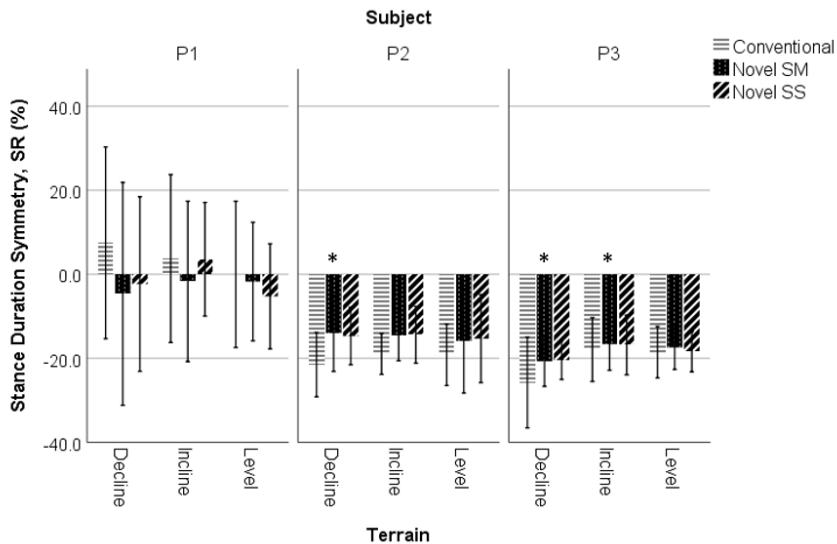


Figure 5.4 Inter-limb symmetry (SR) for stance duration during inclined, level, and declined treadmill walking for each orthotic ankle joint condition. SR = 0 represents symmetry; negative values indicate greater stance duration on the unaffected limb. SS indicates the trial was performed at the subject's self-selected speed; SM refers to the speed matched trial of the novel joint (performed at the self-selected speed for the conventional joint trial). * statistically significant difference between conventional and novel joint conditions (0.05 level, intra-subject comparison).

Step length (distance between successive contralateral HS events), normalized to subject height, was assessed for each orthotic condition (Figure 5.6). Statistically significant differences in step length were observed between ankle joint conditions for most terrains. In general, step lengths on the paretic/AFO side were longer during inclined walking and shorter during declined ambulation. Step length of the paretic/AFO side was increased with the novel joint when speed-matched to the conventional joint (subject P1 - declined: $p=0.010$, inclined: $p=0.003$, level: $p=0.003$; subject P2 - declined: $p=0.033$; subject P3 – declined: $p=0.001$, inclined: $p=0.005$). At self-selected speeds (SS), step length was increased on the paretic/AFO side for subject P2 (declined: $p<0.001$, inclined: $p=0.026$, level: $p<0.001$) and decreased for subjects P1 (level: $p=0.012$).

Inter-limb symmetry in step length was also evaluated to determine the effect of the novel ankle joint on spatial symmetry (Figure 5.6). No significant differences between joints were exhibited by subject P1; this lack of statistical significance was likely influenced by the large variability demonstrated during this subject's gait. Step length symmetry was improved (e.g., decreased SR magnitude) for subject P2 for all terrains when speed was matched (declined: $p=0.004$, inclined: $p=0.001$, level: $p<0.001$); step length symmetry was also improved with the novel joint during declined walking at SS speed ($p<0.001$). In contrast, step length symmetry decreased (e.g., more asymmetric, SR magnitude increased) with the novel ankle joint for subject P3 during decline walking (SM: $p=0.021$, SS: $p=0.029$).

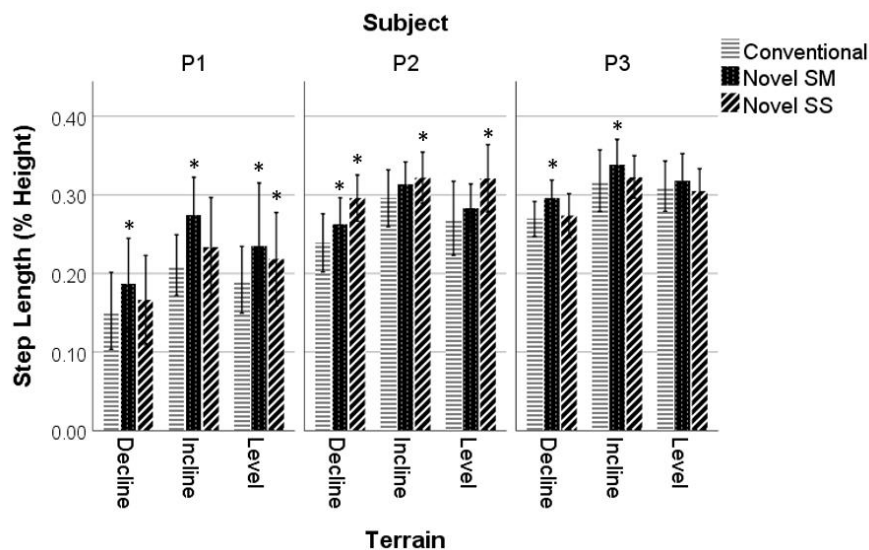


Figure 5.5 Step length on the AFO side (normalized to % height) during treadmill walking across all terrains for each orthotic ankle joint condition. * statistically significant difference between conventional and novel joint conditions (0.05 level, intra-subject comparison). SS indicates the trial was performed at the subject's self-selected speed; SM refers to the speed matched trial of the novel joint (performed at the self-selected speed for the conventional joint trial).

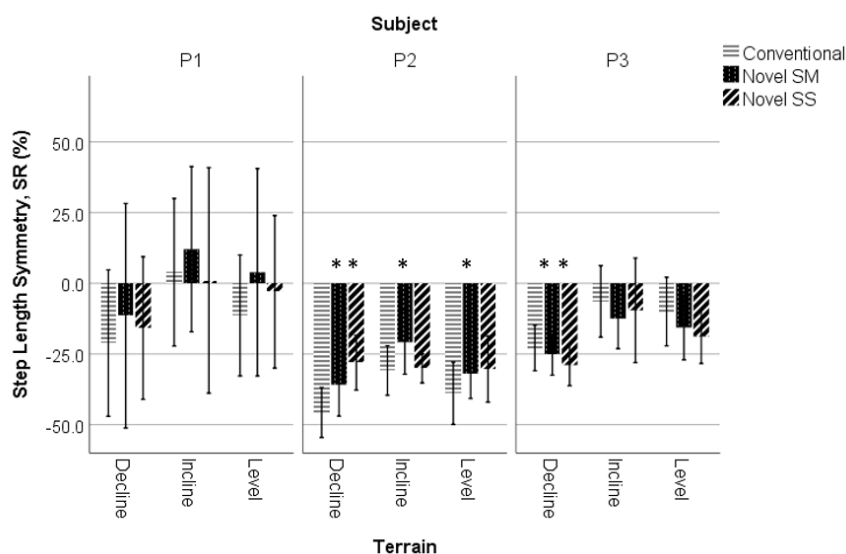


Figure 5.6 Inter-limb symmetry (SR) for step length during inclined, level, and declined treadmill walking for each orthotic ankle joint condition. SR = 0 represents symmetry; negative values indicate greater step length on the unaffected limb. * statistically significant difference between conventional and novel joint conditions (0.05 level, intra-subject comparison). SS indicates the trial was performed at the subject's self-selected speed; SM refers to the speed matched trial of the novel joint (performed at the self-selected speed for the conventional joint trial).

5.3.2 Kinematic Parameters

The kinematic data acquired during treadmill walking were analyzed during the middle 50% of each trial and are presented as a function of percent GC. The results for level terrain walking for each of the post-stroke individuals can be seen in Figure 5.7; the joint angle profiles for inclined and declined treadmill orientation can be found in Appendix D (Figures D.5-6). Subject data is arranged by row; the mean joint angles in the sagittal plane are shown in each column (ankle - left, knee- middle, and hip- right).

The mean ankle angle time series for subject P1 during level treadmill walking exhibits a prolonged dorsiflexion phase from HS to immediately prior to TO, with

increased peak dorsiflexion ($>15^\circ$ for all conditions except novel SS) relative to subjects P2 and P3. Note that stance duration is prolonged relative to both the control subjects and the other post-stroke subjects (P1: TO at 84% GC; controls: TO at 72%; P2 and P3: TO at 62% GC). Stance duration varied between AFO conditions for subject P1 (conventional ankle joint: TO at 84% GC, novel ankle – SS: TO at 86%; novel ankle – SM: 88%). Subject P2 exhibited slight plantarflexion after HS, transitioning towards peak dorsiflexion in mid-late stance, prior to plantarflexing for push off into swing. With the exception of the higher rate of dorsiflexion from early to mid-stance with the conventional ankle joint, no differences in ankle motion were observed with AFO condition. Subject P3 demonstrated pathologic ankle motion during early- to mid-stance; dorsiflexion plateaued prior to achieving peak dorsiflexion at ~52% GC. Differences in stance duration were observed between the conventional and novel joints; stance duration was reduced (2% GC) with the conventional joint.

The knee joint motion profiles and peak flexion also varied for each subject. Subject P1's paretic/AFO limb never achieved full knee extension during stance; the knee remained flexed approximately $5-10^\circ$ through late-stance. Subject P1 also demonstrated premature peak knee flexion with the conventional ankle joint. Subject P2 demonstrated excessive knee flexion (nearly 15°) at HS for all AFO conditions; peak knee flexion of approximately 30° was observed during early swing for all ankle joint conditions. Knee ROM was minimal (less than 20° for subject P3). While some knee flexion was observed at HS, full knee extension during mid-stance was not observed.

Peak hip extension for subject P1 was delayed with all ankle joint conditions, but particularly the novel ankle joint trials. The hip joint motion profiles for subjects P2 and

P3 were similar, with peak hip flexion ($\sim 17^\circ$) at HS and at mid- to late-swing. Sagittal plane hip kinematics were affected by AFO condition for subject P2; in contrast, the hip motion profile for subject P3 showed minimal differences across AFO conditions. Compared to able-bodied subjects, all post-stroke individuals experienced less hip extension ($10\text{-}15^\circ$) during mid stance.

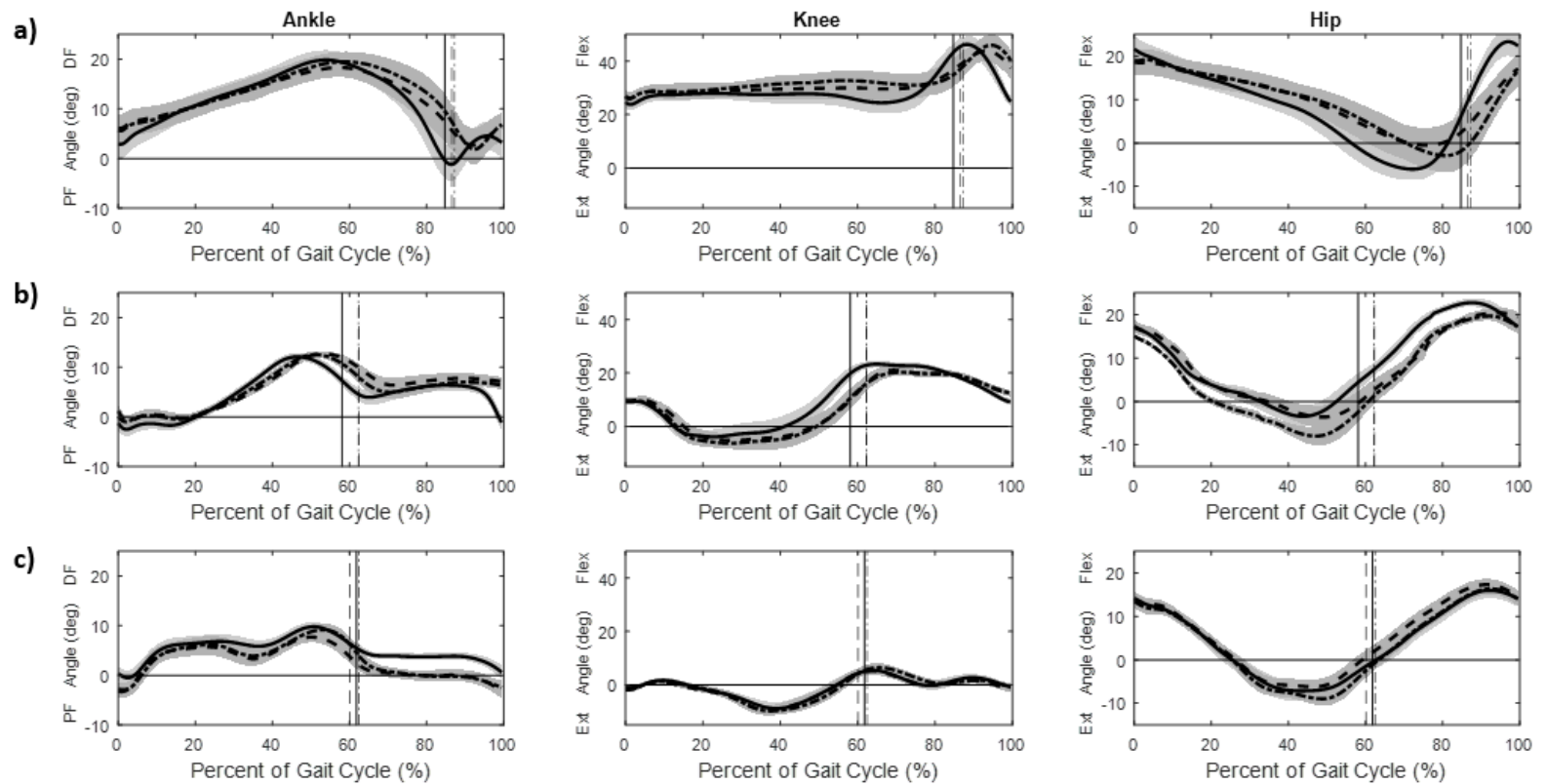


Figure 5.7 Ankle (left), knee (middle), and hip (right) angle time series for the paretic/AFO side of post-stroke subjects during level overground walking – a) Subject P1, b) Subject P2, c) Subject P3. Solid line is the mean of the trials with the conventional joint (light gray shading S.D.), dashed line is the mean of the novel joint at SS (medium gray shading S.D.), and dot-dashed line is the mean of the novel joint at SM (dark gray shading S.D.). The vertical lines (solid – conventional, dashed – novel SS, dot-dash – novel SM) represent TO, the transition from stance to swing.

Kinematic parameters of interest for post-stroke walking included ankle plantarflexion during swing, ankle ROM during stance (early, mid, and late stance), and peak knee and hip flexion during stance.

The peak ankle plantarflexion during swing for treadmill walking is summarized in Figure 5.8, contrasting AFO condition as a function of treadmill orientation.

Plantarflexion during swing was greatest for subject P3; mean values were significantly greater with the novel ankle joint (SM – declined: $p=0.021$, level: $p=0.006$; SS – declined: $p=0.029$, level: $p<0.001$). Significant differences in peak ankle plantarflexion during swing were also observed for subject P2 (SM – declined: $p=0.004$, inclined: $p=0.001$, level: $p<0.001$; SS – declined: $p<0.001$). Little plantarflexion during swing was observed for subject P1 for all AFO conditions.

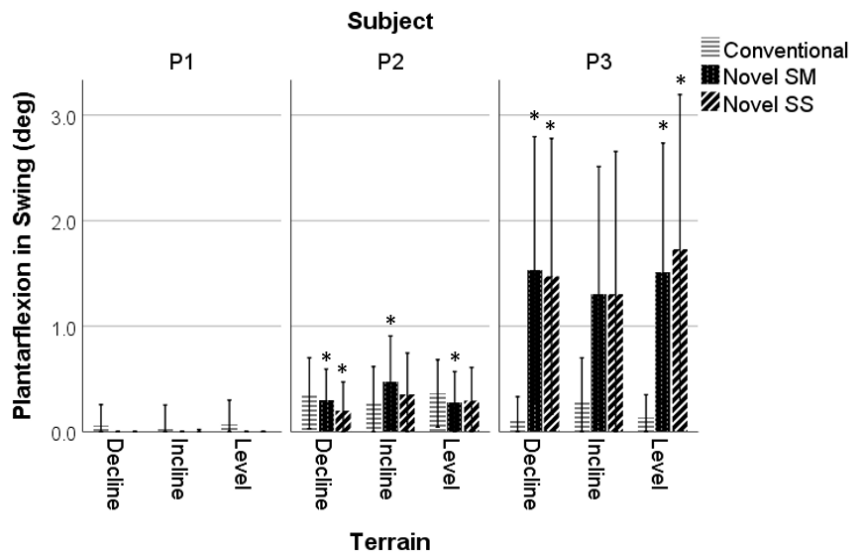
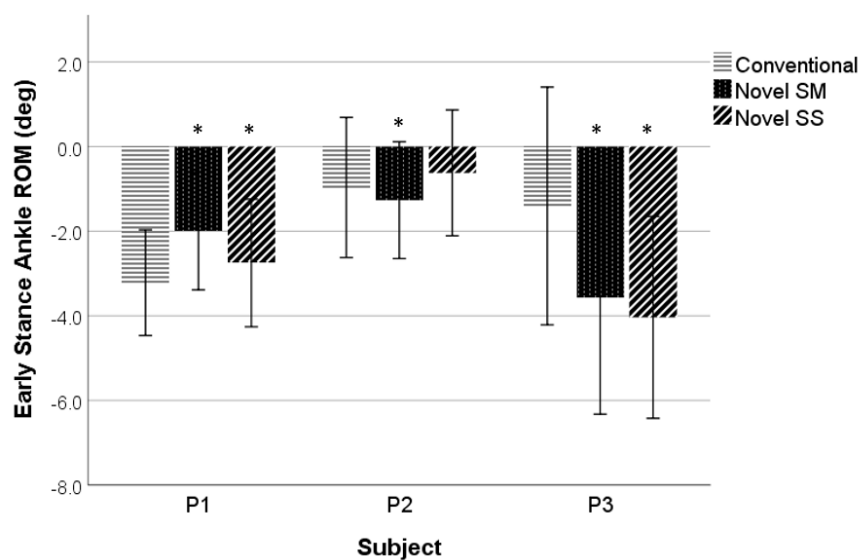


Figure 5.8 Peak plantarflexion on the AFO side during treadmill walking across all terrains for each orthotic ankle joint condition. * statistically significant difference between conventional and novel joint conditions (0.05 level, intra-subject comparison). SS indicates the trial was performed at the subject's self-selected speed; SM refers to the speed matched trial of the novel joint (performed at the self-selected speed for the conventional joint trial).

Ankle ROM during the various sub-phases of stance was evaluated to assess the effects of the novel ankle joint on 1) controlled plantarflexion after heel strike, 2) ankle ROM during mid stance, and 3) plantarflexion during late stance to facilitate push off. This division is consistent with the three rockers. Only the level terrain metrics are presented here, as comparative results between AFO conditions were consistent across terrain conditions. Ankle ROM metrics for inclined and declined treadmill walking can be found in Appendix D (Tables D.5-6).

Ankle ROM during early stance was evaluated to determine whether the novel ankle joint mechanism unlocked at HS to enable plantarflexion to foot flat, where a negative value indicates plantarflexion (Figure 5.9). Statistically significant differences in early stance ROM were seen for all subjects. For subject P1, ankle ROM during early

stance decreased with the novel ankle joint (SM: $p < 0.001$, SS: $p = 0.031$). In contrast, for subject P3, ankle ROM during early stance increased with the novel ankle joint (SM: $p < 0.001$, SS: $p < 0.001$). Ankle ROM during early stance was less for subject P2; despite greater variability, ankle ROM during early stance was significantly different with the novel joint (SM only, $p = 0.042$).



*Figure 5.9 Ankle ROM during early stance on the paretic/AFO side during level treadmill walking for each orthotic ankle joint condition. * statistically significant difference between conventional and novel joint conditions (0.05 level, intra-subject comparison). SS indicates the trial was performed at the subject's self-selected speed; SM refers to the speed matched trial of the novel joint (performed at the self-selected speed for the conventional joint trial).*

During mid-stance, ankle dorsiflexion was assessed to evaluate the effectiveness of the novel orthotic ankle joint to support the second rocker, tibial rotation about the ankle during foot flat (Figure 5.10). Mid-stance ankle dorsiflexion for all subjects was greater for the conventional joint (SS only; P1: $p < 0.001$; P2: $p = 0.012$; P3: $p < 0.001$). In

addition, ankle dorsiflexion during mid-stance was also increased with the conventional joint for SM testing for subjects P1 and P2 ($p=0.001$ and $p<0.001$ respectively).

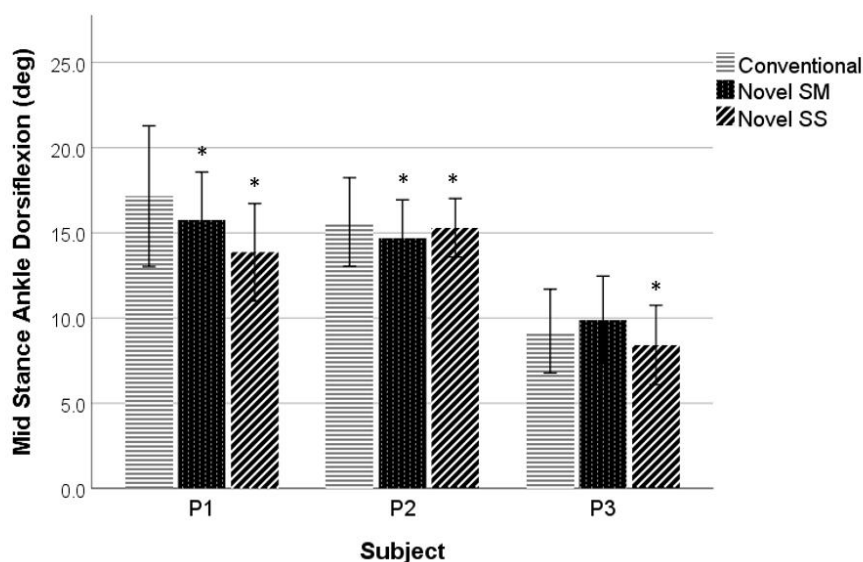


*Figure 5.10 Ankle dorsiflexion during mid-stance on the paretic/AFO side during level treadmill walking for each orthotic ankle joint condition. * statistically significant difference between conventional and novel joint conditions (0.05 level, intra-subject comparison). SS indicates the trial was performed at the subject's self-selected speed; SM refers to the speed matched trial of the novel joint (performed at the self-selected speed for the conventional joint trial).*

Finally, ankle plantarflexion during late stance was quantified to determine whether the novel ankle joint enhanced the ability of the user to provide active push off when transitioning from stance to swing (Figure 5.11). Ankle plantarflexion during late stance was significantly increased with the novel ankle joint for subject P3 only (SM: $p<0.001$, SS: $p=0.001$).

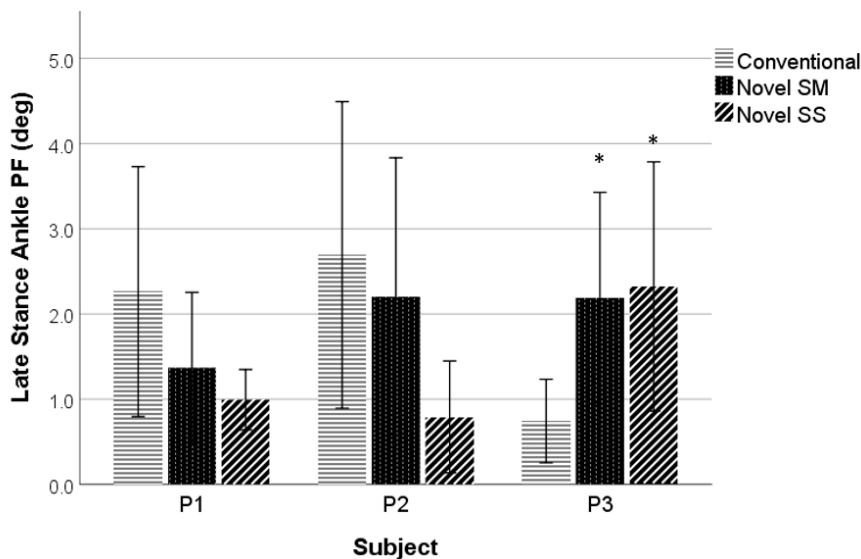
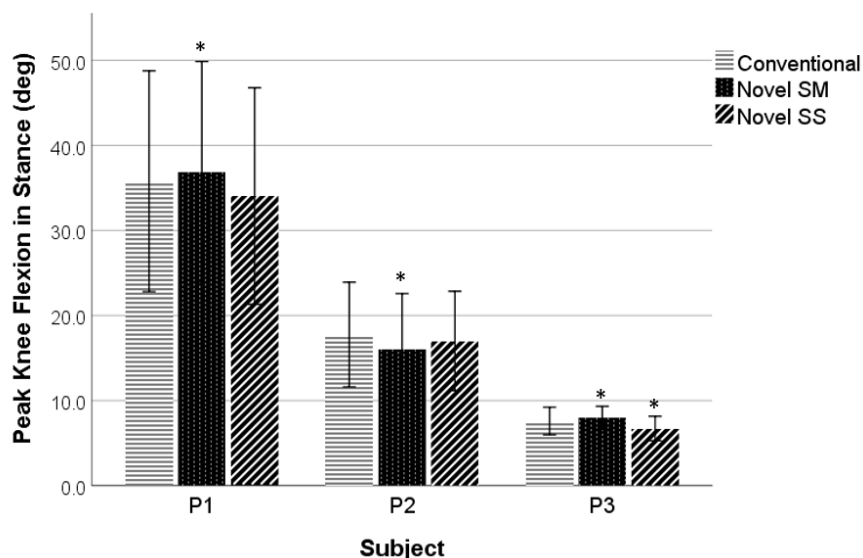


Figure 5.11 Plantarflexion of the ankle during late stance on the paretic/AFO side during level treadmill walking for each orthotic ankle joint condition. * statistically significant difference between conventional and novel joint conditions (0.05 level, intra-subject comparison). SS indicates the trial was performed at the subject's self-selected speed; SM refers to the speed matched trial of the novel joint (performed at the self-selected speed for the conventional joint trial).

In addition to ankle motion, peak knee flexion during stance (specifically the loading phase) on the paretic/AFO side was contrasted to quantify the ability of the novel ankle joint to reduce compensatory gait pathologies (Figure 5.12). As there were no observed differences in knee flexion across terrain, only the results for level treadmill walking are presented here; similar metrics for inclined and declined treadmill walking are summarized in Appendix D (Tables D.3-4). Knee flexion was significantly reduced for subject P2 and P3 with the novel ankle joint at different speeds (P2 SM: $p=0.001$; P3 SS: $p<0.001$). However, the SM trial for subjects P1 and P3 demonstrated a significant increase in knee flexion during the loading response (P1: $p=0.049$; P3: $p<0.001$). Note that subject P3 exhibited much less knee flexion of the paretic/AFO limb during stance than the other post-stroke subjects.

To further assess the effect of the novel joint on compensatory gait pathologies, inter-limb symmetry of knee flexion during stance was calculated via the SR (Figure 5.13). Subject P1 demonstrated low inter-limb asymmetry in stance knee flexion (low magnitude SR) for all trials, with the only significant difference and increase in asymmetry during the SM trial ($p=0.029$). Subject P2 demonstrated a statistically significant increase in knee flexion asymmetry novel joint for the SS trial ($p<0.001$), and despite improvements in symmetry for the SM trial, it was not significant. Subject P3 displayed significantly greater asymmetry with both trials of the novel ankle joint (SM: $p<0.001$; SS: $p<0.001$).



*Figure 5.12 Peak knee flexion during the loading phase of stance on the paretic/AFO side during level treadmill walking for each orthotic ankle joint condition. * statistically significant difference between conventional and novel joint conditions (0.05 level, intra-subject comparison). SS indicates the trial was performed at the subject's self-selected speed; SM refers to the speed matched trial of the novel joint (performed at the self-selected speed for the conventional joint trial).*

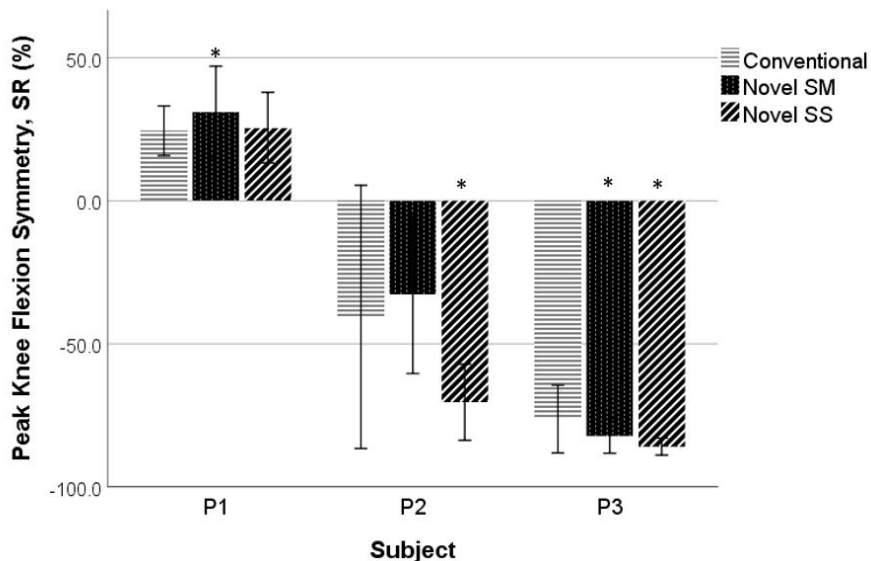


Figure 5.13 Inter-limb symmetry (SR) for peak knee flexion during level treadmill walking for each orthotic ankle joint condition. SR = 0 represents symmetry; negative values indicate greater step length on the unaffected limb. * statistically significant difference between conventional and novel joint conditions (0.05 level, intra-subject comparison). SS indicates the trial was performed at the subject's self-selected speed; SM refers to the speed matched trial of the novel joint (performed at the self-selected speed for the conventional joint trial).

The final kinematic parameter evaluated to assess function of the novel ankle joint was peak hip flexion during stance (raw and in terms of symmetry) (Figure 5.14-15). No significant differences in hip flexion were observed with treadmill orientation; results for inclined and declined treadmill walking are summarized in Appendix D (Tables D.3-4). Both subjects P1 and P2 demonstrated significant reductions in hip flexion during stance with the novel joint (P1-SS only: $p < 0.001$; P2 SS: $p = 0.003$, SM: $p = 0.027$). In contrast, hip flexion during stance increased for subject P3 (SM only, $p = 0.034$). Large variability was observed in the corresponding SRs. Significant differences were only observed for subject P3 (SM: $p < 0.001$) with greater asymmetry (e.g., higher SR) observed for the novel joint trials (Figure 5.15).

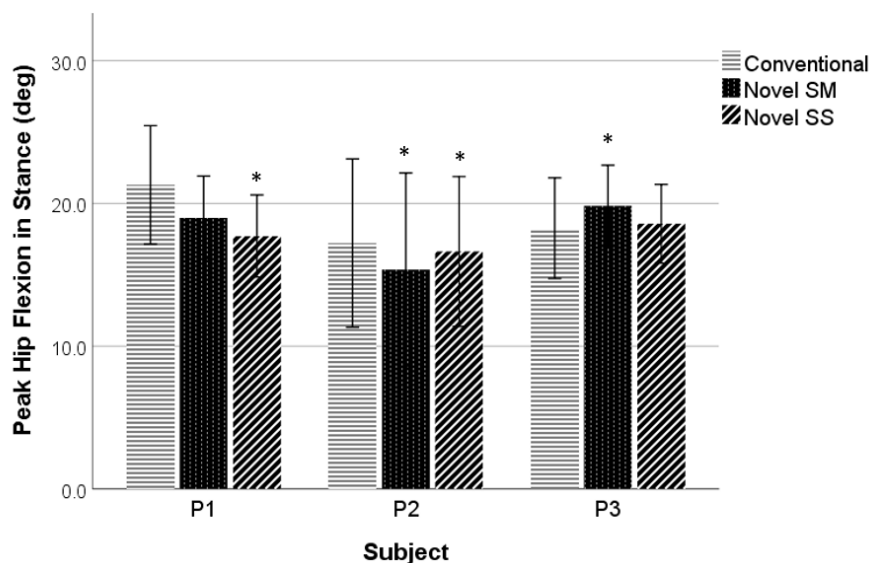


Figure 5.14 Peak hip flexion during stance on the paretic/AFO side during level treadmill walking for each orthotic ankle joint condition. * statistically significant difference between conventional and novel joint conditions (0.05 level, intra-subject comparison). SS indicates the trial was performed at the subject's self-selected speed; SM refers to the speed matched trial of the novel joint (performed at the self-selected speed for the conventional joint trial).

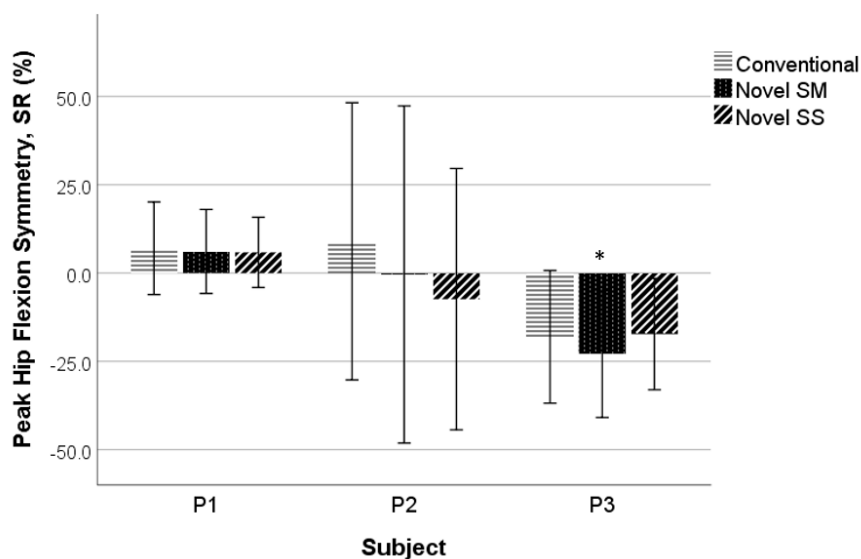


Figure 5.15 Inter-limb symmetry (SR) for peak hip flexion during level treadmill walking for each orthotic ankle joint condition. SR = 0 represents symmetry; negative values indicate greater step length on the unaffected limb. * statistically significant difference between conventional and novel joint conditions (0.05 level, intra-subject comparison). SS indicates the trial was performed at the subject's self-selected speed; SM refers to the speed matched trial of the novel joint (performed at the self-selected speed for the conventional joint trial).

5.4 KINETIC PARAMETERS

While vertical force data were acquired during treadmill walking, the kinetic analyses were limited to overground walking trials. No kinetic data were acquired during overground walking for subject P1, as this individual was unable to complete clean foot strikes on the force plates. A combination of short stride length and slow walking speed made it impossible for the subject to isolate foot strikes without altering their gait pattern.

The kinetic profiles of ankle, knee, and hip moments (normalized to subject mass) can be seen in Figure 5.16; for reference, kinetic data for the able-bodied control subjects is presented in Appendix D (Figure D.4). The peak extension moment at the knee was reduced with the novel versus conventional orthotic joint for both subjects P2 and P3; the knee moment profile for the novel joint more closely matched that for the subject's current AFO. The peak extension moment during loading response was also reduced for the novel joint for both subjects (P2: conventional 0.26Nm/kg, novel 0.07 Nm/kg; P3: conventional 0.29 Nm/kg, novel 0.11 Nm/kg).

The hip moment profiles were more arbitrary, likely due to pelvic marker drop and corresponding errors in inverse dynamics calculations. Marker drop out was extensive for subject P2; the joint moment profiles for the conventional and novel ankle joints are therefore questionable. The hip moment profiles for the subject P3's current AFO and conventional joint AFO were similar, exhibiting peak extension moments of

approximately 0.4 Nm/kg during mid stance. A greater hip extension moment during loading response was noted with the novel ankle joint.

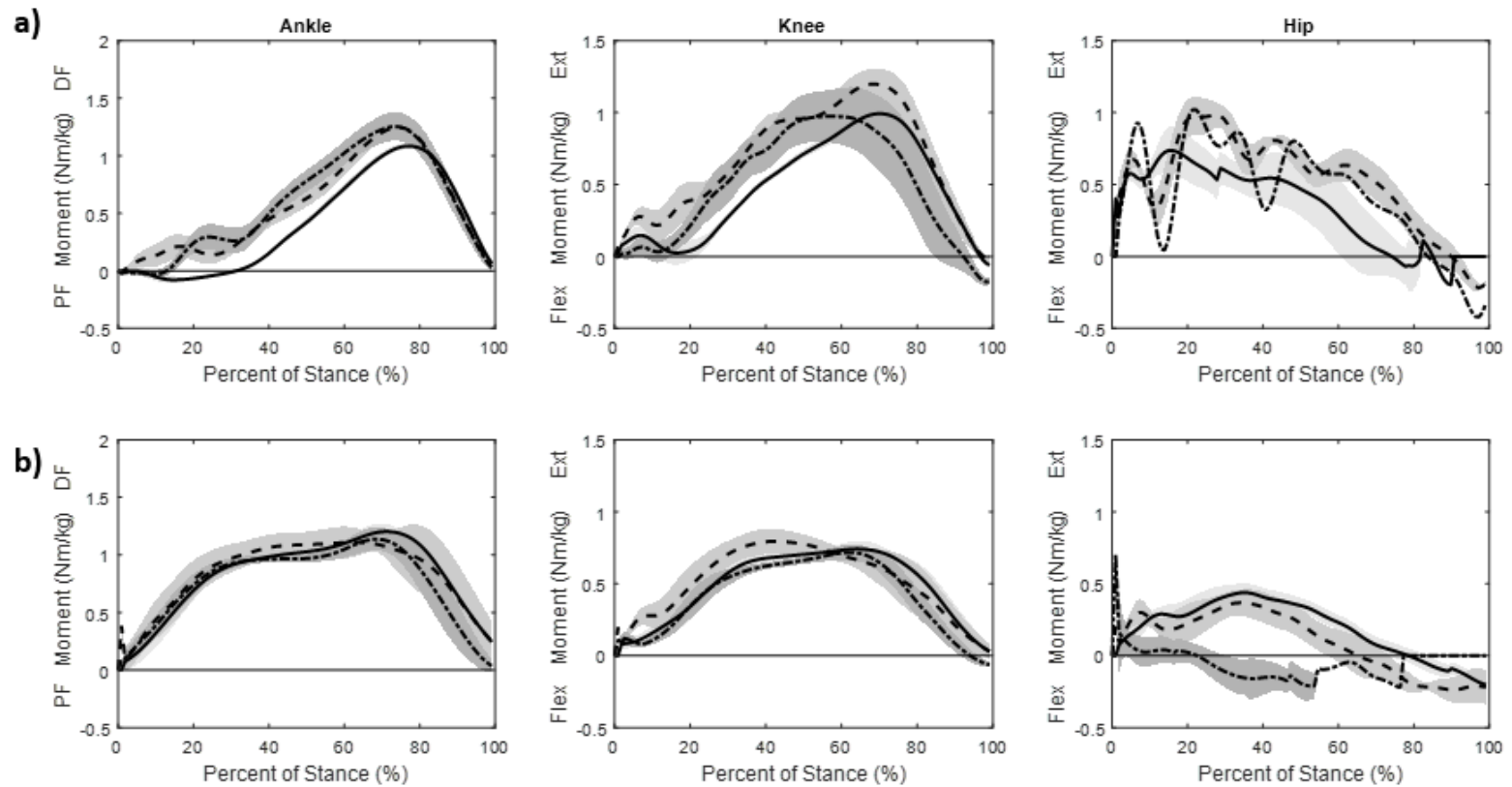


Figure 5.16 Ankle, knee, and hip moments for post-stroke subjects – a) Subject P2, and b) Subject P3, during level overground walking. Solid line is the mean of the trials with subject's current AFO (light gray shading S.D.), dashed is the conventional ankle joint mean (medium gray shading S.D.), and dot-dashed is the novel joint mean (dark gray shading S.D.).

The aforementioned inverse dynamic analyses were conducted to evaluate the peak knee extension moment (raw and symmetry: Figure 5.17-20) and peak hip extension moment of the paretic/AFO limb during stance (Figure 5.19-22). These measures may provide insight into compensatory mechanisms used to accommodate walking with an orthotic brace. While differences on mean peak knee and hip moment were observed between AFO conditions, these differences were not statistically significant.

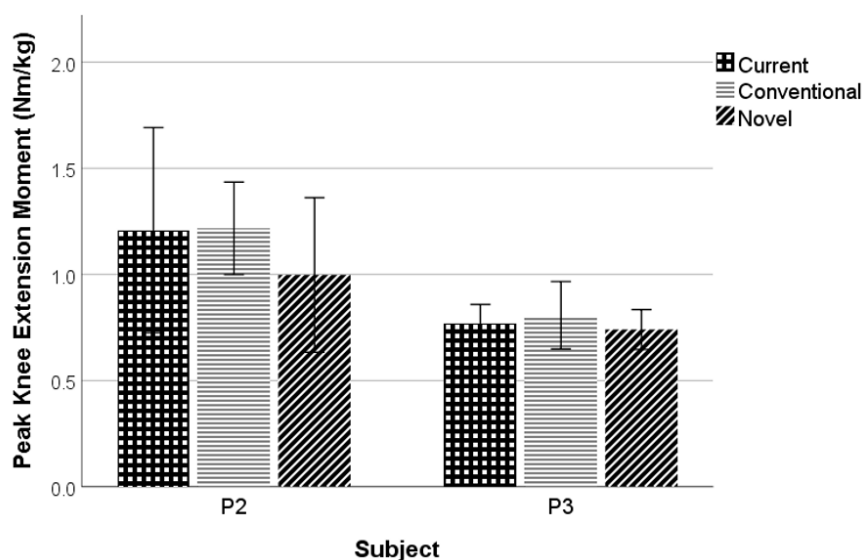


Figure 5.17 Peak knee extension moment during stance for subjects P2 and P3 during overground walking for all ankle joint conditions.

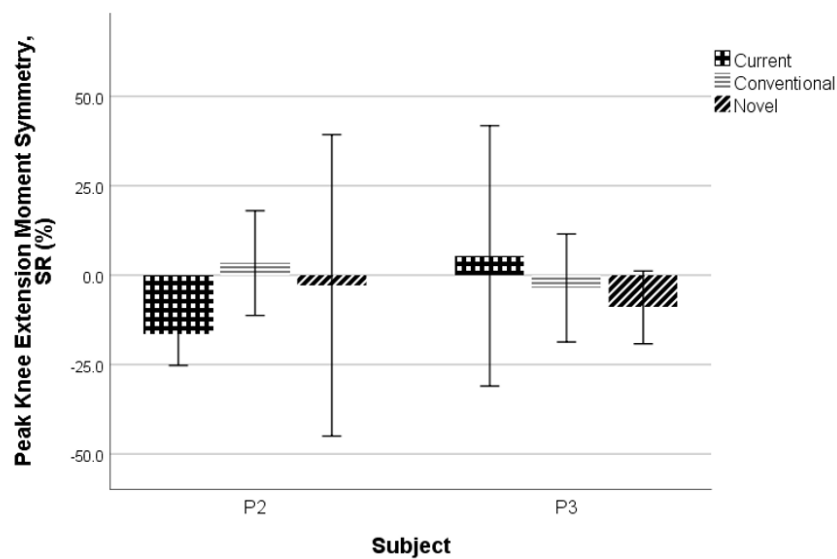


Figure 5.18 Inter-limb symmetry in peak knee extension moment during overground walking for each orthotic ankle joint condition for subjects P2 and P3. SR = 0 represents symmetry; negative values indicate a greater knee extension moment on the unaffected limb.

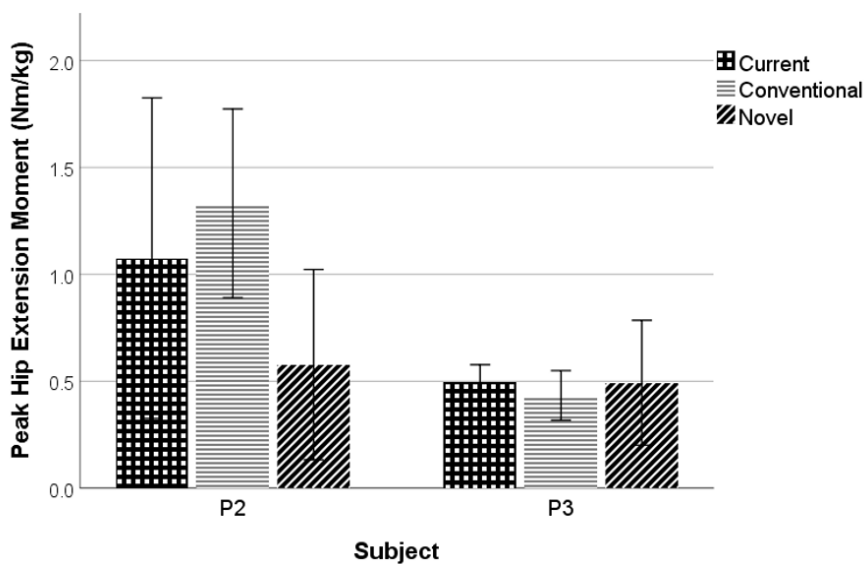


Figure 5.19 Peak hip extension moment during stance for subjects P2 and P3 during overground walking for all ankle joint conditions.

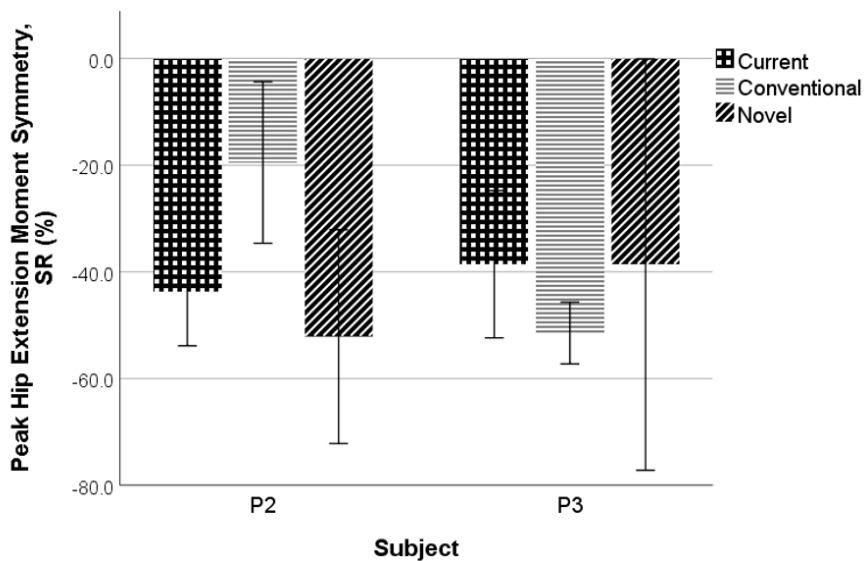


Figure 5.20 Inter-limb symmetry in peak hip extension during overground walking for each orthotic ankle joint condition for subjects P2 and P3. SR = 0 represents symmetry; negative values indicate a greater hip extension moment on the unaffected limb.

5.5 SUBJECT PERCEPTION

The post-testing surveys of subject perception of orthotic joint performance, comfort, and ease of use are shown in Table 5.5.

Table 5.5 Survey responses regarding perceived relative walking performance, comfort, and ease (e.g., reduced exertion or effort) for the novel ankle joint relative to the conventional ankle joint. Scores ranged from -5 to 5; a score of “0” reflects comparable perception; scores greater than 0 favored the novel orthotic ankle joint.

Survey Metric	Able-Bodied			Post-Stroke		
	A1	A2	A3	P1	P2	P3
Walking Performance	2	0	0	4	4	3
Comfort	2	0	0	4	4	2
Perceived Ease	0	2	0	0	4	0

5.6 POWER ANALYSIS

G Power was used to perform a post-hoc power analysis on the difference in means between two dependent measures: 1) the ankle ROM during mid-stance for post-stroke individuals during level treadmill walking and 2) self-selected speed during overground walking. The corresponding effect size was 0.3391 (11.1% power) for ankle ROM and 0.276 (9.67% power) for self-selected speed. To achieve 80% power with the same effect size for future studies contrasting the novel orthotic ankle joint, the ankle ROM effect requires at least 55 subjects to be recruited and self-selected speed requires 82 subjects. These estimations assume that these three post-stroke subjects are representative of the future post-stroke population.

5.7 SUMMARY

The results of the gait analyses for able-bodied subjects demonstrated that novel ankle joint function (e.g., ankle plantarflexion during swing and ankle ROM during stance) was comparable to that for the conventional ankle joint. Subsequent testing of post-stroke individuals also contrasted the effect of the orthotic ankle joint on ankle, knee, and hip joint kinematic and kinetic symmetry. Few metrics (stance duration and step length symmetry) varied significantly with treadmill orientation or terrain. Significant differences between orthotic condition were observed for peak knee flexion during the loading phase of stance, ankle ROM during mid-stance, and step length. These results and their clinical relevance will be discussed in Chapter 6.

6 Discussion

There are little data concerning the comparative function of articulated orthotic ankle joints used in AFOs to prevent drop-foot post stroke. The purpose of this study was to compare a novel design of an ankle joint to a conventional model to investigate whether the novel joint improved mobility and had a positive effect on spatiotemporal, kinematic, and kinetic functional parameters. It was hypothesized that significant differences would be found in compensatory gait pathologies, kinematic and kinetic symmetry between limbs, and spatiotemporal parameters when using the novel versus the conventional orthotic ankle joint. The results of the study, their consistency with current literature data, and support of research hypotheses will be discussed, as will their potential impact on clinical practice. Additionally, study limitations and future directions will be summarized.

6.1 DESIGN POTENTIAL – ABLE-BODIED SUBJECT TESTING

The intent of the preliminary testing of the able-bodied control subjects was to confirm that the novel joint could be swapped with the conventional joint, that the novel joint would not introduce risk during subsequent testing of post-stroke subjects, and that its function was comparable to the conventional joint. Specifically, the related objectives were to demonstrate that:

1. The novel ankle joint could be safely and consistently installed in the same custom AFO as the conventional joint.

2. Self-selected walking speed was increased when using the novel ankle joint versus the conventional joint.
3. Ankle plantarflexion during swing was comparable to the conventional ankle joint to confirm efficacy in the prevention of drop-foot and potential toe drag.
4. Ankle range of motion during stance was enhanced in the novel joint compared to the conventional joint.

As there were no significant changes between metrics of interest based on terrain for able-bodied subjects, only the level treadmill walking is discussed for kinematic parameters.

6.1.1 Objective 1

All three able-bodied subjects successfully completed the testing session with both the conventional and novel ankle joints. No adverse events occurred; no concerns about the novel joint safety or function were observed by the study orthotist or their residents, research personnel or subjects. The novel and conventional ankle joints could be swapped within 10 minutes to facilitate smooth testing order.

6.1.2 Objective 2

During treadmill trials, the average able-bodied walking speed was significantly faster with the novel ankle joint (0.999 ± 0.03 m/s) than the conventional joint (0.864 ± 0.03 m/s). In contrast, during overground walking, only subject C2 demonstrated a significantly faster walking speed with the novel ankle joint (1.12 ± 0.08 m/s) versus the

conventional joint (1.04 ± 0.07 m/s). While these self-selected walking speeds during overground walking are slower than those reported for similarly aged able-bodied subjects (~ 1.34 m/s [17]), the slower speeds may be attributed to the fact that these individuals were wearing an unnecessary assistive device.

6.1.3 Objective 3

For these able-bodied subjects wearing an AFO, ankle plantarflexion during swing never exceeded 5° during treadmill walking for any subject, regardless of orthotic ankle joint condition. Typical able-bodied kinematics during level overground walking without an AFO report peak ankle plantarflexion of nearly 25° in early swing, immediately after TO. The ability of the novel ankle joint to reduce plantarflexion during swing by almost 20° demonstrates that its drop-foot prevention is on par with the conventional ankle joint. Only subject (C2) demonstrated greater plantarflexion with the novel ankle joint than the conventional (novel: $2.80 \pm 1.71^\circ$; conventional: $2.03 \pm 1.58^\circ$).

While not quantified in the literature, it is likely that able-bodied subjects are able to provide sufficient push-off power during late stance to overcome the resistance of the orthotic ankle joint springs. The assumed sufficient push-off power is supported by the observed peak plantarflexion immediately after TO in all individuals, before the springs of the AFO could engage to bring the foot to neutral for the remainder of swing (Appendix D, Figure D.1).

6.1.4 Objective 4

Intra-subject comparison of ankle ROM during stance for the treadmill walking trials noted a significant improvement for subject C1 only (conv: $21.0 \pm 2.48^\circ$, SM: $24.2 \pm 2.57^\circ$). While not statistically significant, the ROM of the novel joint tended to exceed that for the conventional joint for each individual during the SM and/or SS walking speeds. These results may again be attributed to the ability of unimpaired individuals to overpower the AFO resistance, regardless of orthotic ankle joint design, as the typical ankle ROM during stance for able-bodied individuals during ambulation without an AFO is 20-25° [2-3].

6.1.5 Design Potential Summary

The novel ankle joint was thoroughly tested on the three able-bodied subjects to confirm safety and function before proceeding to testing on post-stroke individuals. While the results did not display marked improvements in kinematic parameters between the conventional and novel ankle joints for all subjects, this result can be expected due to the lack of neuromuscular impairment. Individuals with drop-foot will be more dependent on the mechanics of the orthotic ankle joint to facilitate gait than able-bodied subjects [55]. Regardless, these preliminary studies provided a better understanding of the novel orthotic ankle joint function and confirmed its potential and readiness to proceed with future testing.

6.2 POST-STROKE SUBJECT CHARACTERISTICS

Per the subject inclusion and exclusion criteria for post-stroke subjects, all subjects recruited for participation in subsequent preliminary clinical trials to assess the relative efficacy of the novel orthotic ankle joint design were individuals who had experienced a stroke resulting in unilateral drop-foot. Each subject walked with the assistance of an AFO and was able to ambulate for at least 5 minutes without rest or assistance beyond their AFO. These post-stroke subjects, however, were diverse in terms of functional impairment, walking ability, and gait patterns.

Subject P1, who was less than 3 years post-stroke, was the most severely impaired (e.g., Fugl-Myer and Berg Balance scores of 27). She reported infrequent use of her solid AFO for community ambulation, preferring use of a walker for enhanced stability. Her short stature and walking ability restricted her step length such that she could not span the force plates for clean, independent foot contact during overground walking. Her gait was characterized by slow walking speed, prolonged stance duration on the non-paretic limb, short, highly variable step length, inconsistent heel strike initial contact, and crouch gait.

Subject P2 was 5.6 years post-stroke, with limited impairment as demonstrated by his high Fugl-Meyer (56) and Berg Balance (55) scores. He retained some active ankle control. He reported frequent, daily ambulation with his articulated AFO; he receives Botox injections every 3 months to control spasticity in the paretic limb. His gait was characterized by initial contact with the heel, with compensatory knee and hip gait pathologies that predominate with fatigue and limit his active control of the paretic limb.

The final subject, P3, was the youngest of the group; his CVA occurred 11 years prior to testing. His post-stroke functional impairments were modest, as reflected by his Fugl-Myer (46) and Berg Balance (52) scores. While he currently ambulates with the assistance of a functional electrical stimulation device (Bioness L300), he previously used an articulated AFO. He has received Botox injections every 3 months for the past 8 years. This subject demonstrated extreme external tibial rotation ($\sim 20^\circ$) with toe out of the paretic foot. Even when not fatigued, this subject demonstrated minimal knee flexion and had to be prompted to use heel strike first patterns. Compensatory gait pathologies included circumduction, with a hitch during mid-swing.

Step variability may have impacted intra-subject comparisons between orthotic ankle joint conditions. The differences in subject functional level and gait pattern may limit the extrapolation of study results to the general post-stroke population.

6.3 HYPOTHESIS TESTING FOR POST-STROKE INDIVIDUALS

To investigate the functional differences between the novel and conventional ankle joints, spatiotemporal, kinematic, and kinetic parameters during overground and treadmill walking were assessed for the post-stroke subjects. The specific null hypotheses tested are reiterated in Table 6.1.

Table 6.1 Summary of the hypotheses tested.

Hypothesis	Description	Null Hypothesis
1	Self-selected walking speed, stance duration and step length on the paretic limb are <i>increased</i> with the novel joint.	$\bar{X}_{conv} \geq \bar{X}_{novel}$
2	Peak ankle plantarflexion during swing is <i>comparable</i> for the novel to that of the conventional orthotic ankle joint	$\bar{X}_{conv} \leq \bar{X}_{novel}$
3	Ankle ROM during stance is <i>greater</i> with the novel ankle joint	$\bar{X}_{conv} \geq \bar{X}_{novel}$
4	Compensatory gait (peak hip and knee flexion during stance) is <i>reduced</i> with the novel ankle joint	$\bar{X}_{conv} \leq \bar{X}_{novel}$
5	Spatiotemporal, kinematic, and kinetic symmetry is improved (<i>reduced</i> SR) with the novel ankle joint	$\bar{X}_{conv} \leq \bar{X}_{novel}$
6	Perceived exertion is <i>reduced</i> with novel ankle joint.	$\bar{X}_{conv} \leq \bar{X}_{novel}$
	Perceived comfort and walking performance are <i>increased</i> with the novel ankle joint design	$\bar{X}_{conv} \geq \bar{X}_{novel}$

6.3.1 Spatiotemporal Parameters

All spatiotemporal parameters varied by treadmill terrain except for walking speed, which is discussed separately for overground and treadmill trials.

6.3.1.1 Walking Speed

Walking speed is an important indicator of gait function, where increased velocity is generally associated with increased functional ability [7]. It was expected that the novel ankle joint would permit faster self-selected walking speeds due to enhanced ankle mobility.

As shown in Table 5.4, self-selected walking speed increased with the novel ankle joint during overground walking for subjects P2 and P3, relative to both their current AFO (P2: 5.3% increase, P3: 3.4% increase) and the conventional joint (P2: 1.6% increase, P3: 3.0% increase). Note that for subject P1, walking speed decreased with the novel ankle joint compared to her current AFO (solid), as well as the conventional ankle joint. This subject's more extensive functional impairments increased the likelihood of fatigue, despite rest periods between trials and test conditions. In general, self-selected walking speeds were slower on the treadmill for all individuals than during overground walking (treadmill range: 0.268-0.536 m/s, overground range: 0.703-0.847 m/s).

Prior comparisons of solid AFOs to articulated AFOs during overground walking have reported increases in walking speed ranging from 1.65%, 3.82%, and 5.17% for spastic hemiplegia (N=13, [57]), post-stroke (N=15, [58]) and cerebral palsy (N=12, [62]) populations, respectively. Similar increases in walking speed (4.88%) were also observed for a single post-polio subject ambulating in an Adjustable Dynamic Response (ADR) AFO and an articulated AFO with Tamarack joints [38]. The treadmill walking speeds for this study's post-stroke subjects were comparable to those reported for hemiparetic subjects (N=15, 0.43 ± 0.3 m/s) [88].

The improved functional performance in terms of walking speed with the novel orthotic ankle joint is promising, particularly given the study design limitations that may have impacted these findings (see Section 6.5).

6.3.1.2 *Stance Duration*

The stance duration for the paretic (AFO treated side) limb and the stance duration symmetry between limbs were compared for post-stroke individuals to compare the treatment efficacy of the ankle joint conditions. The stance duration of the paretic limb alone ranged from 58-85% of the gait cycle for all treadmill orientations, compared to 74-89% gait cycle for the non-paretic, unaffected limb. These stance durations are substantially prolonged; for example, in young able-bodied subjects, stance duration is typically 60-62% gait cycle [14].

Intra-subject differences in stance duration between orthotic ankle joint conditions were most apparent during non-level treadmill walking. Paretic limb stance duration increased by 5% GC with the novel ankle joint during declined walking for subjects P2 and P3 when walking speed was matched to that for the conventional joint. While only observed for a single subject, P3, stance duration on the paretic limb with the novel joint was also increased (~3%) during the inclined walking when speed was controlled (e.g., SM trial).

Review of inter-limb asymmetry (SR) in stance duration demonstrated that stance was prolonged on the unaffected limb ($SR < 0$), with the exception of subject P1, whose reduced walking ability contributed to large gait variability and inconsistent timing. The inter-limb asymmetry in stance duration observed for subjects P2 and P3, approximately 15-20%, was consistent for all terrains.

For a post-stroke population, stance duration is typically longer on the non-paretic limb to maximize stability. Increased stance duration on the paretic limb likely indicates greater comfort and perhaps enhanced function and/or balance with the orthotic ankle joint condition, as was seen in subjects P2 and P3.

Prolonged stance duration may contribute to slower walking speed. For example, the stance duration of able-bodied subjects was increased 9%, thereby reducing walking speed to match that of a hemiparetic population during overground walking [3]. The significant increase in stance duration is of particular importance as it was observed when *speed was matched or controlled*. These functional improvements were further supported by the statistically significant improvements in stance duration symmetry for subjects P2 and P3, a primary design goal for the novel ankle joint. The findings for stance duration during treadmill ambulation over various grades are consistent with that reported in the literature for 11 able-bodied individuals, where stance duration increased by 0.9% during inclined walking and decreased by the same amount during declined walking [89].

Stance duration is an important indicator of orthotic ankle treatment efficacy, as increased time on the paretic limb reflects improved comfort, balance, and/or stability in bearing weight on that limb. While there were few statistically significant increases in stance duration for the paretic limb, these differences were observed during the speed matched trials and were further supported by improved inter-limb symmetry. Improved symmetry for hemiparetic subjects is often a primary goal of clinicians, reducing risk of future injury.

6.3.1.3 Step Length

Similar to stance duration, step length is a functional measure of subject comfort in loading the paretic limb during gait. The goal of rehabilitation is to improve parity between limbs so that symmetry is improved. Typically, step length increases slightly when walking uphill and more dramatically decreases when walking downhill [90].

Normalized step length varied significantly between ankle joint conditions; these effects were dependent on treadmill orientation. Step length of the paretic limb was increased (4-7% body height) with the novel ankle joint in subject P1 for both SM and SS trials, regardless of treadmill orientation. Similar increases in step length of the paretic limb (3-8% body height) were observed for subject P2. Step length for subject P3 increased during the SM trial for declined and inclined walking with the novel joint; SS trials were comparable to conventional joint step lengths. Paretic limb step length decreased during declined walking for all subjects and increased for inclined walking, which match the trends seen in stance duration. There were no consistent trends between SM or SS trials.

Regardless of AFO condition or terrain, step length was longer for the non-paretic limb as noted by the corresponding negative SR values observed for subjects P2 and P3. Only subject P2 had reduced asymmetry using the novel ankle joint that was consistent with increased step length on the paretic limb, implying that higher functional scores lead to improved gains in step length with the novel ankle joint. The trends seen in asymmetry on the paretic limb were opposite of changes in normalized step length on the paretic

limb: the SR increased for declined walking and decreased for inclined walking regardless of condition.

While prior studies of subjects ambulating with an AFO demonstrated a longer step length for the paretic limb and positive SR values ([57]: SR = 4.56%, [59]: SR = 11.7%, [38]: SR = 35.9%), this inconsistency may be attributed to inherent variability in the post-stroke population. For example, many of the subjects tested by Lewallen et al. relied on canes or other assistive mobility devices. In addition, other studies allowed acclimation periods of multiple days with the AFO device before testing and examined overground level walking, where this study only allowed 20 minutes of acclimation before testing. In general, the trends of step length asymmetry are inconsistent in chronic stroke survivors, regardless of AFO use [27], [91], [92].

The results of step length as a function of ankle joint design were generally inconclusive, as only subject P2 consistently demonstrated improved step length on the paretic limb, and by extension a reduction in interlimb asymmetry. Declined terrain proved the most difficult to traverse with the AFO, as step length on the paretic limb decreased, increasing inter-limb asymmetry, and this was not sufficiently remedied by the novel ankle joint.

6.3.1.4 Spatiotemporal Parameters Summary

Hypotheses 1, 2 and 5 were partially supported by the results from this study: improvements in walking speed, stance duration, and step length were consistently seen in 1-2 individuals over each terrain type. These improvements led to reduced inter-limb

asymmetry, decreasing the disparity from drop-foot. However, these results were not consistent among all individuals, so the hypotheses were not fully supported.

6.3.2 *Kinematic Parameters*

There were distinct differences in kinematic joint profiles at the ankle, knee, and hip between subjects resulting from intra-subject variability mentioned previously (see Section 6.2).

Subject P1 displayed a prolonged dorsiflexion phase from 0-55% GC, which was a result of inconsistent gait timing averaged over all the cycles for one trial. The crouched gait of Subject P1 meant that the knee was consistently flexed throughout the first 80% GC, before a period of rapid flexion and extension during swing. The same trend was seen at the hip, where gradual extension through late swing achieved only -5° extension prior to TO. The excessive knee flexion demonstrates a decreased ability to ambulate with a normal gait pattern and is reflected in the low Fugl-Meyer and Berg Balance scores.

The ankle angle time series for subject P2 most closely approached that for able-bodied subjects, with distinct phases for early to mid-stance, continuing through early swing. His Fugl-Meyer scores were high, and he retained some voluntary control of the paretic ankle joint. However, excessive extension during mid-stance was observed at the knee; during swing, however, insufficient extension was observed in preparation for HS. The hip angle profile differed only from that of able-bodied subjects in this study in terms

of maximum extension during late stance, peaking at 10° with the novel ankle joint (able-bodied peak extension: 25°).

The gait of subject P3 was characterized by an almost fully extended knee throughout the gait cycle and limited control of the ankle. The ankle angle time series was similar to subject P2; slight plantarflexion to foot flat was achieved, dorsiflexion continued through mid-stance, and some plantarflexion prior to TO. While the subject's Fugl-Meyer scores were similar in magnitude to P2, subject P3 had deficits in sensory perception that may have contributed to differences seen in the slight double dorsiflexion peak during mid-stance. The diminished ROM of the knee (5° extension to 5° flexion) was apparent. The subject achieved slightly greater extension of the hip during late stance, but this did not exceed that of the able-bodied subjects.

As only peak ankle plantarflexion during swing differed significantly in terms of terrain, the remaining kinematic parameters are only compared using level treadmill walking.

6.3.2.1 Peak Ankle Plantarflexion During Swing

Peak plantarflexion during swing is indicative of remnant drop-foot or the efficacy of the orthotic ankle joint function in preventing drop-foot. Without an AFO, post-stroke subjects with drop-foot experience $10\text{-}20^\circ$ of plantarflexion during swing. While solid AFOs restrict this plantarflexion completely, articulated AFOs aim to retain the clinically recommended $5\text{-}7^\circ$, thereby preventing tripping without compromising existing functional mechanics [19-20].

Peak plantarflexion during swing for these post stroke subjects wearing AFOs ranged from 0-1.4° with the conventional ankle joint and 0-3.2° with the novel ankle joint (Figure 5.8). Both plantarflexion ranges were less than able-bodied subjects ambulating in the AFOs who were tested in this study; their healthy limbs were able to overpower the orthotic ankle joint springs to allow up to 4.5° plantarflexion after TO. As both orthotic ankle joints limit plantarflexion, this finding confirms the efficacy of both designs in treating drop foot. Modest differences in peak ankle plantarflexion during swing were observed by terrain; these differences were not consistent across subjects and did not increase plantarflexion sufficiently to suggest increased risk foot clearance with terrain condition for either design.

In contrast to the ankle kinematics observed for this study's able-bodied subjects for whom peak plantarflexion was observed immediately after TO, peak plantarflexion for the post-stroke subjects was observed during late swing. The delayed peak plantarflexion reflect the post-stroke subjects' difficulty in preparation for initial contact with the heel and may be attributed to plantarflexor spasticity or dorsiflexor weakness of the paretic limb. However, as plantarflexion during swing never exceeded 4° (e.g., clinical guideline for articulated AFOs, for any condition [19-20]), the novel ankle joint may be recommended for the prevention of drop-foot. However, the ankle angles reported here are small, within the accuracy range of the motion capture system due in part to skin motion artifact.

6.3.2.2 *Ankle ROM During Stance*

Ankle ROM during stance was divided into the traditional three rockers: 1) plantarflexion motion of the foot from heel strike to foot flat, 2) dorsiflexion of the ankle as the shank rotates over the foot, and 3) powered plantarflexion to propel the limb into swing. In subjects wearing an AFO, ankle ROM in all three rockers can be attenuated by the device, even if residual ankle function remains. For individuals poststroke with drop-foot, the prevention of drop-foot is the primary treatment objective, regardless of the impact on ankle ROM during stance. The novel ankle joint was designed to enable greater ROM during all three rockers during stance compared to the conventional ankle joint.

6.3.2.2.1 *Early Stance (First Rocker)*

During early stance, the orthotic ankle joint and the dorsiflexors act to control foot flat, slowly decelerating the foot as contact progresses from the heel at initial contact to the forefoot. The use of an AFO, even an articulated model, limits this ability by forcing the user to either work against the springs or adopt a foot contact instead of heel contact approach. The novel ankle joint was designed to unlock at heel strike, eliminating the need for the individual to fight the springs to achieve the traditional first rocker style. It was expected that the novel ankle joint would allow greater plantarflexion than the conventional ankle joint. At HS, the able-bodied subjects in this study were able to achieve up to 8° of plantarflexion while wearing their AFOs, compared to literature values of almost 10° in an able-bodied population without AFOs [14].

Greater plantarflexion during early stance was exhibited with the novel ankle joint for subject P3 for both speed trials (conv: 1.40 ± 2.81 , SM: $3.58 \pm 2.75^\circ$, SS: $4.04 \pm 2.39^\circ$). Due to greater kinematic variability demonstrated by subject P2, a significant increase in ankle plantarflexion with the novel joint was only observed during the SM trial (0.3° increase). Only Subject P1 demonstrated significantly reduced ankle plantarflexion with the novel orthotic ankle joint for both the speed trials (conv: $3.22 \pm 1.25^\circ$, SM: $2.00 \pm 1.39^\circ$, SS: $2.75 \pm 1.51^\circ$).

Although subject P3 experienced the greatest improvements in the first rocker with the novel ankle joint, the maximum plantarflexion was 6.5° ; while less than that observed for able-bodied individuals, this result is particularly promising. Despite the ankle being slightly dorsiflexed at HS, the subjects were able to achieve foot flat gradually, without foot slap. Further tuning of the novel joint spring stiffness might further enhance the unlocking mechanism, as was demonstrated by Yamamoto et al. with a novel oil damper ankle joint [52].

6.3.2.2.2 *Mid-Stance (Second Rocker)*

The second rocker of stance involves ankle dorsiflexion as the shank rotates over the foot and the body center of mass advances. For able-body subjects without an AFO, this angle typically includes $20\text{-}25^\circ$ of ankle dorsiflexion. For the three able-bodied subjects wearing the novel ankle joint, approximately 21° ankle dorsiflexion was observed. It was expected that the unlocking mechanism of the novel ankle joint would facilitate greater motion than the conventional joint. As walking speed affects ankle ROM [93], only the SM trials will be discussed.

Ankle ROM during mid-stance differed significantly between ankle joint designs, although the trends were inconsistent between subjects. Ankle ROM significantly decreased with the novel ankle joint for subject P1 (conv: 17.2°, SM: 15.8°). While subject P2 demonstrated significant differences between conventional and novel conditions, the difference was only 0.9° which may not be clinically relevant. Subject P3 demonstrated limited dorsiflexion during the second rocker when compared to the other individuals and also displayed a significant decrease in ankle ROM with the novel joint (conv: 9.2°, SM: 9.90°).

The novel ankle joint did not enhance ankle dorsiflexion during the second rocker of treadmill walking as expected. Past studies have reported greater mid-stance ankle ROM with other designs of articulated ankle joints (oil damper: $20.14 \pm 8.01^\circ$ [52], spring piston slider: 19° [69]), suggesting that there needs to be further design changes and/or additional tuning of the joint springs to achieve higher levels of mobility.

6.3.2.2.3 *Late Stance (Third Rocker)*

During late stance, the plantarflexors provide active push-off to propel the limb into swing. Ankle plantarflexion typically occurs during late stance, although the associated third rocker reflects rotation about the metatarsal heads. For the able-bodied subjects evaluated with an AFO in this study, plantarflexion during the third rocker remained between 8-16°, which is attenuated from the nearly 20° of powered plantarflexion for able-bodied subjects tested without an AFO in the literature [4]. As the novel ankle joint remains unlocked throughout weight bearing, this design was expected

to permit greater plantarflexion (and plantarflexor activity) during late stance in post-stroke subjects.

Subject P3 demonstrated increased ankle plantarflexion during late stance with the novel ankle joint for both trials (conv: $0.74 \pm 0.49^\circ$, SM: $2.19 \pm 1.24^\circ$, SS: $2.32 \pm 1.46^\circ$). Ankle plantarflexion during late stance was highly variable for subjects P1 and P2; mean peak plantarflexion decreased by approximately 1° with the novel versus conventional ankle joint, although these differences were not statistically significant. It was expected that subjects P2 and P3 would have demonstrated greater plantarflexion during the third rocker than P1, as they had much higher functional scores and retained some control of the affected limb. However, though P1 displayed greater flaccidity than the other two subjects, both subjects P2 and P3 received regular Botox injections to control the spasticity in the affected limb. These injections may have affected their ability to control the plantarflexors and attenuated powered plantarflexion during the third rocker.

Residual plantarflexor function is variable in individuals post-stroke with drop-foot, and walking studies have reported these individuals may be capable of $0-14^\circ$ of plantarflexion when walking *without* an assistive device [52], [53], [58]. AFO treatment, regardless of design, generally restricts ankle plantarflexion during late stance, and articulated AFOs, including this novel ankle joint, typically limit powered plantarflexion to 4° [52], [53], [58]. Instead, non-articulated AFOs that emphasize energy absorption and return (posterior leaf-spring and Dual Carbon Fiber Spring AFOs) have been demonstrated to preserve the range of motion during push off up to $12-16^\circ$ respectively, offering potential future design considerations [58].

This study did not test walking ability without an AFO and as such it is unclear whether these subjects would be able to provide a greater level of plantarflexion than what was observed.

6.3.2.3 *Knee Flexion during Stance*

The treatment of drop-foot with AFOs often compromises knee kinematics during the first rocker of stance. For able-bodied individuals, the knee is extended at heel strike and slightly flexes at foot flat. For post-stroke individuals, the use of an AFO pulls the tibia forward to compensate for the restricted motion of the ankle, increasing knee flexion during loading and increasing potential knee instability. Therefore, the unlocking mechanism of the novel ankle joint is expected to decrease knee flexion of the paretic limb during stance due and reduce interlimb asymmetry compared to the conventional joint.

Subject P1 overall consistently demonstrated almost 20° greater knee flexion during the loading response for all ankle joint conditions relative to the other two subjects; this was due to her crouched gait. This knee flexion of P1 during the loading response was significantly increased with the novel joint for the SM condition (conv: $35.8 \pm 12.9^\circ$, SM: $36.9 \pm 12.9^\circ$), which was also observed for subject P3 (conv: $7.60 \pm 1.62^\circ$, SM: $7.98 \pm 1.34^\circ$). In contrast, knee flexion was significantly reduced for subject P2 with the novel joint during the SM condition (conv: $17.8^\circ \pm 6.2$, SM: $16.1 \pm 6.51^\circ$) and subject P3 during the SS condition (conv: $7.60 \pm 1.62^\circ$, SS: $6.72 \pm 1.43^\circ$).

The corresponding interlimb asymmetry (SR) in knee flexion was assessed to determine whether the novel ankle joint was able to return the limbs to parity. Symmetrical gait correlates strongly with stages of recovery, fall risk, and walking speed, all of which improve functional outcomes for the individual [27].

The interlimb asymmetry for knee flexion during the loading response varied. Subject P1 consistently demonstrated greater knee flexion with the paretic limb (e.g., $SR > 0$), while subjects P2 and P3 conversely demonstrated greater knee flexion with the unaffected limb ($SR < 0$). This effect was especially pronounced for subject P3; the paretic limb retained knee extension during the loading response while the unaffected limb exhibited healthy knee flexion, resulting in asymmetry levels greater than 75%. Even though subject P3's peak paretic limb knee flexion during the loading response decreased for the SS trial, knee flexion during loading response of the *unaffected* limb increased; the corresponding asymmetry therefore increased. Similar bilateral knee flexion occurred for subject P2 during the SS trial.

The comparison of articulated ankle joints in AFOs performed by Mulroy et al. determined that an ankle joint which assisted dorsiflexion during swing demonstrated lower knee flexion during the loading response (17.4°) when compared to a device which only inhibited drop-foot (20.3°) [37]. Despite the novel ankle joint unlocking at HS to permit greater mobility, it appears that the ability to increase the initial angle of dorsiflexion at HS has a greater impact on decreasing abnormal flexion of the knee during the loading response. This response was also seen in the able-bodied subjects tested in this study with an AFO, where ankle joint conditions were comparable in producing $16\text{-}22^\circ$ of knee flexion during the loading response.

The design goal for the novel ankle joint was to unlock the ankle at heel strike thereby supporting the first rocker to facilitate foot flat, enhance knee stability, and decrease knee flexion during loading response. All subjects displayed slightly lower knee flexion with the novel ankle joint while speed matched, but the same trend was not observed for the SS condition. Surprisingly, while ankle plantarflexion in the first rocker was improved for subject P3, knee flexion during loading response and interlimb asymmetry were not. However, subject P3 generally walked with an extended knee, which could contribute to successful actuation of the novel ankle joint and prevent knee flexion from occurring in the first place.

6.3.2.4 Hip Flexion during Stance

The amount of hip flexion during loading phase is linked to that at the knee; both are affected by use of an AFO. The forward shifting of the tibia due to a rigid AFO compromises knee joint motion, which in turn, can be transferred to the hip [28]. Hip flexion was assessed in terms of peak magnitude and interlimb asymmetry to assess the impact of the novel ankle joint on walking functional performance; both hip flexion and interlimb hip flexion asymmetry during loading response were expected to decrease.

Subjects P1 and P2 demonstrated less hip flexion with the novel orthotic ankle joint, although this was true only for subject P1's SM trial (P1 – SM:19.8°; P2 – SM:14.8, SS: 15.8°). Only subject P3 during the SM condition displayed greater hip flexion for the loading response with the novel joint (conv: $17.7 \pm 3.48^\circ$, SM: $20.4 \pm 2.81^\circ$).

The interlimb asymmetry in hip flexion during loading response was variable between subjects, although similar trends were observed to those seen in the peak values. Subject P1 exhibited greater peak hip flexion during loading response with the paretic limb (e.g., $SR > 0$); her hip flexion asymmetry range was modest (conv: 7.03%, SS: 5.86%). In contrast, subjects P2 and P3 typically exhibited greater hip flexion during loading response with the unaffected limb (e.g., $SR < 0$); the standard deviation of SR for subject P2 exceeded 35% for all conditions. The only statistically significant difference in interlimb asymmetry in hip flexion during the loading response due to ankle joint condition was observed for subject P3, where the conventional joint resulted in greater hip flexion symmetry than the SM trial, corresponding to the difference in peak hip flexion (conv: -18.0%, SM: -22.9%).

The peak hip flexion values seen here are comparable to those reported for the novel oil damper AFO ankle joint ($23.9 \pm 5.58^\circ$) and another double action joint design ($20.6 \pm 11.4^\circ$), both of which are greater than walking without an AFO ($19.7 \pm 10.9^\circ$) [52], [59]. It appears that there are currently no designs of ankle joint that reduce flexion at the hip without first reducing that of the knee, which none of the studies reported as achieving lower than 16.3° [59]. It may be that the novel ankle joint design did not sufficiently increase the mobility of the ankle during the first rocker for post-stroke subjects; as mentioned in Section 6.3.2.2.1 even able-bodied subjects wearing AFOs were able to maintain at least 8° , which contributed to lower knee and hip flexion than the post-stroke subjects.

Though each individual exhibited lower peak hip flexion on the paretic limb for at least one trial of the novel ankle joint when compared to the conventional design, there

were no real improvements in asymmetry level. The large values for hip flexion SR standard deviation indicate that neither of the joints are able to produce consistent changes in interlimb symmetry by solely controlling peak hip flexion.

6.3.2.5 *Kinematic Parameters Summary*

Ankle plantarflexion during swing was controlled by the novel ankle joint at a sufficient level to prevent drop foot, supporting Hypothesis 2. Future designs may require stiffer springs for individuals with poor voluntary plantarflexion control.

The novel ankle joint did not demonstrate consistent increases in ankle ROM during all three rockers; Hypothesis 3 was only partially supported. Ankle plantarflexion during the first rocker was the most promising functional improvement.

Despite the improvements seen in first rocker ankle ROM, reduced knee flexion of the paretic limb during loading response and the corresponding interlimb symmetry in knee flexion was not supported. Reduced hip flexion of the paretic limb during loading response, however, was more commonly observed; but this did not produce meaningful changes in interlimb hip asymmetry. Hypothesis 4 and 5 are rejected based on these findings.

6.3.3 *Kinetic Parameters*

The examination of kinetic parameters in gait analysis help to more fully describe the individual's ability to walk and compensatory gait pathologies that may guide design of AFOs. These kinetic parameters were measured during overground level walking, and

there was no data collected for subject P1 due to short strides and low walking speed. While the orthotic ankle joint affected temporal, spatial, and kinematic measures, these differences resulted in no significant differences in the corresponding kinetic parameters (hip and knee flexion/extension moments in the sagittal plane only) between AFO conditions. The observed trends in these kinetic parameters and their associated interlimb asymmetry are discussed (Hypothesis 5).

6.3.3.1 *Knee Extension Moment*

The internal knee extension moment during the loading response is elevated in AFO users due to the limited ankle ROM and rigid nature of the AFO. A reduction in this extension moment is considered an improvement in walking ability, and articulated AFOs are considered advantageous at lowering this moment when compared to solid AFOs [37]. The extension moment and corresponding interlimb asymmetry were assessed to determine if the novel ankle joint reduced abnormal forces on the knee by further increasing the ankle mobility over a conventional articulated joint.

Subjects P2 and P3 demonstrated comparable knee extension moments during loading response between their current AFO and the conventional ankle joint (P2 – curr: 1.21 ± 0.48 , conv: 1.22 ± 0.22 ; P3 – curr: 0.77 ± 0.09 , conv: 0.81 ± 0.16 Nm/kg). Both individuals exhibited a lower knee extension moment with the novel ankle joint, although only modestly for subject P3 (P2: 1.0 ± 0.36 Nm/kg, P3: 0.74 ± 0.09 Nm/kg). The lack of significance may be attributed to the reduced number of trials during these overground trials for kinetic analysis, in contrast to the large number of trials for the treadmill walking for which the peak knee flexion was analyzed.

The corresponding interlimb asymmetry in knee extension moment during loading response was more varied, with an almost even distribution between sign of SR. Subject P2 had a larger variability in asymmetry with the novel ankle joint than with both the current AFO and conventional joint (curr: $-16.3 \pm 8.9\%$, conv: $3.37 \pm 14.7\%$, novel: $-2.86 \pm 42\%$); the opposite trend was seen for subject P3 (curr: $5.40 \pm 36.4\%$, conv: $-3.58 \pm 15.1\%$, $-9.02 \pm 10.2\%$). The large variation may be attributed to the ability of the unaffected limb to compensate for the paretic side, but it is more likely that there were difficulties with data collection over the larger capture volume, when coupled with fewer gait cycles, that increased the variability between trials. The inverse dynamics calculations rely on accurate kinematic information from motion capture; incorrect joint angles propagate error.

Mulroy et al. found that two types of articulated ankle joints were able to reduce the knee extension moment during the loading response, but this effect was attenuated in individuals with greater impairment [37]. While subject P3 had similar functional scores to subject P2, the obvious differences in gait compensation (e.g., P3's constantly extended knee and paretic limb circumduction) could compromise optimal performance of the ankle condition to alter kinetics at this joint.

6.3.3.2 Hip Extension Moment

Similar to the knee, the extension moment at the hip was examined to investigate the ability of the novel ankle joint to decrease abnormal kinetics during the loading phase of stance. Immediately after HS, the mechanics of current orthotic ankle joints pull the tibia forward and produce instability through the knee to the hip. The hip extension

moment during the loading phase was similar across joint conditions for the able-bodied subjects of this study while wearing an AFO (range: 0.2-0.35 Nm/kg), though this could change in a post-stroke population. It is expected that the novel joint would lower peak hip extension moments and improve inter-limb asymmetry during the loading response when compared to the conventional joint due to the unlocking mechanism.

Hip extension moments were highly variable in the two post stroke subjects, most likely due to the extensive marker drop from a limited field of vision on the left side of the capture volume and obstruction of markers. As a result, the hip joint moment profiles are questionable, especially for subject P2, as can be seen in the large standard deviation (Figure 5.18). While the results require further trials to be fully trusted, peak hip extension moments for P2 followed the same trend observed for the knee extension moments: the novel AFO produced the lowest moment (curr: 1.08 ± 0.75 Nm/kg, conv: 1.33 ± 0.44 Nm/kg, novel: 0.58 ± 0.44 Nm/kg). Similarly, subject P3 demonstrated comparable peak hip extension moments for all three conditions, ranging from 0.43-0.5 Nm/kg.

The trends in interlimb asymmetry in hip extension moment with orthotic joint conditions varied for each subject. For subject P2, the novel joint resulted in increased asymmetry (novel: $-52.1 \pm 20.0\%$, conv: $-19.5 \pm 15.1\%$). For subject P3, hip moment asymmetry was decreased with the novel joint (conv: $-51.5 \pm 5.79\%$, novel: $-38.6 \pm 38.5\%$), although the large standard deviation suggests issues with data capture.

It's possible that the different ankle joint conditions produced different stiffnesses, attenuating the moment seen at the hip. Haight et al. determined that a compliant AFO produced lower hip extension moments than one with increased spring

stiffness [23]. Based on these findings, subject P2 responded to the novel ankle joint as being less stiff than the conventional, while P3 had approximately the same response for all joints. This may indicate that the AFO joints were improperly tuned for subject P3, who as the largest subject, might require stiffer springs to produce greater changes in function. Unfortunately, none of the prior studies reported hip extension moments bilaterally so interlimb asymmetry could not be compared.

6.3.3.3 Kinetic Parameters Summary

As there were no statistically significant differences in knee or hip extension moment or the corresponding interlimb asymmetry measures, Hypothesis 5 was not supported.

6.3.4 Subject Perception

Subject perception is critical to the adoption of novel medical devices, as a therapy may not be utilized if the user does not perceive it as helpful or comfortable. Post-testing surveys were administered to identify potential design concerns that compromised user comfort or perceived performance. Without metabolic testing, self-reported perceived exertion was the sole measure to assess the novel joint's ease of use. It was expected that users would consider the novel joint as comparable or superior to the conventional in terms of perceived exertion and comfort, and superior in walking performance.

The post-testing surveys administered to able-bodied subjects after use of the conventional and novel ankle joint AFOs were inconclusive for all metrics (walking performance, comfort, and perceived ease of use). In general, the two joint conditions were seen as identical, which can be expected from a group of individuals who do not need an AFO to ambulate, as any condition would be expected to be less comfortable than unassisted walking.

For post-stroke individuals, the novel ankle joint ranked higher in walking performance and comfort compared to the conventional model. While only subject P2 ranked the novel ankle joint as “superior” to the conventional joint for perceived exertion, neither of the other two individuals scored it “worse” than the conventional joint. A potential factor for lower perceived ease scores could be related to fatigue, as all novel ankle joint trials on the treadmill were last in the testing order. All subjects noted feeling some fatigue during the SM trials, but this fatigue was likely due more to extended ambulation over advanced terrain two times previously than the novel ankle joint making walking more difficult.

6.3.4.1 Subject Perception Summary

In general Hypothesis 6 was supported; perceived exertion was reduced and both comfort and walking performance were improved with the novel ankle joint for these post-stroke individuals.

6.4 CLINICAL RELEVANCE

The novel joint design demonstrated modest improvements in ankle joint mobility during early and late stance, walking speed during level overground trials, and step length when compared to the conventional joint. These results indicate the novel ankle joint design may be viable for clinical use, pending further research to refine prescription and indications for use.

6.4.1 *Prescription*

The intended market or population for the novel ankle joint was, and remains, a less impaired unilateral post stroke population with drop-foot, namely: individuals who are able to:

- 1) walk with a heel strike first pattern as required to actuate the locking mechanism
- 2) control plantarflexion activation
- 3) maintain quadriceps strength to control at least 20° of knee ROM in the sagittal plane to prevent paretic limb circumduction

The novel ankle joint is contraindicated for individuals such as subject P1 who lack the necessary coordination and strength to take advantage of the increased mobility of the ankle joint. In fact, the increased flexibility of the joint may compromise their stability; a solid AFO or articulated AFO with pin stops would be more appropriate. If trials continued for these individuals, clinicians should preface use with physical therapy to

strengthen the quadriceps, gastrocnemius, and tibialis anterior muscles to increase inherent stability before using the device.

6.4.2 Design Refinements

Future refined designs of the novel ankle joint should address the unlocking mechanism and adjustability of the stop tabs to enhance performance. The unlocking mechanism was not actuated as smoothly as expected; energy was absorbed due to soft tissue compression at heel or foot strike. The failure of the springs to disengage efficiently was compounded by the inability of some individuals to walk with a heel strike first gait pattern, which requires the design to be more sensitive to suboptimal “foot” strikes. To further this goal, stiffer springs or modifications to permit pin stops might be added to increase the ankle dorsiflexion angle at heel strike. Testing also revealed a need for tuning adjustability in the permitted ankle ROM while unlocked; limited ROM during stance may necessitate redesign of the stop tabs. These might be shaped for each individual via a custom template and attached to the main body of the joint with screws for easy removal but may not be feasible due to increased cost and maintenance.

6.4.3 Fabrication and Fitting

It is recommended that the fabrication of the novel ankle joint and AFO be revised to enhance performance. While the Gaffney Free Motion joint permitted translational motion and may have been appropriate for this preliminary research study, this joint limited smooth walking ability. Clinical AFO use should incorporate a

conventional dorsiflexion assist joint medially or use the novel ankle joint bilaterally. In addition, the spring plunger holes should be altered. These holes were limited in diameter and placement due to the design constraints of matching the approximate size and shape of the conventional joint, making spring selection difficult and restricting individual tuning. In the future, the diameter of the holes should be increased, as should the number of holes and/or placement options to more effectively actuate unlocking at heel strike.

As mentioned previously, the current design of the novel ankle joint does not permit the use of pin stops in place of spring plungers to improve support of the foot during swing. Pins are an important clinical tool for preventing drop-foot in some individuals. As such, the orthotist was limited in his ability to effectively fit subject P1 to maximize functional ability, which could be addressed through the design modifications listed above.

6.5 STUDY LIMITATIONS

There were several study limitations and their causes can be categorized into subject population, experimental protocol, and kinematic analysis.

6.5.1 *Subject Sample Size*

The initial intent of the study was to recruit 10 post-stroke subjects to have sufficient power for statistical analysis of self-selected overground walking speed and ankle ROM during stance (see Chapter 4, Section 4.5). The subject selection criteria were constrained to chronic post-stroke subjects with drop-foot, a disparate population for

whom the novel orthotic ankle joint might benefit. Despite recruitment from two post-stroke databases, only 3 subjects were recruited and tested during the grant funded study duration. While the post-stroke recruitment databases were fairly extensive, the specific selection criteria (AFO use, no additional assistive device during ambulation, and walking duration for five minutes without rest) disqualified many potential study participants.

The difficulty in recruitment may have contributed to the lack of differences seen in parameters between conditions, limiting the power to 11.1% when considering differences in ankle ROM during mid-stance and 9.67% for self-selected walking speed. As such, if this group of individuals is representative of the post-stroke population with drop-foot, 55-82 subjects would need to be recruited for there to be demonstrable changes in joint condition.

The paired t-test was chosen to compare the effects of ankle joint condition but is associated with error due to unequal sample sizes. This test requires the same number of cycles to be present for each condition for comparison, which was difficult to achieve with marker drop out or cycle exclusion. While the power may have been slightly reduced by using this test, most metrics had at least 15-70 clean cycles each.

6.5.2 Experimental Protocol Design

The test protocol was designed to minimize orthotic joint changes (AFO donning/doffing), subject safety, and risk of potential fatigue. Specifically, the protocol dictated that the testing order was current AFO, followed by conventional joint trials and

then novel joint trials, all while switching between overground and treadmill testing conditions. However, this single test session protocol limited acclimation time to 10-20 minutes with the various ankle joint conditions as the subjects were not given the device to use at home. Prior AFO use may also have biased the results, as mentioned previously, only one subject regularly used an AFO to ambulate in the community; one subject relied on a walker and another the Bioness FES device for community ambulation. All these factors could contribute to a feeling of instability with the novel ankle joint, which requires a specific gait pattern (heel strike first) to unlock the mechanism to increase mobility. As such, individuals could be walking with a suboptimal gait pattern, reducing the efficacy of the joint, increasing fatigue, and reducing subject comfort.

The optimized test protocol listed above also prevented randomization of ankle joint conditions. The subjects began with their current AFO to establish familiarity with the testing procedures before moving to the conventional ankle joint condition and finally the novel ankle joint. The goal of performing novel ankle joint trials last was to ensure subject familiarity with the testing tasks before introducing a novel and potentially unsettling condition. The lack of randomization may have introduced training effects and subjects may have experienced more fatigue at the end of trials with the novel ankle joint, especially when traversing difficult terrain, despite ample time given for breaks between conditions and trials. The fatigue experienced as testing continued could affect the selection of walking speed, kinematics of the final treadmill trials, and subject perception of perceived exertion while using the novel joint. Because novel ankle joint testing was performed last, most of these effects would be exhibited there, potentially explaining

disparities between SS and SM trials despite some subjects performing both sets of trials at the same speed.

6.5.3 *Kinematic Analysis*

The traditional Helen Hayes marker system for gait analysis was modified in this study to minimize potential pelvic marker drop out during treadmill and overground walking. However, pelvic marker dropout remained problematic due to the treadmill safety harness, railings, and subject's swinging arms – despite redundant cameras. While gait cycles with gaps of more than 10 frames were omitted from analysis, polynomial marker interpolation, together with marker-skin movement artifact, have been reported to contribute to kinematic errors ranging from 5-8° flexion/extension [94], [95]. Such error magnitudes exceed the observed variations within ankle joint conditions and the within trial variability in joint ROM and peak values. While the Helen Hayes marker system is common, this marker set poorly approximates joint centers for overweight individuals for whom marker placement over bony landmarks is imprecise [77].

This study only explored the metrics of interest in the sagittal plane, as the ankle joint conditions being tested only attempted to control gait in this anatomical plane. However, pelvic obliquity in the coronal plane has been found to significantly change with AFO use in chronic stroke patients used to wearing AFOs daily [96], [97]. Additionally, some subjects benefit from the use of anterior or posterior AFOs to control inversion/eversion of the paretic foot that results after a stroke [67]. It is expected that only the pelvis or ankle kinematics and kinetics would benefit from analysis in the coronal plane, and only for individuals with apparent gait pathologies. The excessive

tibial rotation and circumduction of subject P3 were not characterized well by measurements in the sagittal plane, and as such it is unknown whether the novel ankle joint had a positive effect on these gait pathologies.

With the exception of self-selected walking speed overground, the kinematic and spatiotemporal parameters (stance duration, step length, ankle plantarflexion during swing, ankle ROM during stance, knee and hip flexion during stance) were based solely on the treadmill walking trials, thereby maximizing the number of gait cycles while controlling speed over level and non-level terrain to minimize fall risk. However, treadmill walking differs from overground walking [83] and the sustained, controlled durations of inclined, level and declined walking differs from community ambulation which typically includes short ramps and for which individuals may adjust their speed and cadence. Specifically, for able-bodied subjects, level treadmill versus overground walking was found to affect hip ROM and cadence [83]. Subjects in this study were aware that they would be ambulating for an extended period of time while traversing the advanced terrain, and the inability to modulate the speed during the trial could encourage them to select a slower speed than may have been possible using the novel ankle joint. Walking speed has a large effect on kinematics of the knee and ankle [98], and selection of a suboptimal speed with the novel joint could mask its true effects on modifying ankle mobility.

6.6 PROTOCOL MODIFICATIONS AND FUTURE STUDIES

Based on the current study, future analysis of the training effects of the novel ankle joint design on spatiotemporal and kinematic characteristics should be explored.

Modifications to the testing protocol to address the above limitations should be performed to reduce experimental error in the results.

Future work should concentrate on the long-term effects of the novel ankle joint design to determine whether training with the device could continue to improve gait past initial prescription. At least 15 subjects should be recruited from several clinician offices or support groups and should be excluded if there is poor plantarflexion control, a non-heel strike first walking pattern, or weak quadriceps that results in reduced paretic knee flexion. Each subject will be cast for one AFO that will support swapping of the novel and conventional ankle joints between acclimation sessions. The AFO will integrate one joint on each side of the ankle, so that the effects of the joints can be isolated. At the fitting session, the first ankle joint condition will be randomly assigned before complete tuning of the device occurs. The subject will be blinded to which condition they are currently using.

The fully tuned and fitted AFO will be provided to the individual for an initial one-week acclimation period before baseline testing, requiring gradual AFO use (e.g., 1-2 hours/day) [6]. Walking performance with the AFO will be measured with the same spatiotemporal and kinematic parameters evaluated in the current study (walking speed, stance duration, step length, ankle plantarflexion and ROM, knee and hip flexion) during treadmill walking over level terrain only. The testing session should include 3 trials, each consisting of 5 minutes of walking and a 10-minute break between trials to rest.

The subject will continue use of the AFO for a one-month training period at home with an activity monitor and diary to record use of the AFO for quantifying the amount of training. The second testing session should be recorded after the one-month training

period to measure changes in the same parameters as an effect of the prolonged use. The process will then be repeated with the other ankle joint (one-week acclimation, baseline testing, one-month training, and final testing session) to fully measure the efficacy of the novel ankle joint design.

After a period of acclimation and training it is expected that the novel ankle joint will outperform the conventional ankle joint by:

- 1) increasing self-selected walking speed
- 2) improving inter-limb asymmetry for stance duration and step length
- 3) increasing ankle ROM during the first and third rockers
- 4) reducing knee flexion during the loading response

The results of this proposed future study should make clarify how the novel ankle joint design modifies spatiotemporal and kinematic parameters of community ambulation, the effect of training on using the novel ankle joint effectively, and the relative benefits of the novel ankle joint when compared to a conventional articulated design.

6.7 Summary

In summary, gait analysis performed on post-stroke subjects walking with the novel and conventional orthotic ankle joints were assessed to isolate the following trends (Table 6.2).

Table 6.2 Hypothesis testing results and trends.

Hypothesis	Supported?	Trend
1	Yes	Self-selected walking speed overground was greatest with the novel ankle joint for most subjects, subject P2 selected a faster treadmill walking speed.
2	Yes	Ankle plantarflexion was comparable for all subjects but P3, even then it was enough to provide foot clearance.
3	Partially	Improvements in walking speed, stance duration, and step length were seen for all individuals. Ankle ROM was consistently improved during all rockers for all individuals.
4	Partially	Knee flexion during the loading response was not reduced, but hip flexion during stance for two or the three subjects was improved.
5	No	In general, asymmetry between limbs was increased for kinetic and kinematic variables using the novel ankle joint but were dependent on subject.
6	Yes	Perceived exertion was lower with the novel ankle joints, perceived comfort and walking performance were improved.

This study was able to characterize walking mechanics with different designs of articulated AFO joints for both overground and treadmill walking, enhancing the limited present literature.

7 Conclusion

This study investigated the function of a novel design for an orthotic ankle joint for thermoplastic AFOs to treat drop-foot for individuals post-stroke and compared it to a conventional design for both a preliminary population of able-bodied individuals as well as a small post-stroke population. Conventional articulated ankle joints perform superiorly to solid AFOs in promoting healthy gait kinematics and kinetics but fail to preserve normal ankle mobility or decrease abnormal knee and hip motion during early stance. While a great deal of research had been performed to characterize walking with AFOs, few studies have investigated the function of novel joint designs for articulated AFOs and their explicit role in improving gait. To address this lack of knowledge, the novel ankle joint design in this study was assessed in terms of its ability on spatiotemporal, kinematic, and kinetic parameters.

The novel ankle joint was for the post-stroke population in the U.S. that experiences drop-foot and regularly walks in the community with an AFO. To facilitate testing, the device had to be the approximate size, shape, and weight of a conventional articulated ankle joint (Becker Double Action) and permit adjustability for subject specific tuning. The design objectives of the device were to 1) remain locked during swing to prevent drop-foot, before 2) unlocking during weight bearing to permit less restricted rotation during stance. The novel ankle joint design was evaluated before human subject testing using common engineering tools to address risks and modes of failure.

Initial gait testing of the ankle joint was performed on three able-bodied individuals to ensure device safety and function before proceeding to the target population. This testing session involved overground walking to quantify kinetic variables and treadmill walking to isolate the spatiotemporal and kinematic effects of AFO joint type; the treadmill trials also supported investigation of level, inclined and declined walking. The session revealed that use of the novel ankle joint produced faster self-selected walking speeds, controlled plantarflexion during swing, and produced comparable ankle ROM during stance to the conventional design. Based on these positive preliminary results, three post-stroke individuals who exhibited drop-foot and walked with an AFO were recruited to conduct gait testing with the different ankle joint conditions.

The testing of the novel ankle joint on post-stroke individuals was accomplished safely and the following key findings were isolated:

- Self-selected walking speed for overground walking significantly improved with the novel ankle joint for two subjects, one of which also selected a faster speed for treadmill walking over inclined/declined terrain.
- The spatiotemporal results were mixed, as 1-2 subjects demonstrated improvements in stance duration and step length using the novel ankle joint, but these were not consistent across all trials, so hypothesis 1 was partially supported.
- Peak ankle plantarflexion during swing was controlled effectively with the novel ankle joint, supporting hypothesis 2 (peak ankle plantarflexion during swing is *comparable* for the novel to that of the conventional joint).

- Ankle ROM during stance was more variable between individuals. Only the first rocker (ankle ROM during loading response) was consistently improved with the novel joint; hypothesis 3 (ankle ROM during stance is *greater* with the novel joint) was only partially supported.
- Despite the consistent improved ankle ROM during loading response with the novel orthotic ankle joint, neither knee nor hip flexion during loading response was consistently nor significantly reduced. Hypothesis 4 (compensatory gait is *reduced* with the novel joint) was rejected.
- No significant changes were found between kinetic variables, making it impossible to fully support hypothesis 5 (kinetic symmetry is *improved* with the novel joint). Finally, subject perception of the novel ankle joint was generally positive, especially for the post-stroke users of the device. The novel joint rated highly in terms of comfort and walking performance and performed comparably to the conventional ankle joint in perceived exertion (hypothesis 6 was supported).

Based on the results of this study, further design refinement and testing should be conducted before clinical adoption of the novel ankle joint to treat drop-foot. The prescription of this novel ankle joint should be restricted to individuals walking with a heel strike first pattern, who are able to control plantarflexion activation, and have adequate strength in their quadriceps to control knee ROM. A number of design refinements, including the removal of the Gaffney joint over the medial malleolus, integration of pin stops, and improved spring selection should be made to expand the group of potential users.

While this study has added to the body of literature a promising novel mechanical design and preliminary comparative functional analysis, these results must be interpreted with caution. First, the sample size of this study was small (N=3) and was composed of diverse individuals who walked with inconsistent gait patterns. Second, the subjects were likely not given sufficient time to adapt to changes in ankle joint function to maximize their effects (e.g., one week of gradually increased use time is generally accepted clinical practice). Finally, the test protocol should randomize ankle joint conditions to minimize potential training and/or fatigue effects. With the above suggested changes, it should be possible to further define the effects of the novel ankle joint on the gait of post stroke subjects and provide more detailed clinical recommendations.

BIBLIOGRAPHY

- [1] E. J. Benjamin, M. Blaha, S. Chiuve *et al.*, “Heart Disease and Stroke Statistics-2017 Update: A Report From the American Heart Association.,” *Circulation*, vol. 135, no. 10, pp. e146–e603, Mar. 2017.
- [2] R. Bohannon, M. Morton, and J. Wilkholm, “Importance of four variables of walking to patients with stroke,” *Int. J. Rehabil. Res.*, vol. 14, no. 3, pp. 246–250, 1991.
- [3] J. F. Lehmann, S. M. Condon, R. Price, and B. J. DeLateur, “Gait abnormalities in hemiplegia: their correction by ankle-foot orthoses.,” *Arch. Phys. Med. Rehabil.*, vol. 68, no. 11, pp. 763–71, Nov. 1987.
- [4] D. Levine, J. Richards, and M. Whittle, *Whittle’s Gait Analysis*, 5th ed. Elsevier Ltd, 2012.
- [5] M. Alam, I. A. Choudhury, and A. Bin Mamat, “Mechanism and design analysis of articulated ankle foot orthoses for drop-foot,” *Scientific World Journal*. pp. 1–14, 2014.
- [6] D. Nawoczenski and M. Epler, *Orthotics in Functional Rehabilitation of the Lower Limb*. W.B. Saunders, 1997.
- [7] L. N. Awad, J. A. Palmer, R. T. Pohlig, S. A. Binder-Macleod, and D. S. Reisman, “Walking Speed and Step Length Asymmetry Modify the Energy Cost of Walking After Stroke,” *Neurorehabil. Neural Repair*, vol. 29, no. 5, pp. 416–423, Jun. 2015.
- [8] D. Lloyd-Jones, R. Adams, M. Carthenon, G. De Simone, T. . Ferguson, and K. Flegal, “Heart Disease and Stroke Statistics - 2009 Update,” *Circulation*, vol. 119, no. 3, pp. e21–e181, 2009.
- [9] R. L. Sacco *et al.*, “An updated definition of stroke for the 21st century: a statement for healthcare professionals from the American Heart Association/American Stroke Association.,” *Stroke*, vol. 44, no. 7, pp. 2064–2089, Jul. 2013.

- [10] A. R. Fugl-Meyer, L. Jääskö, I. Leyman, S. Olsson, and S. Steglind, "The post-stroke hemiplegic patient. 1. a method for evaluation of physical performance.," *Scand. J. Rehabil. Med.*, vol. 7, no. 1, pp. 13–31, 1975.
- [11] K. Berg, S. Wood-Dauphine, J. I. Williams, and D. Gayton, "Measuring balance in the elderly: preliminary development of an instrument," *Physiother. Canada*, vol. 41, no. 6, pp. 304–311, Nov. 1989.
- [12] J. Barton, S. Tedesco, T. Healy, and B. O'Flynn, "Potential for smart knee device to cut down on knee surgery recovery time," *Eng. J.*, 2017.
- [13] J. Rose and J. Gamble, *Human Walking*. 1994.
- [14] J. Perry and J. Burnfield, *Gait Analysis Normal and Pathological Function*, 2nd ed. Thorofare: SLACK Incorporated, 2010.
- [15] C. Shupe, "Abnormal biomechanics of the feet and pudendal neuropathy," in *Pudendal Neuralgia and Lower Extremity Biomechanics*, 2011.
- [16] Z. O. Abu-Faraj, P. A. Smith, G. F. Harris, and S. Hassani, "Human Gait and Clinical Movement Analysis," in *Wiley Encyclopedia of Electrical and Electronics Engineering*, 2015, pp. 1–34.
- [17] T. Oberg, A. Karsznia, and K. Oberg, "Basic gait parameters: reference data for normal subjects, 10-79 years of age.," *J. Rehabil. Res. Dev.*, vol. 30, no. 2, pp. 210–223, 1993.
- [18] C. L. Lewis and D. P. Ferris, "Walking with increased ankle pushoff decreases hip muscle moments," *J. Biomech.*, vol. 41, no. 10, pp. 2082–2089, Jul. 2008.
- [19] J. M. Finley, A. Long, A. J. Bastian, and G. Torres-Oviedo, "Spatial and Temporal Control Contribute to Step Length Asymmetry during Split-Belt Adaptation and Hemiparetic Gait," *Neurorehabil. Neural Repair*, vol. 29, no. 8, pp. 786–795, 2015.
- [20] S. Tyson, H. Thornton, and A. Downes, "The effect of a hinged ankle-foot orthosis on hemiplegic gait: four single case studies," *Proceedings Inst. Mech. Eng. D J. Automot. Eng.*, vol. 14, no. 2, pp. 75–85, 1998.

- [21] B. Silver-Thorn, A. Herrmann, T. Current, and J. McGuire, "Effect of ankle orientation on heel loading and knee stability for post-stroke individuals wearing ankle-foot orthoses," *Prosthet. Orthot. Int.*, vol. 35, no. 2, pp. 150–162, 2011.
- [22] D. J. J. Bregman, J. Harlaar, C. G. M. Meskers, and V. de Groot, "Spring-like Ankle Foot Orthoses reduce the energy cost of walking by taking over ankle work," *Gait Posture*, vol. 35, no. 1, pp. 148–153, 2012.
- [23] D. J. Haight, E. Russell Esposito, and J. M. Wilken, "Biomechanics of uphill walking using custom ankle-foot orthoses of three different stiffnesses," *Gait Posture*, vol. 41, no. 3, pp. 750–756, Mar. 2015.
- [24] E. Owen, "The importance of being earnest about shank and thigh kinematics especially when using ankle-foot orthoses," *Prosthet. Orthot. Int.*, vol. 34, no. 3, pp. 254–269, 2010.
- [25] M. Błażkiewicz, I. Wiszomirska, K. Kaczmarczyk, G. Brzuszkiewicz-Kuźmicka, and A. Wit, "Mechanisms of compensation in the gait of patients with drop foot," *Clin. Biomech.*, vol. 42, pp. 14–19, Feb. 2017.
- [26] J. C. Wall and G. I. Turnbull, "Gait asymmetries in residual hemiplegia," *Arch. Phys. Med. Rehabil.*, vol. 67, no. 8, pp. 550–553, Aug. 1986.
- [27] C. K. Balasubramanian, M. G. Bowden, R. R. Neptune, and S. A. Kautz, "Relationship Between Step Length Asymmetry and Walking Performance in Subjects With Chronic Hemiparesis," *Arch. Phys. Med. Rehabil.*, vol. 88, no. 1, pp. 43–49, Jan. 2007.
- [28] S. J. Olney, M. P. Griffin, T. N. Monga, and I. D. McBride, "Work and power in gait of stroke patients," *Arch. Phys. Med. Rehabil.*, vol. 72, no. 5, pp. 309–314, Apr. 1991.
- [29] D. Surr and T. Cook, *Prosthetics & Orthotics*. 1990.
- [30] T. Kobayashi, M. S. Orendurff, M. L. Singer, F. Gao, and K. B. Foreman, "Contribution of ankle-foot orthosis moment in regulating ankle and knee motions during gait in individuals post-stroke," *Clin. Biomech.*, vol. 45, pp. 9–13, 2017.

- [31] S. F. Tyson and R. M. Kent, "Effects of an ankle-foot orthosis on balance and walking after stroke: A systematic review and pooled meta-analysis," *Arch. Phys. Med. Rehabil.*, vol. 94, no. 7, pp. 1377–1385, 2013.
- [32] J. F. Lehmann, P. C. Esselman, M. J. Ko, J. C. Smith, B. J. DeLateur, and A. J. Dralle, "Plastic ankle-foot orthoses: evaluation of function.," *Arch. Phys. Med. Rehabil.*, vol. 64, no. 9, pp. 402–7, Sep. 1983.
- [33] Center for Prosthetics Orthotics Inc., "Double Upright Adjustable Joint AFO." [Online]. Available: <http://cpo.biz/double-upright-adjustable-joint-af/>. [Accessed: 30-Jul-2018].
- [34] Dallas Cowboys Forum, "Drop Foot. A Death Sentence Or Diluted Talking Point For Jaylon Smith?" [Online]. Available: <https://cowboyszone.com/threads/drop-foot-a-death-sentence-or-diluted-talking-point-for-jaylon-smith.378684/>. [Accessed: 30-Jul-2018].
- [35] Bracemasters International LLC., "Ankle Foot Orthosis." [Online]. Available: http://www.bracemasters.com/products/AFO_ankle_foot_orthosis.php. [Accessed: 30-Jul-2018].
- [36] T. Kobayashi *et al.*, "An articulated ankle-foot orthosis with adjustable plantarflexion resistance, dorsiflexion resistance and alignment: A pilot study on mechanical properties and effects on stroke hemiparetic gait," *Med. Eng. Phys.*, vol. 44, pp. 94–101, 2017.
- [37] S. J. Mulroy, V. J. Eberly, J. K. Gronely, W. Weiss, and C. J. Newsam, "Effect of AFO design on walking after stroke: Impact of ankle plantar flexion contracture," *Prosthet. Orthot. Int.*, vol. 34, no. 3, pp. 277–292, 2010.
- [38] T. Bowman, "Single-Case Study: Traditional Thermoplastic AFO Versus Adjustable Dynamic Response - A Crossover Single-Case Study," *Proceedings Inst. Mech. Eng. D J. Automot. Eng.*, vol. 22, no. 2, pp. 84–90, 2010.
- [39] B. J. May and M. A. Lockard, *Prosthetics & Orthotics in Clinical Practice*. 2011.
- [40] Musculoskeletal Key, "Principles of Lower Extremity Orthoses." [Online]. Available: <https://musculoskeletalkey.com/principles-of-lower-extremity-orthoses/>. [Accessed: 30-Jul-2018].

- [41] Cascade O&P Distributor, “Gaffney Hinge Kit.” [Online]. Available: <https://www.cascade-usa.com/gaffney-hinge-kit.html>. [Accessed: 30-Jul-2018].
- [42] Align Clinic, “Ankle Foot Orthotics (AFO).” [Online]. Available: <http://www.align-clinicwi.com/ankle-foot-orthotics-afo.html>. [Accessed: 30-Jul-2018].
- [43] SPS, “Heavy Duty Oklahoma Ankle Joint.” [Online]. Available: <https://www.spsco.com/becke-heavy-duty-oklahoma-ankle-joint.html>. [Accessed: 30-Jul-2018].
- [44] J. M. Carlson, “The story behind orthotic flexure joint technology,” Blaine, MN, 1998.
- [45] H. Naito, Y. Akazawa, K. Tagaya, T. Matsumoto, and M. Tanaka, “An Ankle-Foot Orthosis with a Variable-Resistance Ankle Joint Using a Magnetorheological-Fluid Rotary Damper,” *J. Biomech. Sci. Eng.*, vol. 4, no. 2, pp. 182–191, 2009.
- [46] J. Furusho *et al.*, “Development of Shear Type Compact MR Brake for the Intelligent Ankle-Foot Orthosis and Its Control; Research and Development in NEDO for Practical Application of Human Support Robot,” in *2007 IEEE 10th International Conference on Rehabilitation Robotics*, 2007, pp. 89–94.
- [47] S. M. Cain, K. E. Gordon, and D. P. Ferris, “Locomotor adaptation to a powered ankle-foot orthosis depends on control method,” *J. Neuroeng. Rehabil.*, vol. 4, no. 1, p. 48, Dec. 2007.
- [48] J. Carberry *et al.*, “Parametric design of an active ankle foot orthosis with passive compliance,” in *2011 24th International Symposium on Computer-Based Medical Systems (CBMS)*, 2011, pp. 1–6.
- [49] A. Schmid *et al.*, “Improvements in speed-based gait classifications are meaningful,” *Stroke*, vol. 38, no. 7, pp. 2096–2100, 2007.

- [50] T. Kobayashi, M. L. Singer, M. S. Orendurff, F. Gao, W. K. Daly, and K. B. Foreman, "The effect of changing plantarflexion resistive moment of an articulated ankle-foot orthosis on ankle and knee joint angles and moments while walking in patients post stroke," *Clin. Biomech.*, vol. 30, no. 8, pp. 775–780, 2015.
- [51] D. J. J. Bregman, V. De Groot, P. Van Diggele, H. Meulman, H. Houdijk, and J. Harlaar, "Polypropylene Ankle Foot Orthoses to Overcome Drop-Foot Gait in Central Neurological Patients: A Mechanical and Functional Evaluation," *Prosthet. Orthot. Int.*, vol. 34, no. 3, pp. 293–304, Sep. 2010.
- [52] S. Yamamoto, M. Fuchi, and T. Yasui, "Change of rocker function in the gait of stroke patients using an ankle foot orthosis with an oil damper: immediate changes and the short-term effects," *Prosthet. Orthot. Int.*, vol. 35, no. 4, pp. 350–359, Dec. 2011.
- [53] J. Romkes and R. Brunner, "Comparison of a dynamic and a hinged ankle-foot orthosis by gait analysis in patients with hemiplegic cerebral palsy," *Gait Posture*, vol. 15, pp. 18–24, 2002.
- [54] Y. L. Kerkum, A. I. Buizer, J. C. van den Noort, J. G. Becher, J. Harlaar, and M.-A. Brehm, "The Effects of Varying Ankle Foot Orthosis Stiffness on Gait in Children with Spastic Cerebral Palsy Who Walk with Excessive Knee Flexion," *PLoS One*, vol. 10, no. 11, Nov. 2015.
- [55] R. van Swigchem, M. Roerdink, V. Weerdesteyn, A. C. Geurts, and A. Daffertshofer, "The Capacity to Restore Steady Gait After a Step Modification Is Reduced in People With Poststroke Foot Drop Using an Ankle-Foot Orthosis," *Phys. Ther.*, vol. 94, no. 5, pp. 654–663, 2014.
- [56] M. L. Singer, T. Kobayashi, L. S. Lincoln, M. S. Orendurff, and K. B. Foreman, "The effect of ankle-foot orthosis plantarflexion stiffness on ankle and knee joint kinematics and kinetics during first and second rockers of gait in individuals with stroke," *Clin. Biomech.*, vol. 29, no. 9, pp. 1077–1080, 2014.
- [57] J. Lewallen, J. Miedaner, S. Amyx, and J. Sherman, "Effect of Three Styles of Custom Ankle Foot Orthoses on the Gait of Stroke Patients While Walking on Level and Inclined Surfaces," *JPO J. Prosthetics Orthot.*, vol. 22, no. 2, pp. 78–83, Apr. 2010.

- [58] K. Desloovere *et al.*, “How can push-off be preserved during use of an ankle foot orthosis in children with hemiplegia? A prospective controlled study,” *Gait Posture*, vol. 24, no. 2, pp. 142–151, 2006.
- [59] R. G. Burdett, D. Borello-France, C. Blatchly, and C. Potter, “Gait comparison of subjects with hemiplegia walking unbraced, with ankle-foot orthosis, and with Air-Stirrup brace,” *Phys. Ther.*, vol. 68, no. 8, pp. 1197–203, Aug. 1988.
- [60] K. J. Nolan, K. K. Savalia, A. H. Lequerica, and E. P. Elovic, “Objective Assessment of Functional Ambulation in Adults with Hemiplegia using Ankle Foot Orthotics after Stroke,” *PM&R*, vol. 1, no. 6, pp. 524–529, Jun. 2009.
- [61] H. Gök, A. Küçükdeveci, H. Altinkaynak, G. Yavuzer, and S. Ergin, “Effects of ankle-foot orthoses on hemiparetic gait,” *Clin. Rehabil.*, vol. 17, no. 2, pp. 137–139, Mar. 2003.
- [62] S. A. Radtka, S. R. Skinner, and M. E. Johanson, “A comparison of gait with solid and hinged ankle-foot orthoses in children with spastic diplegic cerebral palsy,” *Gait Posture*, vol. 21, pp. 303–310, 2005.
- [63] B. Burkett, J. Smeathers, and T. Barker, “Walking and running inter-limb asymmetry for Paralympic trans-femoral amputees, a biomechanical analysis,” *Prosthet. Orthot. Int.*, vol. 27, no. 1, pp. 36–47, Apr. 2003.
- [64] N. Nelson, “Investigation of the Effects of Prosthetic Knee Condition on Novice Transfemoral Amputee Runners,” 2018.
- [65] S. Yamamoto, A. Hagiwara, T. Mizobe, O. Yokoyama, and T. Yasui, “Gait improvement of hemiplegic patients using an ankle-foot orthosis with assistance of heel rocker function,” *Prosthet. Orthot. Int.*, vol. 33, no. 4, pp. 307–323, 2009.
- [66] C. D. M. Simons, E. H. F. van Asseldonk, H. van der Kooij, A. C. H. Geurts, and J. H. Buurke, “Ankle-foot orthoses in stroke: Effects on functional balance, weight-bearing asymmetry and the contribution of each lower limb to balance control,” *Clin. Biomech.*, vol. 24, no. 9, pp. 769–775, Nov. 2009.

- [67] C. C. Chen *et al.*, “Kinematic features of rear-foot motion using anterior and posterior ankle-foot orthoses in stroke patients with hemiplegic gait,” *Arch. Phys. Med. Rehabil.*, vol. 91, no. 12, pp. 1862–1868, 2010.
- [68] S. Kesikburun, F. Yavuz, Ü. Güzelküçük, E. Yaşar, and B. Balaban, “Effect of ankle foot orthosis on gait parameters and functional ambulation in patients with stroke,” *Orig. Artic. Turk J Phys Med Rehab*, vol. 63, no. 2, pp. 143–151, 2017.
- [69] S. Yamamoto, M. Ebina, S. E. Kubo, T. Hayashi, Y. Akita, and Y. Hayawaka, “Development of an Ankle-Foot Orthosis with Dorsiflexion Assist Part 2: Structure and Evaluation,” *J. Prosthetics Orthot.*, vol. 11, no. 2, pp. 24–28, 1999.
- [70] K. M. Robinette *et al.*, “Final Report, Volume I: Summary,” in *Civilian American and European Surface Anthropometry Resource (CAESAR)*, United States Air Force Research Laboratory, 2002.
- [71] Becker Orthopedic, “Ankle Joint Components - Catalog Section 5,” 2016.
- [72] T. L. Saaty, “Decision making with the analytic hierarchy process,” 2008.
- [73] E. Baker, P. Volgewede, T. Current, and B. Silver-Thorn, “Design of a novel ankle joint for an AFO for individuals with drop-foot evaluated on able-bodied subjects.,” *Biomed. Sci. Instrum.*, vol. 55, no. 2, pp. 367–372, 2019.
- [74] E. Feyzullahoglu and Z. Saffak, “The tribological behaviour of different engineering plastics under dry friction conditions,” *Mater. Des.*, vol. 29, no. 1, pp. 205–211, Jan. 2008.
- [75] Gaffney Technology, “Gaffney Hinge Joints,” 2016. [Online]. Available: <https://www.gaffneytechnology.com/products>. [Accessed: 08-Nov-2018].
- [76] G. Sheng-Hsien Teng and M. Shin-Yann Ho, “Failure mode and effects analysis: An integrated approach for product design and process control,” *Int. J. Qual. Reliab. Manag.*, vol. 13, no. 5, pp. 8–26, Jul. 1996.

- [77] Visual3D, “Marker Set Guidelines - Helen Hayes Pelvis.” [Online]. Available: https://www.c-motion.com/v3dwiki/index.php?title=Marker_Set_Guidelines. [Accessed: 31-Jul-2018].
- [78] D. P. Ferris, K. E. Gordon, G. S. Sawicki, and A. Peethambaran, “An improved powered ankle–foot orthosis using proportional myoelectric control,” *Gait Posture*, vol. 23, no. 4, pp. 425–428, Jun. 2006.
- [79] C-Motion WIKI Documentation, “Segment Coordinate System,” 2016. [Online]. Available: https://www.c-motion.com/v3dwiki/index.php/Segment_Coordinate_System. [Accessed: 30-Apr-2019].
- [80] D. N. Filzah Pg Damit, S. M. N. A. Senanayake, O. A. Malik, and P. N. bin P. Tuah, “Instrumented measurement analysis system for soldiers’ load carriage movement using 3-D kinematics and spatio-temporal features,” *Measurement*, vol. 95, pp. 230–238, Jan. 2017.
- [81] Brookside Press, “2.06 Range of Motion.” [Online]. Available: http://brooksidepress.org/basic_patient_care/lessons/lesson-2-positioning-the-patient/2-06-range-of-motion/. [Accessed: 31-Jul-2018].
- [82] A. West, “The Knee-Hip Connection: Muscles and movement,” *Inyegar Yoga*, 2017. [Online]. Available: <https://annwestyoga.com/the-knee-hip-connection-muscles-and-movement/>. [Accessed: 28-Jun-2019].
- [83] F. Alton, L. Baldey, S. Caplan, and M. C. Morrissey, “A kinematic comparison of overground and treadmill walking,” *Clin. Biomech.*, vol. 13, no. 6, pp. 434–440, Sep. 1998.
- [84] University of Texas at Dallas, “Gait Terminology.” [Online]. Available: <https://www.utdallas.edu/atec/midori/Handouts/walkingGraphs.htm>. [Accessed: 01-Apr-2019].
- [85] S. Jun and X. Zhou, “A comparative study of human motion capture and computational analysis tools,” in *The 2nd International Digital Modeling Symposium*, 2003.

- [86] C-Motion WIKI Documentation, “Inverse Dynamics,” 2015. [Online]. Available: https://c-motion.com/v3dwiki/index.php/Inverse_Dynamics. [Accessed: 30-Apr-2019].
- [87] D. G. E. Robertson, G. Caldwell, J. Hamill, G. Kamen, and S. Whittlesey, *Research Methods in Biomechanics*. 2004.
- [88] J. M. Finley and A. J. Bastian, “Associations between Foot Placement Asymmetries and Metabolic Cost of Transport in Hemiparetic Gait,” *Neurorehabil. Neural Repair*, vol. 31, no. 2, pp. 168–177, 2017.
- [89] S. Kimel-Naor, A. Gottlieb, and M. Plotnik, “The effect of uphill and downhill walking on gait parameters: A self-paced treadmill study,” *J. Biomech.*, vol. 60, pp. 142–149, Jul. 2017.
- [90] K. Kawamura, A. Tokuhira, and H. Takechi, “Gait analysis of slope walking: a study on step length, stride width, time factors and deviation in the center of pressure.,” *Acta Med. Okayama*, vol. 45, no. 3, pp. 179–84, Jun. 1991.
- [91] M. A. Dettman, M. Linder, and S. Sepic, “Relationships among walking performance, postural stability, and functional assessments of the hemiplegic patient,” *Am. J. Phys. Med. Rehabil.*, vol. 66, no. 2, pp. 77–90, 1987.
- [92] C. M. Kim and J. J. Eng, “Symmetry in vertical ground reaction force is accompanied by symmetry in temporal but not distance variables of gait in persons with stroke,” *Gait Posture*, vol. 18, no. 1, pp. 23–28, Aug. 2003.
- [93] S. van Hove, B. Leenstra, P. Willems, M. Poeze, and K. Meijer, “The effect of age and speed on foot and ankle kinematics assessed using a 4-segment foot model,” *Medicine (Baltimore)*, vol. 96, no. 35, p. e7907, Sep. 2017.
- [94] A. Cappozzo, F. Catani, A. Leardini, M. Benedetti, and U. Della Croce, “Position and orientation in space of bones during movement: experimental artefacts,” *Clin. Biomech.*, vol. 11, no. 2, pp. 90–100, Mar. 1996.
- [95] A. Cappello, A. Cappozzo, P. F. La Palombara, L. Lucchetti, and A. Leardini, “Multiple anatomical landmark calibration for optimal bone pose estimation,” *Hum. Mov. Sci.*, vol. 16, no. 2–3, pp. 259–274, Apr. 1997.

- [96] T. H. Cruz and Y. Y. Dhaher, "Impact of ankle-foot-orthosis on frontal plane behaviors post-stroke," *Gait Posture*, vol. 30, no. 3, pp. 312–316, Oct. 2009.

- [97] C. D. M. Nikamp, M. S. H. Hobbelink, J. van der Palen, H. J. Hermens, J. S. Rietman, and J. H. Bourke, "A randomized controlled trial on providing ankle-foot orthoses in patients with (sub-)acute stroke: Short-term kinematic and spatiotemporal effects and effects of timing," *Gait Posture*, vol. 55, pp. 15–22, Jun. 2017.

- [98] C. Kirtley, M. W. Whittle, and R. J. Jefferson, "Influence of walking speed on gait parameters," *J. Biomed. Eng.*, vol. 7, no. 4, pp. 282–288, Oct. 1985.

APPENDIX A: ALTERNATIVE DESIGNS

The first of the three designs used a cam and spring-loaded pin (Figure A.1).

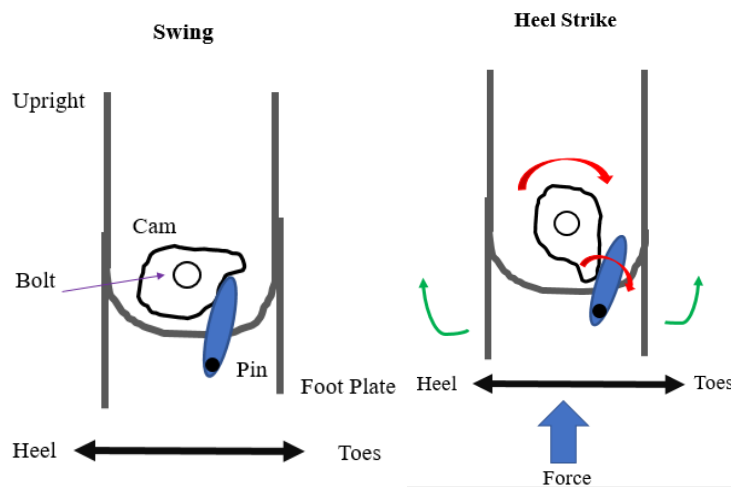


Figure A.1 Cam design with spring-loaded pin and unique cam shape.

The function of the cam is to take the rotational motion of the ankle and translate it into linear motion. There is a total of three pieces: upright, cam, and footplate that connected with a bolt through the center of each piece. The footplate pin presses against a notch on the cam during swing, preventing plantarflexion from drop foot. As soon as pressure from initial contact is applied, the pin pushes against the cam to rotate past the notch, leaving the cam free to rotate. The cam moves with the footplate, enabling plantarflexion from initial contact through push off. During pre-swing, the cam reengages against the pin and locks until the next heel strike.

The second proposed design consists of a pair of twisting plates to be inserted between the footplate and upright, connected by a bolt with a wave spring along its length (Figure A.2).

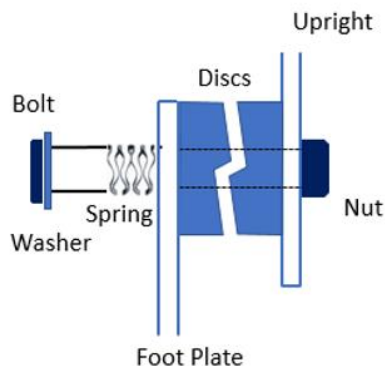


Figure A.2 Locking discs design.

The discs are in contact; any rotation causes the discs to twist apart. Plantarflexion is limited to approximately 10° ; dorsiflexion is unconstrained. The spring resists this motion during swing; once the user makes initial contact, this spring force is overcome by the GRF. The resistance can be modified by changing the spring stiffness to adjust for differences in individual size and mass.

The final design uses linear displacement at initial contact and push off, powered by spring actuation, to lock the joint during swing while keeping stance free (Figure A.3).

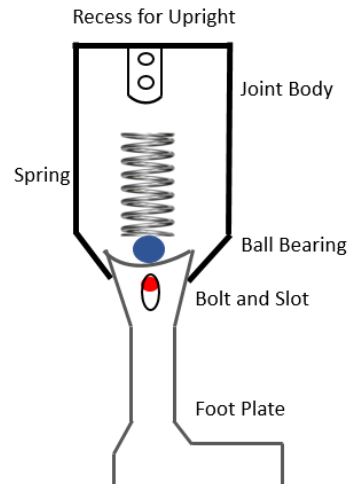


Figure A.3 Initial prototype design sketch of linear spring system.

The body of the joint is solid, with a slot in the bottom for the footplate to insert. A bolt secures the footplate to the inside, with a spring and ball bearing assembly to lock vertical movement during swing. The force from initial contact pushes the footplate up; the mechanism is free to roll under the ball bearing and stance is uninhibited. The range of motion is controlled by the width and angle of the walls of the joint body, rather than a complex locking mechanism.

APPENDIX B: DESIGN EVALUATION TOOLS

Table B.1 Bill of materials including manufacturer, specifications, cost, and function in the novel ankle joint design.

Component Number	Name	Manufacturer	Specifications	Cost (ea.)	Function
1	Joint Body	Custom Machine Shop Order	Aluminum 7075-T6	\$400 (machine time) +\$10 material	Connects thermoplastic brace pieces, holds springs and stirrup
2	Stirrup	Becker Orthopedic	Double Action Y-Stirrup Adult		Unites ankle joint and plastic footplate
3	Upright	Becker Orthopedic		Ordered with double action joint	Links upper brace and ankle joint
4	Spring Plungers	Misumi USA	M6 x1.0mm Heavy & Very Heavy Force	\$5.95	Resist drop-foot during swing, depress during stance
5	Main Bolt	Becker Orthopedic	3/8" specialty Chicago Bolt	~\$3	Hold together joint body and stirrup
6	Upright Bolts	Fastenal	3/16" bolt and nut	\$0.32	Couple upright and joint body

Table B.2 Full FMEA for the novel ankle joint design to determine likely failure modes and severity.

Process Function	Failure Mode	Effect(s) of Failure	Severity	Cause(s) of Failure	Occurrence	Controls	Detection	RPN
Stop Tabs	Too weak	Tabs break, footplate supported by main bolt	5	Improper material, machining, weight	2	Proper material, machinist training	5	50
	Angled incorrectly	Footplate sits crookedly	4	Improper machining	2	Proper machinist training, visual inspection	1	8
	Over worn	Footplate sits low, only supported by main bolt	3	Excessive wear	2	Brace changed every 3 years	1	6
Center Slot	Too small	Limited ROM, increased shear on the center bolt, may not fit	3	Improper machining	2	Proper machinist training, visual inspection	1	6
	Too big	Footplate position imprecise	3	Improper machining	2	Proper machinist training, visual inspection	1	6
	Too far up	Footplate hits stop before full ROM	4	Improper machining	2	Proper machinist training, visual inspection	1	8
	Too far down	Increased main bolt shear	3	Improper machining	2	Proper machinist training, visual inspection	1	6
	Not centered	Footplate sits crookedly	4	Improper machining	2	Proper machinist training, visual inspection	1	8
Spring Holes	Walls too thin	Springs get pushed out	7	Design flaw, improper machining	3	Proper machinist training	4	84
Spring Plungers	Too weak	Springs break	7	Incorrect material selection, larger subject	4	Proper spring selection and orthotist tuning	4	112
	Too weak	Springs provide insufficient resistance	3	Incorrect material selection, weight	3	Orthotist tuning	3	27
Upright Recess	Too shallow	Upright pushes out, no upper brace support	4	Improper machining	2	Proper machinist training	1	8
Footplate Interface	Too thin	Footplate dents body	6	Improper material, machining, design	3	Proper machinist training, visual inspection	5	90
Upright Screw Holes	Too high	Upright shears screws	6	Improper machining, design	3	Proper machinist training	1	18
Joint Surface	Too rough	Footplate jams	3	Bad finish	4	Machinists are properly trained, proper material	2	24
Center Bolt	Too long	Possible jamming, footplate not secured	5	Improper material selection	2	Proper dimensioning, visual inspection	1	10
Joint Body	No torsion resistance	Joint snaps in half	7	Improper material, design flaw	1	Proper material, brace absorbs torsional forces	6	42

APPENDIX C: SUBJECT FITNESS ASSESSMENTS AND PERCEPTION SURVEY

FUGL-MEYER ASSESSMENT LOWER EXTREMITY (FMA-LE)
Assessment of sensorimotor function

ID: _____
 Date: _____
 Examiner: _____

Fugl-Meyer AR, Jaasko I, Leyman I, Olsson S, Steglind S: The post-stroke hemiplegic patient. 1. a method for evaluation of physical performance. Scand J Rehabil Med 1975, 7:13-31.

E. LOWER EXTREMITY				
I. Reflex activity, supine position		none	can be elicited	
Flexors: knee flexors		0	2	
Extensors: patellar, achilles (at least one)		0	2	
Subtotal I (max 4)				
II. Volitional movement within synergies, supine position		none	partial	full
Flexor synergy: Maximal hip flexion (abduction/external rotation), maximal flexion in knee and ankle joint (palpate distal tendons to ensure active knee flexion).	Hip flexion	0	1	2
	Knee flexion	0	1	2
	Ankle dorsiflexion	0	1	2
Extensor synergy: From flexor synergy to the hip extension/adduction, knee extension and ankle plantar flexion. Resistance is applied to ensure active movement, evaluate both movement and strength (compare with the unaffected side)	Hip extension	0	1	2
	Knee adduction	0	1	2
	Knee extension	0	1	2
	Ankle plantar flexion	0	1	2
Subtotal II (max 14)				
III. Volitional movement mixing synergies, sitting position, knee 10cm from the edge of the chair/bed		none	partial	full
Knee flexion from actively or passively extended knee	no active motion less than 90° active flexion, palpate tendons of hamstrings more than 90° active flexion	0	1	2
Ankle dorsiflexion compare with unaffected side	no active motion limited dorsiflexion complete dorsiflexion	0	1	2
Subtotal III (max 4)				
IV. Volitional movement with little or no synergy, standing position, hip at 0°		none	partial	full
Knee flexion to 90° hip at 0°, balance support is allowed	no active motion or immediate, simultaneous hip flexion less than 90° knee flexion and/or hip flexion during movement at least 90° knee flexion without simultaneous hip flexion	0	1	2
Ankle dorsiflexion compare with unaffected side	no active motion limited dorsiflexion complete dorsiflexion	0	1	2
Subtotal IV (max 4)				
V. Normal reflex activity, supine position, assessed only if full score of 4 points is achieved in part IV, compare with the unaffected side		0 (IV), hyper	lively	normal
Reflex activity: knee flexors, Patellar, Achilles,	0 points on part IV or 2 of 3 reflexes markedly hyperactive 1 reflex markedly hyperactive or at least 2 reflexes lively maximum of 1 reflex lively, none hyperactive	0	1	2
Subtotal V (max 2)				
Total E (max 28)				

FMA-LE PROTOCOL Rehabilitation Medicine, University of Gothenburg

F. COORDINATION/SPEED, supine, after one trial with both legs, eyes closed, heel to knee cap of the opposite leg, 5 times as fast as possible		marked	slight	none			
Tremor	at least 1 completed movement	0	1	2			
Dysmetria at least 1 completed movement	pronounced or unsystematic slight and systematic no dysmetria	0	1	2			
Time start and end with the hand on the knee	at least 6 seconds slower than unaffected side 2-5 seconds slower than unaffected side less than 2 seconds difference	≥ 6s	2 - 5s	< 2s			
Total F (max 6)							
H. SENSATION, lower extremity eyes closed, compare with the unaffected side		anaesthesia	hypoesthesia or dysesthesia	normal			
Light touch	leg footsole	0	1	2			
		less than 3/4 correct or absence	3/4 correct or considerable difference	correct 100%, little or no difference			
Position small alterations in the position	hip knee ankle great toe (IP-joint)	0 0 0 0	1 1 1 1	2 2 2 2			
Total H (max 12)							
J. PASSIVE JOINT MOTION, lower extremity supine position, compare with the unaffected side		only few degrees	decreased	normal	J. JOINT PAIN during passive motion, lower extremity		
					pronounced pain during movement or very marked pain at the end of the movement	some pain	no pain
Hip	Flexion Abduction External rotation Internal rotation	0 0 0 0	1 1 1 1	2 2 2 2	0 0 0 0	1 1 1 1	2 2 2 2
Knee	Flexion Extension	0 0	1 1	2 2	0 0	1 1	2 2
Ankle	Dorsiflexion Plantar flexion	0 0	1 1	2 2	0 0	1 1	2 2
Foot	Pronation Supination	0 0	1 1	2 2	0 0	1 1	2 2
Total (max 20)					Total (max 20)		
E. LOWER EXTERMTY					/28		
F. COORDINATION / SPEED					/6		
TOTAL E-F (motor function)					/34		
H. SENSATION					/12		
J. PASSIVE JOINT MOTION					/20		
J. JOINT PAIN					/20		

Figure C.1 Fugl-Meyer Assessment for the lower extremities [10].

a) Berg Balance Scale

Name: _____ Date: _____
 Location: _____ Rater: _____

ITEM DESCRIPTION	SCORE (0-4)
Sitting to standing	_____
Standing unsupported	_____
Sitting unsupported	_____
Standing to sitting	_____
Transfers	_____
Standing with eyes closed	_____
Standing with feet together	_____
Reaching forward with outstretched arm	_____
Retrieving object from floor	_____
Turning to look behind	_____
Turning 360 degrees	_____
Placing alternate foot on stool	_____
Standing with one foot in front	_____
Standing on one foot	_____
Total	_____

GENERAL INSTRUCTIONS

Please document each task and/or give instructions as written. When scoring, please record the lowest response category that applies for each item.

In most items, the subject is asked to maintain a given position for a specific time. Progressively more points are deducted if:

- the time or distance requirements are not met
- the subject's performance warrants supervision
- the subject touches an external support or receives assistance from the examiner

Subject should understand that they must maintain their balance while attempting the tasks. The choices of which leg to stand on or how far to reach are left to the subject. Poor judgment will adversely influence the performance and the scoring.

Equipment required for testing is a stopwatch or watch with a second hand, and a ruler or other indicator of 2, 5, and 10 inches. Chairs used during testing should be a reasonable height. Either a step or a stool of average step height may be used for item # 12.

b)

SITTING TO STANDING

INSTRUCTIONS: Please stand up. Try not to use your hand for support.

- () 4 able to stand without using hands and stabilize independently
- () 3 able to stand independently using hands
- () 2 able to stand using hands after several tries
- () 1 needs minimal aid to stand or stabilize
- () 0 needs moderate or maximal assist to stand

STANDING UNSUPPORTED

INSTRUCTIONS: Please stand for two minutes without holding on.

- () 4 able to stand safely for 2 minutes
- () 3 able to stand 2 minutes with supervision
- () 2 able to stand 30 seconds unsupported
- () 1 needs several tries to stand 30 seconds unsupported
- () 0 unable to stand 30 seconds unsupported

If a subject is able to stand 2 minutes unsupported, score full points for sitting unsupported. Proceed to item #4.

SITTING WITH BACK UNSUPPORTED BUT FEET SUPPORTED ON FLOOR OR ON A STOOL

INSTRUCTIONS: Please sit with arms folded for 2 minutes.

- () 4 able to sit safely and securely for 2 minutes
- () 3 able to sit 2 minutes under supervision
- () 2 able to sit 30 seconds
- () 1 able to sit 10 seconds
- () 0 unable to sit without support 10 seconds

STANDING TO SITTING

INSTRUCTIONS: Please sit down.

- () 4 sits safely with minimal use of hands
- () 3 controls descent by using hands
- () 2 uses back of legs against chair to control descent
- () 1 sits independently but has uncontrolled descent
- () 0 needs assist to sit

TRANSFERS

INSTRUCTIONS: Arrange chair(s) for pivot transfer. Ask subject to transfer one way toward a seat with armrests and one way toward a seat without armrests. You may use two chairs (one with and one without armrests) or a bed and a chair.

- () 4 able to transfer safely with minor use of hands
- () 3 able to transfer safely definite need of hands
- () 2 able to transfer with verbal cuing and/or supervision
- () 1 needs one person to assist
- () 0 needs two people to assist or supervise to be safe

STANDING UNSUPPORTED WITH EYES CLOSED

INSTRUCTIONS: Please close your eyes and stand still for 10 seconds.

- () 4 able to stand 10 seconds safely
- () 3 able to stand 10 seconds with supervision
- () 2 able to stand 3 seconds
- () 1 unable to keep eyes closed 3 seconds but stays safely
- () 0 needs help to keep from falling

STANDING UNSUPPORTED WITH FEET TOGETHER

INSTRUCTIONS: Place your feet together and stand without holding on.

- () 4 able to place feet together independently and stand 1 minute safely
- () 3 able to place feet together independently and stand 1 minute with supervision
- () 2 able to place feet together independently but unable to hold for 30 seconds
- () 1 needs help to attain position but able to stand 15 seconds feet together
- () 0 needs help to attain position and unable to hold for 15 seconds

Figure C.2a-b Berg Balance Test assessment of fall risk a) page 1 and b) page 2) [11]

c)

REACHING FORWARD WITH OUTSTRETCHED ARM WHILE STANDING

INSTRUCTIONS: Lift arm to 90 degrees. Stretch out your fingers and reach forward as far as you can. (Examiner places a ruler at the end of fingertips when arm is at 90 degrees. Fingers should not touch the ruler while reaching forward. The recorded measure is the distance forward that the fingers reach while the subject is in the most forward lean position. When possible, ask subject to use both arms when reaching to avoid rotation of the trunk.)

- 4 can reach forward confidently 25 cm (10 inches)
- 3 can reach forward 12 cm (5 inches)
- 2 can reach forward 5 cm (2 inches)
- 1 reaches forward but needs supervision
- 0 loses balance while trying/requires external support

PICK UP OBJECT FROM THE FLOOR FROM A STANDING POSITION

INSTRUCTIONS: Pick up the shoe/slipper, which is in front of your feet.

- 4 able to pick up slipper safely and easily
- 3 able to pick up slipper but needs supervision
- 2 unable to pick up but reaches 2-5 cm (1-2 inches) from slipper and keeps balance independently
- 1 unable to pick up and needs supervision while trying
- 0 unable to try/needs assist to keep from losing balance or falling

TURNING TO LOOK BEHIND OVER LEFT AND RIGHT SHOULDERS WHILE STANDING

INSTRUCTIONS: Turn to look directly behind you over toward the left shoulder. Repeat to the right. (Examiner may pick an object to look at directly behind the subject to encourage a better twist turn.)

- 4 looks behind from both sides and weight shifts well
- 3 looks behind one side only other side shows less weight shift
- 2 turns sideways only but maintains balance
- 1 needs supervision when turning
- 0 needs assist to keep from losing balance or falling

TURN 360 DEGREES

INSTRUCTIONS: Turn completely around in a full circle. Pause. Then turn a full circle in the other direction.

- 4 able to turn 360 degrees safely in 4 seconds or less
- 3 able to turn 360 degrees safely one side only 4 seconds or less
- 2 able to turn 360 degrees safely but slowly
- 1 needs close supervision or verbal cuing
- 0 needs assistance while turning

PLACE ALTERNATE FOOT ON STEP OR STOOL WHILE STANDING UNSUPPORTED

INSTRUCTIONS: Place each foot alternately on the step/stool. Continue until each foot has touched the step/stool four times.

- 4 able to stand independently and safely and complete 8 steps in 20 seconds
- 3 able to stand independently and complete 8 steps in > 20 seconds
- 2 able to complete 4 steps without aid with supervision
- 1 able to complete > 2 steps needs minimal assist
- 0 needs assistance to keep from falling/unable to try

STANDING UNSUPPORTED ONE FOOT IN FRONT

INSTRUCTIONS: (DEMONSTRATE TO SUBJECT) Place one foot directly in front of the other. If you feel that you cannot place your foot directly in front, try to step far enough ahead that the heel of your forward foot is ahead of the toes of the other foot. (To score 3 points, the length of the step should exceed the length of the other foot and the width of the stance should approximate the subject's normal stride width.)

- 4 able to place foot tandem independently and hold 30 seconds
- 3 able to place foot ahead independently and hold 30 seconds
- 2 able to take small step independently and hold 30 seconds
- 1 needs help to step but can hold 15 seconds
- 0 loses balance while stepping or standing

STANDING ON ONE LEG

INSTRUCTIONS: Stand on one leg as long as you can without holding on.

- 4 able to lift leg independently and hold > 10 seconds
- 3 able to lift leg independently and hold 5-10 seconds
- 2 able to lift leg independently and hold ≥ 3 seconds
- 1 tries to lift leg unable to hold 3 seconds but remains standing independently.
- 0 unable to try of needs assist to prevent fall

Figure C.2c Berg Balance Test assessment of fall risk c) page 3 [11]

Design and Evaluation of a Novel Ankle Joint for an Ankle Foot Orthosis for Individuals with Drop-Foot

Post Testing Session Survey

Please rate the AFO with the new ankle joint in terms of **walking performance** compared to the default study-provided AFO:

-5 (Worse)	-4	-3	-2	-1	0 (Same)	1	2	3	4	5 (Superior)

Please rate the AFO with the new ankle joints in terms of **comfort** compared to the default study-provided AFO

-5 (Worse)	-4	-3	-2	-1	0 (Same)	1	2	3	4	5 (Superior)

Please rate the AFO with the new ankle joints in terms of **perceived exertion** compared to the default study-provided AFO:

-5 (More Fatiguing)	-4	-3	-2	-1	0 (Same)	1	2	3	4	5 (Less Fatiguing)

Additional Comments:

Figure C.3 Subject perception survey to determine relative walking performance, comfort, and perceived exertion with the two orthotic ankle designs.

Inverse Dynamics Equations of Motion

$$\delta = \frac{3M}{L(R_{proximal}^2 + R_{distal}R_{proximal} + R_{distal}^2)\pi} \quad (\text{Eq C.1})$$

$$a_1 = \frac{9}{20\pi} \quad (\text{Eq C.2})$$

$$a_2 = \frac{(1+x+x^2+x^3+x^4)}{(1+x+x^2)^2} \quad (\text{Eq C.3})$$

$$b_1 = \frac{3}{80} \quad (\text{Eq C.4})$$

$$b_2 = \frac{(1+4x+10x^2+4x^3+x^4)}{(1+x+x^2)^2} \quad (\text{Eq C.5})$$

where M = mass of the segment, L = length of the segment, R = radius of the segment (proximal or distal), x = ratio between the proximal and distal segment radii [86], [87].

APPENDIX D: RAW METRICS

Table D.1 Spatiotemporal and kinematic parameters for the AFO side (right) of able-bodied subjects for each ankle condition during the middle 145 seconds of level treadmill walking. Conv = conventional ankle joint, NSS = novel ankle joint trial at self-selected speed, NSM = novel ankle joint trial at speed matched to the conventional trial.

	C1			C2			C3		
	Conv	NSS	NSM	Conv	NSS	NSM	Conv	NSS	NSM
Stance Duration (% GC)	0.78 ±0.05	0.77 ±0.05	0.78 ±0.06	0.78 ±0.06	0.78 ±0.05	0.78 ±0.07	0.71 ±0.03	0.69 ±0.04	0.69 ±0.09
Step Length (% Height)	0.53 ±0.03	0.53 ±0.03	0.55 ±0.05	0.55 ±0.05	0.53 ±0.03	0.56 ±0.05	0.59 ±0.02	0.57 ±0.02	0.57 ±0.07
Peak Knee Flexion stance (deg)	19.8 ±9.54	22.1 ±9.30	17.6 ±12.1	16.9 ±4.94	20.1 ±5.00	17.8 ±4.87	16.8 ±6.02	23.4 ±3.83	19.1 ±9.32
Peak Hip Flexion stance (deg)	21.2 ±8.44	33.2 ±10.8	27.1 ±9.38	13.0 ±5.44	12.3 ±4.97	12.3 ±5.52	9.92 ±6.23	17.0 ±6.34	17.3 ±6.03

Table D.2 Spatiotemporal and kinematic parameters for the AFO side (right) of able-bodied subjects for each ankle condition during the middle 145 seconds of incline treadmill walking. Conv = conventional ankle joint, NSS = novel ankle joint trial at self-selected speed, NSM = novel ankle joint trial at speed matched to the conventional trial.

	C1			C2			C3		
	Conv	NSS	NSM	Conv	NSS	NSM	Conv	NSS	NSM
Ankle PF swing (deg)	0.24 ±0.29	0.71 ±0.64	1.09 ±1.11	2.23 ±1.64	2.95 ±1.62	1.56 ±1.12	2.52 ±2.03	1.27 ±1.04	2.16 ±1.48
Ankle ROM stance (deg)	20.8 ±2.69	21.7 ±2.60	23.9 ±2.59	25.6 ±2.15	26.3 ±1.38	26.2 ±2.33	23.7 ±2.23	22.1 ±2.71	21.7 ±2.30
Stance Duration (% GC)	0.82 ±0.06	0.78 ±0.03	0.81 ±0.04	0.83 ±0.05	0.81 ±0.03	0.82 ±0.04	0.69 ±0.04	0.71 ±0.02	0.72 ±0.02
Step Length (% Height)	0.54 ±0.04	0.53 ±0.03	0.56 ±0.04	0.59 ±0.04	0.53 ±0.03	0.56 ±0.03	0.58 ±0.02	0.58 ±0.02	0.58 ±0.02
Peak Knee Flexion stance (deg)	18.1 ±8.17	21.1 ±8.90	14.9 ±13.2	15.5 ±4.66	17.7 ±4.62	17.5 ±5.01	16.8 ±6.27	16.3 ±4.64	15.1 ±8.18
Peak Hip Flexion stance (deg)	24.7 ±8.52	33.2 ±9.68	27.5 ±9.17	13.0 ±4.98	12.4 ±4.22	12.6 ±5.06	10.0 ±6.41	17.4 ±5.98	17.1 ±5.71

Table D.3 Spatiotemporal and kinematic parameters for the AFO side (right) of able-bodied subjects for each ankle condition during the middle 145 seconds of decline treadmill walking. Conv = conventional ankle joint, NSS = novel ankle joint trial at self-selected speed, NSM = novel ankle joint trial at speed matched to the conventional trial.

	C1			C2			C3		
	Conv	NSS	NSM	Conv	NSS	NSM	Conv	NSS	NSM
Ankle PF swing (deg)	0.24 ±0.29	0.69 ±0.63	1.06 ±1.02	2.11 ±1.63	2.83 ±1.66	1.54 ±1.13	2.58 ±2.06	1.34 ±1.11	2.11 ±1.44
Ankle ROM stance (deg)	21.1 ±2.72	22.0 ±2.71	24.4 ±2.70	25.7 ±2.22	26.4 ±1.38	26.4 ±2.33	23.6 ±2.21	22.1 ±2.82	21.8 ±2.38
Stance Duration (% GC)	0.77 ±0.05	0.77 ±0.04	0.77 ±0.04	0.79 ±0.06	0.76 ±0.05	0.76 ±0.06	0.72 ±0.03	0.71 ±0.02	0.72 ±0.03
Step Length (% Height)	0.53 ±0.03	0.53 ±0.03	0.55 ±0.04	0.55 ±0.06	0.52 ±0.03	0.54 ±0.05	0.59 ±0.03	0.57 ±0.02	0.59 ±0.02
Peak Knee Flexion stance (deg)	17.7 ±7.79	20.5 ±8.47	14.3 ±11.7	15.6 ±4.37	18.0 ±4.54	17.4 ±4.65	19.0 ±7.13	22.4 ±3.43	17.1 ±8.51
Peak Hip Flexion stance (deg)	22.4 ±7.94	32.6 ±9.81	26.8 ±9.04	12.7 ±4.96	12.0 ±4.28	12.1 ±5.09	10.8 ±6.65	17.6 ±6.25	17.5 ±5.92

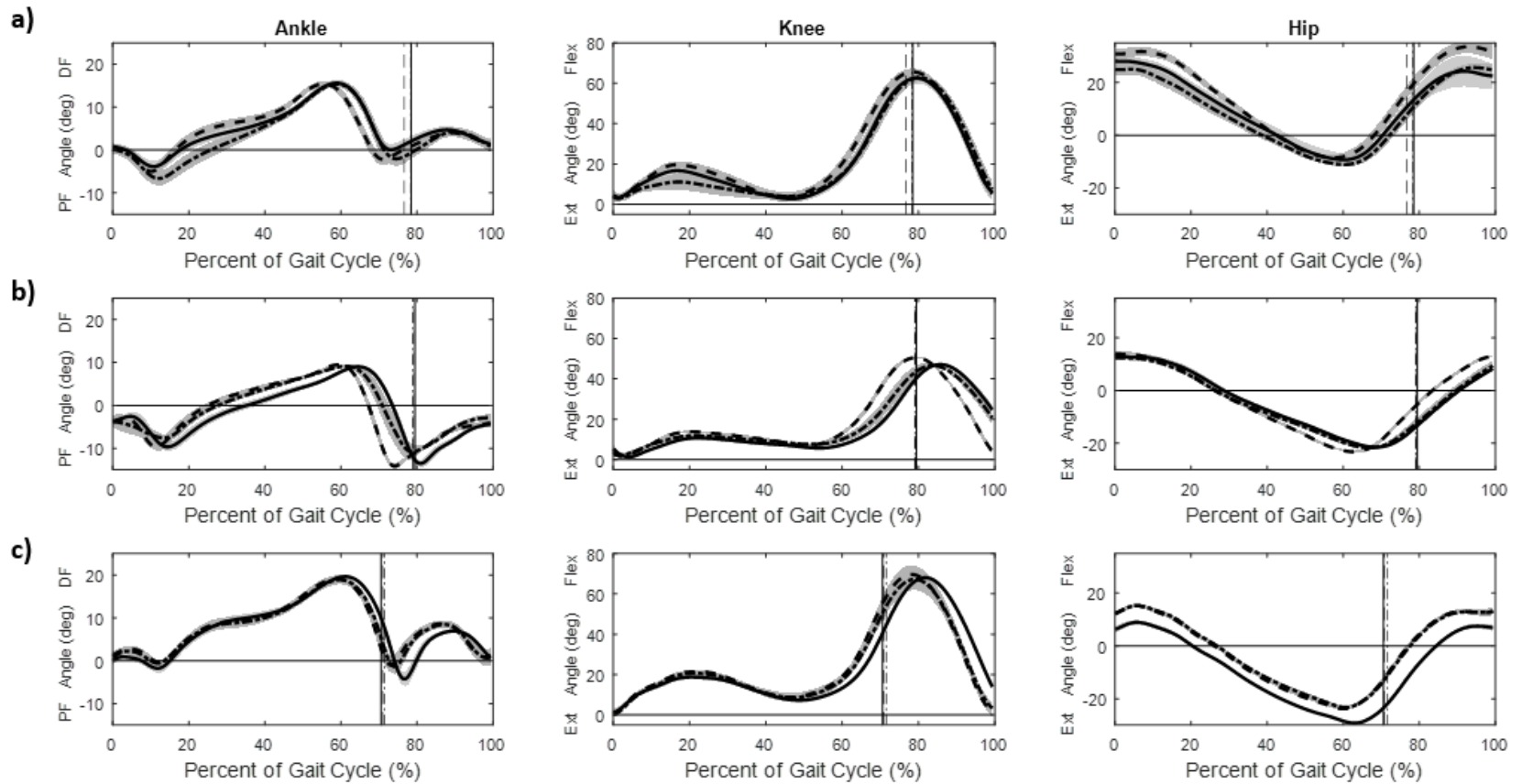


Figure D.1 Ankle (left), knee (middle), and hip (right) angle time series for the paretic/AFO side of able-bodied subjects for level treadmill walking— a) Subject C1, b) Subject C2, c) Subject C3. Solid line is the mean of the trials with the conventional joint (light gray shading S.D.), dashed line is the mean of the novel joint at SS (medium gray shading S.D.), and dot-dashed line is the mean of the novel joint at SM (dark gray shading S.D.).

The vertical lines (solid – conventional, dashed – novel SS, dot-dash – novel SM) represent TO, the transition from stance to swing.

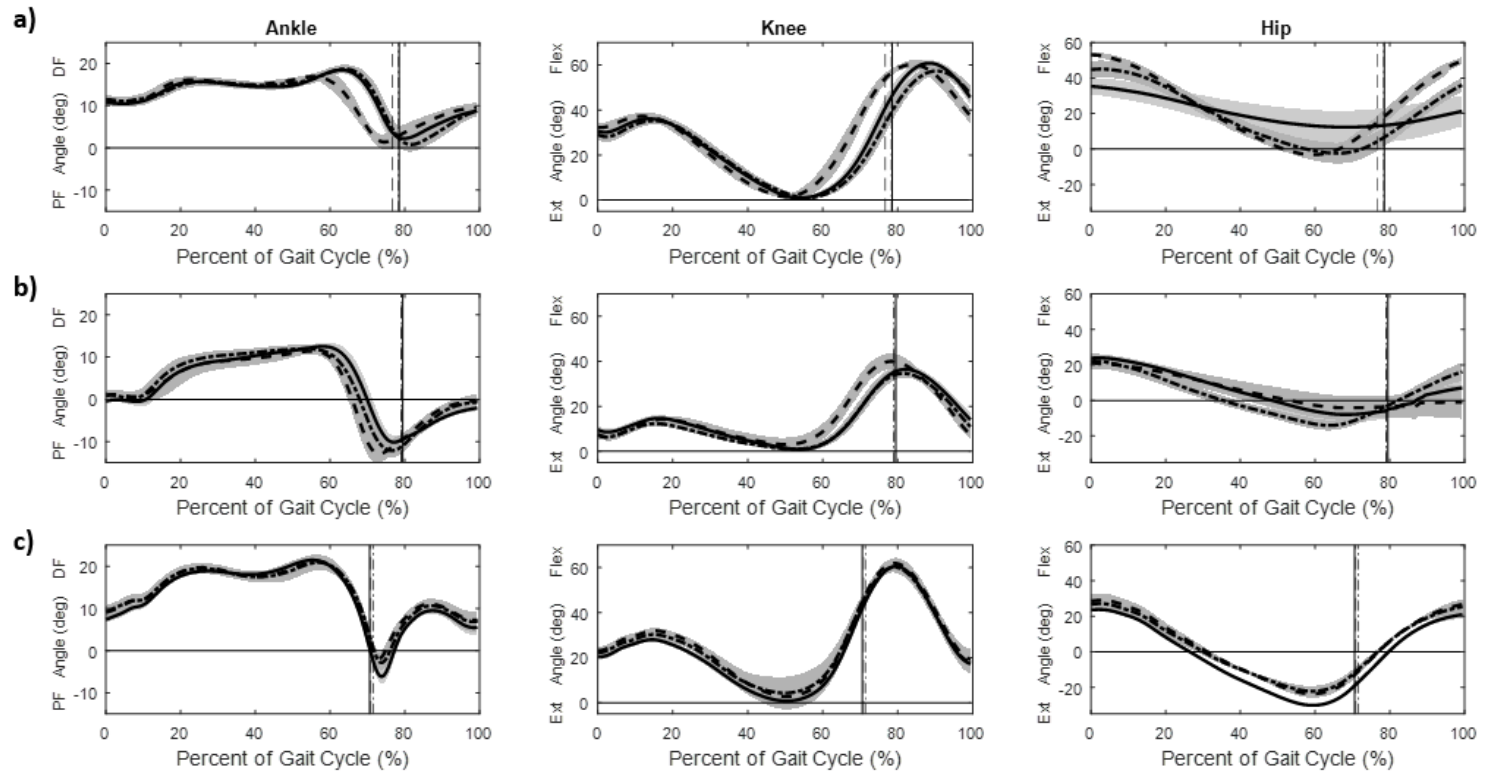


Figure D.2 Ankle (left), knee (middle), and hip (right) angle time series for the paretic/AFO side of able-bodied subjects for inclined treadmill walking– a) Subject C1, b) Subject C2, c) Subject C3. Solid line is the mean of the trials with the conventional joint (light gray shading S.D.), dashed line is the mean of the novel joint at SS (medium gray shading S.D.), and dot-dashed line is the mean of the novel joint at SM (dark gray shading S.D.).

The vertical lines (solid – conventional, dashed – novel SS, dot-dash – novel SM) represent TO, the transition from stance to swing.

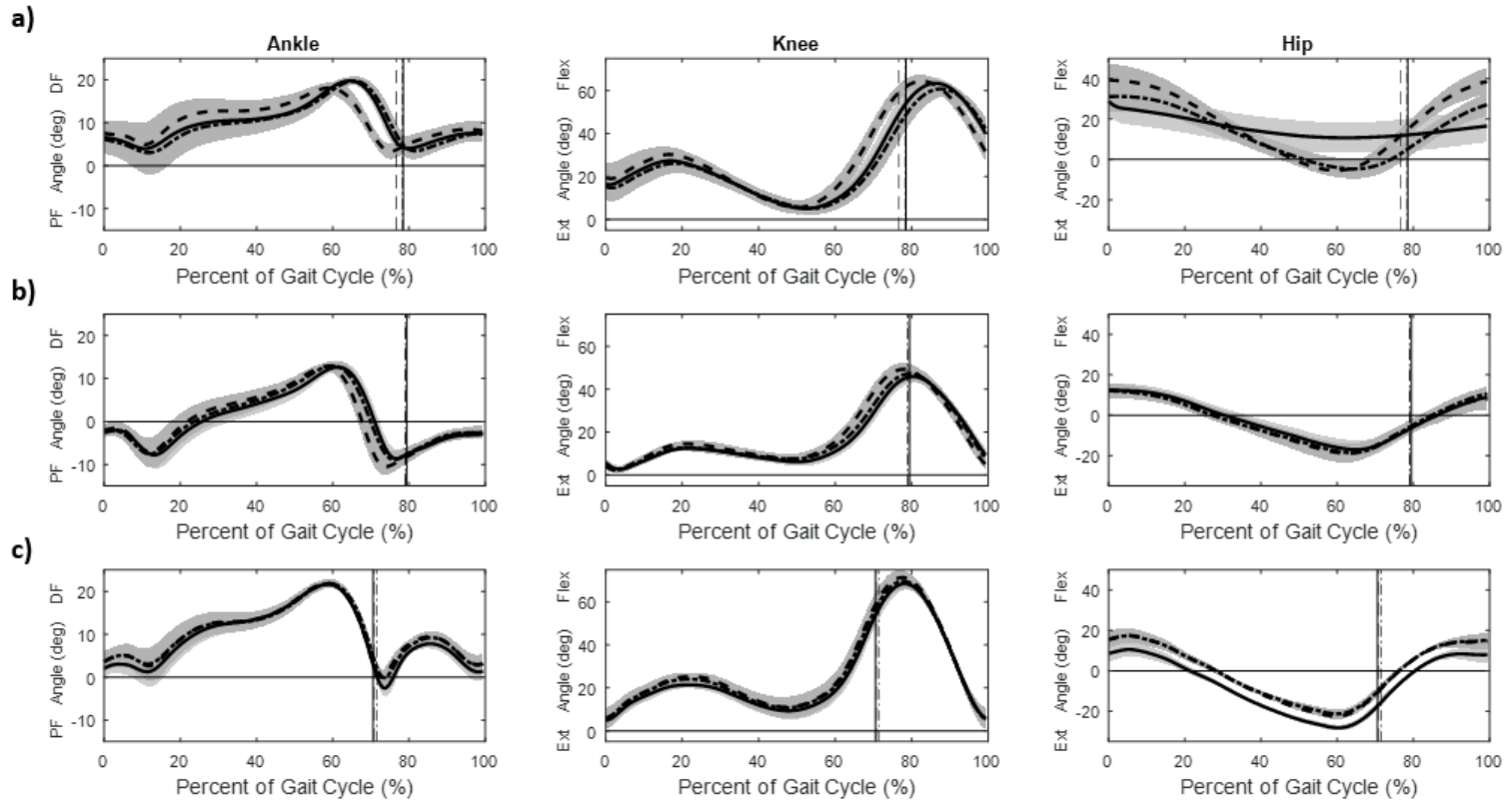


Figure D.3 Ankle (left), knee (middle), and hip (right) angle time series for the paretic/AFO side of able-bodied subjects for declined treadmill walking— a) Subject C1, b) Subject C2, c) Subject C3. Solid line is the mean of the trials with the conventional joint (light gray shading S.D.), dashed line is the mean of the novel joint at SS (medium gray shading S.D.), and dot-dashed line is the mean of the novel joint at SM (dark gray shading S.D.).

The vertical lines (solid – conventional, dashed – novel SS, dot-dash – novel SM) represent TO, the transition from stance to swing.

Table D.4 Kinetic parameters for able-bodied subjects during overground walking for each ankle joint condition; raw metrics are for the AFO side (right leg). No AFO = no AFO trial, Conv = conventional ankle joint, Novel = novel ankle joint.

	C1			C2			C3		
	No AFO	Conv	Novel	No AFO	Conv	Novel	No AFO	Conv	Novel
Peak Knee Extension Moment (Nm/kg)	0.26 ±0.08	0.28 ±0.03	0.41 ±0.36	1.12 ±0.06	1.19 ±0.16	0.76 ±0.26	0.61 ±0.29	0.58 ±0.17	0.61 ±0.05
Peak Hip Extension Moment (Nm/kg)	0.60 ±0.05	0.60 ±0.07	0.77 ±0.28	1.27 ±0.15	1.55 ±0.28	0.89 ±0.45	0.48 ±0.24	0.56 ±0.05	0.35 ±0.03

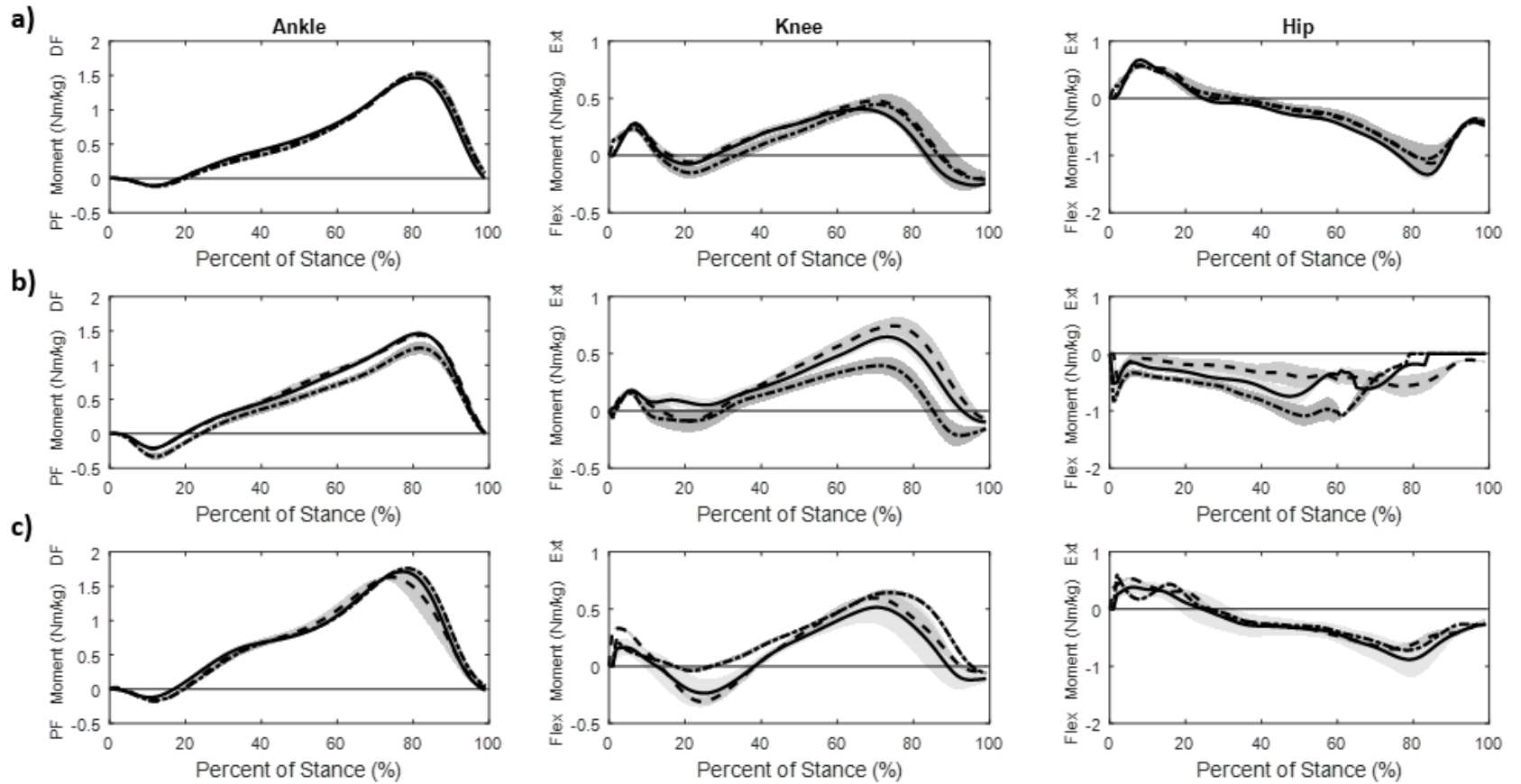


Figure D.4 Ankle, knee, and hip moments for the paretic/AFO side of control subjects – a) Subject C1, b) Subject C2, c) Subject C3 - walking over level ground. Solid line is the mean of the trials with no AFO (light gray shading S.D.), dashed is the conventional ankle joint mean (medium gray shading S.D.), and dot-dashed is the novel joint mean (dark gray shading S.D.).

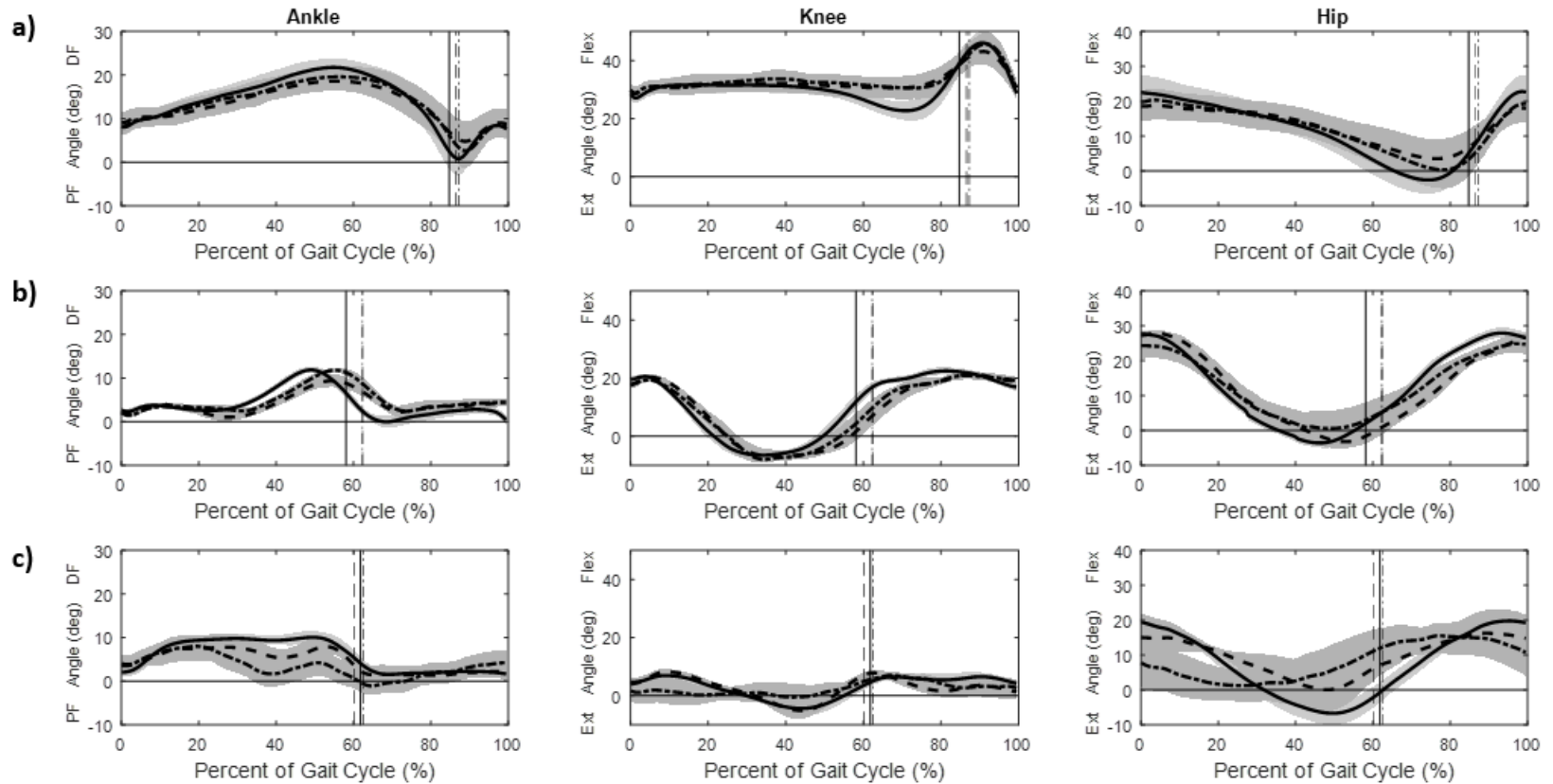


Figure D.5 Ankle (left), knee (middle), and hip (right) angle time series for the paretic/AFO side of post-stroke subjects for inclined treadmill walking— a) Subject P1, b) Subject P2, c) Subject P3. Solid line is the mean of the trials with the conventional joint (light gray shading S.D.), dashed line is the mean of the novel joint at SS (medium gray shading S.D.), and dot-dashed line is the mean of the novel joint at SM (dark gray shading S.D.).

The vertical lines (solid – conventional, dashed – novel SS, dot-dash – novel SM) represent TO, the transition from stance to swing.

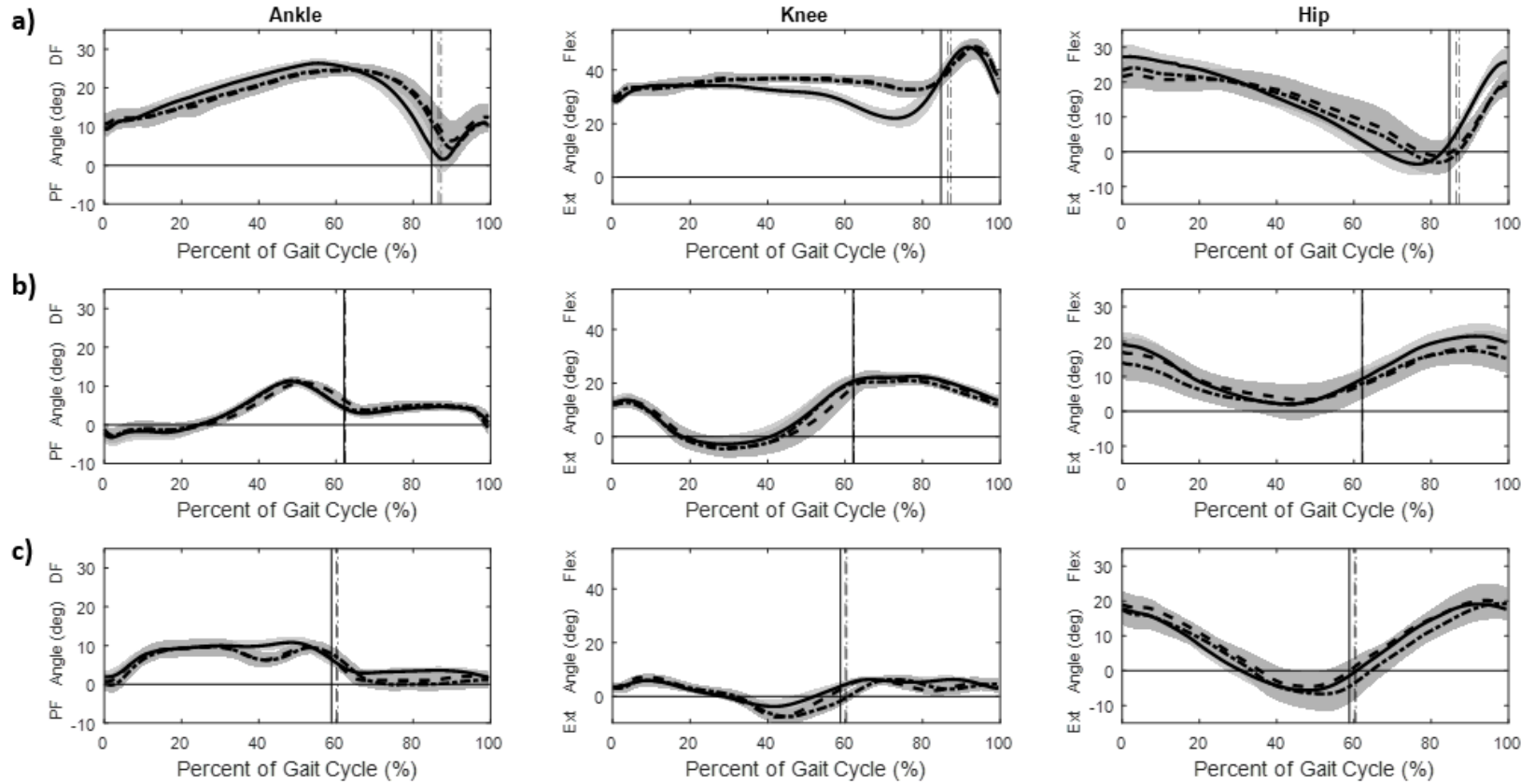


Figure D.6 Ankle (left), knee (middle), and hip (right) angle time series for the paretic/AFO side of post-stroke subjects for declined treadmill walking— a) Subject P1, b) Subject P2, c) Subject P3. Solid line is the mean of the trials with the conventional joint (light gray shading S.D.), dashed line is the mean of the novel joint at SS (medium gray shading S.D.), and dot-dashed line is the mean of the novel joint at SM (dark gray shading S.D.).

The vertical lines (solid – conventional, dashed – novel SS, dot-dash – novel SM) represent TO, the transition from stance to swing.

Table D.5 Spatiotemporal and kinematic parameters for the AFO side (right) of post-stroke subjects for each ankle condition during the middle 50% of incline treadmill walking. Conv = conventional ankle joint, NSS = novel ankle joint trial at self-selected speed, NSM = novel ankle joint trial at speed matched to the conventional trial.

	P1			P2			P3		
	Conv	NSS	NSM	Conv	NSS	NSM	Conv	NSS	NSM
Ankle ROM early stance (deg)	-3.29 ±1.26	-2.95 ±1.64	-2.34 ±1.49	-0.99 ±1.66	-0.74 ±1.71	-1.22 ±1.50	-2.01 ±2.65	-4.05 ±2.40	-3.81 ±2.78
Ankle ROM mid stance (deg)	16.4 ±4.22	13.9 ±3.28	15.9 ±2.62	15.1 ±2.86	14.4 ±2.38	14.6 ±2.22	8.83 ±2.46	8.59 ±2.40	10.0 ±2.42
Ankle PF late stance (deg)	1.96 ±1.29	1.28 ±0.52	1.05 ±0.76	2.61 ±1.95	0.87 ±0.53	1.89 ±1.56	0.87 ±0.53	2.15 ±1.46	2.16 ±1.46
Peak Knee Flexion stance (deg)	34.1 ±4.81	32.8 ±5.59	31.1 ±6.78	23.6 ±4.18	21.6 ±3.60	22.1 ±3.06	6.82 ±1.55	8.01 ±1.32	1.06 ±1.27
Peak Hip Flexion stance (deg)	22.8 ±3.73	18.4 ±3.98	18.9 ±3.99	29.7 ±5.30	29.9 ±6.38	25.3 ±5.27	20.1 ±3.56	15.6 ±3.61	9.10 ±3.70

Table D.6 Spatiotemporal and kinematic parameters for the AFO side (right) of post-stroke subjects for each ankle condition during the middle 50% of decline treadmill walking. Conv = conventional ankle joint, NSS = novel ankle joint trial at self-selected speed, NSM = novel ankle joint trial at speed matched to the conventional trial.

	P1			P2			P3		
	Conv	NSS	NSM	Conv	NSS	NSM	Conv	NSS	NSM
Ankle ROM early stance (deg)	-3.21 ±1.25	-2.92 ±1.65	-2.31 ±1.51	-0.91 ±1.85	-0.29 ±1.77	-1.00 ±1.60	-1.72 ±2.68	-3.83 ±2.42	-3.40 ±2.75
Ankle ROM mid stance (deg)	16.7 ±4.34	13.8 ±3.19	16.1 ±2.86	16.0 ±2.71	15.1 ±2.48	15.1 ±2.28	9.26 ±2.48	8.29 ±2.72	9.86 ±2.66
Ankle PF late stance (deg)	1.86 ±1.24	1.11 ±0.28	0.93 ±0.82	2.70 ±1.93	0.87 ±0.67	1.87 ±1.70	0.87 ±0.55	2.21 ±1.46	2.33 ±1.35
Peak Knee Flexion stance (deg)	35.6 ±5.09	34.5 ±5.93	32.8 ±7.04	13.4 ±3.89	13.3 ±3.23	12.9 ±2.87	6.65 ±1.40	8.08 ±1.43	7.02 ±1.39
Peak Hip Flexion stance (deg)	25.9 ±3.56	18.4 ±3.73	20.9 ±3.73	19.9 ±4.82	18.4 ±5.75	14.0 ±4.95	18.0 ±3.84	19.3 ±3.32	18.8 ±3.46